

UNIVERSITY OF SÃO PAULO

Faculty of Pharmaceutical Sciences

Graduate Program in Food Sciences

Department of Food and Experimental Nutrition

**Docosahexaenoic fatty acid nanoencapsulated with Anti-PECAM-1 as strategy to
increase atherosclerotic plaque stability**

Matheus de Castro Leão

São Paulo

2022

UNIVERSITY OF SÃO PAULO
Faculty of Pharmaceutical Sciences
Graduate Program in Food Sciences
Department of Food and Experimental Nutrition

**Docosahexaenoic fatty acid nanoencapsulated with Anti-PECAM-1 as strategy to
increase atherosclerotic plaque stability**

Matheus de Castro Leão

Original Version

Ph. D. Thesis presented for the degree of
DOCTOR OF SCIENCE

Advisor: Profa. Dr. Inar Castro Erger

São Paulo
2022

Autorizo a reprodução e divulgação total ou parcial deste trabalho, por qualquer meio convencional ou eletrônico, para fins de estudo e pesquisa, desde que citada a fonte.

Ficha Catalográfica elaborada eletronicamente pelo autor, utilizando o programa desenvolvido pela Seção Técnica de Informática do ICMC/USP e adaptado para a Divisão de Biblioteca e Documentação do Conjunto das Químicas da USP

Bibliotecária responsável pela orientação de catalogação da publicação:
Marlene Aparecida Vieira - CRB - 8/5562

L438d Leão, Matheus de Castro
Docosahexaenoic fatty acid nanoencapsulated with
Anti-PECAM-1 as strategy to increase
atherosclerotic plaque stability / Matheus de
Castro Leão. - São Paulo, 2022.
97 p.

Tese (doutorado) - Faculdade de Ciências
Farmacêuticas da Universidade de São Paulo.
Departamento de Alimentos e Nutrição Experimental -
Programa de Pós-Graduação em Ciência dos Alimentos.
Orientador: Erger, Inar Castro

1. Aterosclerose . 2. Nanocápsulas. 3. Ácido
docosahexaenoico. 4. Polarização. 5. Inflamação. I.
T. II. Erger, Inar Castro, orientador.

Matheus de Castro Leão

**DOCOSAHEXAENOIC FATTY ACID NANOENCAPSULATED WITH ANTI-PECAM-1 AS
STRATEGY TO INCREASE ATHEROSCLEROTIC PLAQUE STABILITY**

Commission of Thesis for the degree of Doctor of Science

1° Examiner

2° Examiner

3° Examiner

4° Examiner

5° Examiner

São Paulo, _____, 2022.

ACKNOWLEDGMENTS

First of all, I would like to express my sincere gratitude to my advisor Prof. Inar Castro Erger for all support during these years of the post-graduation program. Her advices about professional and personal aspects of the life were precious.

I would greatly like to thank the professors Adriana Raffin Pohlmann and Silvia Guterres for all support during the initial phase of my study, carried out in the UFRGS. Their expertise and collaboration became this thesis possible.

I take this opportunity to thank Dr. Aline Alvez, who helped me at the beginning of the project. Thank you for your patience and for all the support!

I want to thank all the students of the nanotechnology laboratory of UFRGS, especially Dr. Luíza Frank, who was always present!

I also want to thank Prof. Sandra Farsky for her collaboration, and Dr. Silvana Sandri with all my heart for her immeasurable assistance. I want to thank my great lab friend Milena, who helped me very much! Thank you, Mayara Uchiyama for the partnership and for the advices! Thank you, Pablo and Gustavo! I have no words to express my gratitude!

I would like to thank my lab colleagues, who have always been together and helped me to overcome the difficulties of each day. Especially Gabriela Grassmann, Marina Nogueira and Thiago Motta. Thank you very much!

I also thank the students of scientific initiation, Isabela and Sarah, who are carrying out the next steps of my research.

My particular gratitude to my family, that gave to me the basis to arrive here. To my loving parents Francisco and Simone, my sisters Ranile and Thaís, my brother-in-law Joshua, my cousin Jonatas and my uncles Lenira and Danilo. You helped me to overcome very difficult moments. Thank you for your encouragement and spiritual care.

Finally, I would like to thank myself for not give up on this challenge and to overcome the unexpected adversities that happened more recently. Thank you, Matheus!

This research would not have been available without the financial support of FAPESP (Process 2019/ 21029-3), the scholarship of CNPq (166541/2017-6) and without the excellent work of the Food and Experimental Nutrition Department post-graduation staff.

“The important thing is not to stop questioning. Curiosity has its own reason for existence.”

Albert Einstein

RESUMO

LEAO, M. C. **Ácido graxo docosahexaenoico nanoencapsulado com anti-PECAM-1 como uma estratégia para aumentar a estabilidade de placas ateroscleróticas.** 2022. 97f. Tese (Doutorado) – Faculdade de Ciências Farmacêuticas, Universidade de São Paulo, São Paulo, 2022.

As doenças cardiovasculares (DCVs) são a principal causa de mortalidade no mundo, sendo os eventos isquêmicos responsáveis por 85% das mortes. A aterosclerose é uma inflamação crônica das artérias associada aos eventos isquêmicos das DCVs, na qual o sistema imunológico inato e adaptativo estão envolvidos desde a formação inicial das estrias gordurosas até a ruptura das placas ateroscleróticas. Pesquisas recentes direcionadas à redução da inflamação sistêmica têm mostrado resultados controversos, pois essa abordagem pode aumentar a susceptibilidade do paciente a infecções. Nesse sentido, novas estratégias direcionadas ao tecido lesionado são necessárias. No que se refere a medicamentos anti-inflamatórios ou suplementos alimentares, o ácido docosahexaenóico (DHA) tem sido relatado como um precursor natural de oxilipinas pró-resolutivas. Baseado nesse contexto, o objetivo deste estudo foi desenvolver nanocápsulas contendo óleo de alga como fonte de DHA e vetorizar essas nanopartículas com o anticorpo anti-PECAM-1 em sua superfície, visando direcioná-las ao endotélio inflamado. Inicialmente, a nanocápsula multiparede metal-complexa funcionalizada contendo óleo de alga em seu núcleo (MLNC-DHA-a1) foi desenvolvida, apresentando um diâmetro médio de 163 ± 5 nm, formato esférico, onde a eficiência de conjugação do anti-PECAM-1 (200 $\mu\text{g}/\text{mL}$) foi de 94,80% sem toxicidade significativa em HUVECs nas concentrações de 1.14 a 2.9×10^{11} nanocápsulas/mL. As nanocápsulas apresentaram uma estabilidade de 2h, o que representa tempo suficiente para a sua aplicação clínica. A seguir, ensaios de viabilidade celular foram realizados em outras linhagens de células para avaliar a toxicidade das nanocápsulas. As concentrações de 0.14 a 1.40×10^{11} de nanocápsulas/mL não afetaram significativamente a viabilidade celular de macrófagos murinos imortalizados (RAW 264.7) e U-937 após 24, 48 e 72 h de tratamento. Por fim, os macrófagos (RAW 264.7) foram incubados com 0.75×10^{11} MLNC-DHA-a1/mL durante 4 h e apresentam uma captação significativa das nanocápsulas, observada por microscopia hiperespectral de campo escuro (CytoViva®). Uma vez captadas pelos macrófagos murinos imortalizados (RAW 264.7), as nanoformulações MLNC-DHA-a1 promoveram um forte aumento da polarização do fenótipo M2 em comparação com as células controle não tratadas. Nossos resultados sugerem que o óleo de alga rico em DHA presente no núcleo lipídico das nanocápsulas, não reduziu a viabilidade celular e estimulou uma maior polarização de macrófagos para o tipo M2, sendo assim uma terapia potencial para controlar a inflamação crônica e cicatrizar ou estabilizar placas ateroscleróticas.

Palavras-chave: Aterosclerose, nanocápsulas, ácido docosahexaenoico, polarização, inflamação.

ABSTRACT

LEAO, M. C. **Docosahexaenoic fatty acid nanoencapsulated with Anti-PECAM-1 as strategy to increase atherosclerotic plaque stability**. 2022. 97f. Thesis (PhD) – Faculty of Pharmaceutical Sciences, University of São Paulo, São Paulo, 2022.

Cardiovascular diseases (CVDs) are the main cause of mortality worldwide, being the ischemic heart disease responsible for 85% of deaths. Atherosclerosis is a chronic inflammation of the arteries that underlies ischemic forms of CVD and involves the innate and adaptive immune systems, from initial fatty streak formation to atherosclerotic plaque ruptures, which defines the beginning and end stages of disease, respectively. Recent research on the reduction of systemic inflammation in order to treat CVD is controversial, since results show that this reduced inflammation can also increase patient susceptibility to general infection. Therefore, new tissue-targeting strategies are necessary. Docosahexaenoic fatty acid (DHA) is a natural bioactive precursor of pro-resolving oxylipins that can reduce inflammation. Based on these factors, the objective of this study was to develop a nanocapsule containing algae oil as a DHA source and apply anti-PECAM-1 on its surface to drive it to the inflamed endothelium. Initially, a surface-functionalized metal-complex multi-wall nanocapsule containing algae oil in its nucleus (MLNC-DHA-a1) was developed. This nanocapsules presented a mean diameter of 163 ± 5 nm, was spherical in shape, showed 94.80% conjugation efficiency using 200 $\mu\text{g}/\text{mL}$ of anti-PECAM-1 on the surface, and did not show significant toxicity toward HUVECs at concentrations from 0.14 to 2.90×10^{11} nanocapsules/mL. The nanocapsules were also stable for 2 h, sufficient time to allow for clinical applications. In cell viability assays, concentrations of 0.14 to 1.40×10^{11} nanocapsules/mL did not significantly affect the viability of immortalized murine macrophages (RAW 264.7) and U-937 cells after 24, 48, and 72 h of treatment. Finally, macrophages were incubated with 0.75×10^{11} MLNC-DHA-a1 nanocapsules/mL for 4 h and showed a significant uptake, observed using dark-field hyperspectral microscopy (CytoViva®). Once inside murine macrophages (RAW 264.7), MLNC-DHA-a1 nanocapsules promoted a strong increase in M2 phenotype polarization compared to non-treated control cells. Our results suggest that DHA-enriched algae oil, as part of a lipid core nanocapsules, does not reduce cell viability and improves macrophage phenotype, making it a promising potential therapy for controlling chronic inflammation and healing or stabilizing atherosclerotic plaques.

Key words: atherosclerosis, nanocapsules, docosahexaenoic acid, polarization, inflammation

ABBREVIATIONS

apoB-LP, apolipoprotein B; ARA, arachidonic fatty acid; CAM, cell adhesion molecules; COX, cyclooxygenases; CRP, c-reactive protein; CT, computed chromatography; CVDs, cardiovascular diseases; CYP450, cytochrome P 450; DAMPs, Damage-associated molecular pattern; DHA, docosahexaenoic acid; EPA, eicosapentaenoic acid; FDA, Food and Drug Administration; GPR120, G protein coupled receptor; HUVEC, Human umbilical vein endothelial cells; ICAM-1, Intracellular Adhesion Molecule-1; IL, interleukins; LDL, low-density lipoprotein; LDL^(-/-), *Knockout* for LDL receptor; LNC, lipid core nanocapsule; LOX, lipoxygenases; LPS, lipopolysaccharide; LTB₄, leukotriene B₄; MCP-1, monocyte chemoattractant protein-1; MCT, medium-chain triglyceride; MLNC, multi-wall lipid core nanocapsules; MLNC-DHA-a1, surface-functionalized metal-complex multi-wall nanocapsules containing algae oil; N3FA, omega 3 fatty acids; NF-κB, Nuclear factor kappa-light-chain-enhancer of activated B cells; OxLDL, oxidized low-density lipoprotein; PAMPs, pathogens-associated molecular patterns; PCL, poli(E-caprolactone); PECAM-1 or CD31, Platelet endothelial cell adhesion molecule; PGE₂, prostaglandin E₂; PMNs, polymorphonuclear neutrophils; PPAR_γ, transcriptor factor Peroxisome proliferator-activated receptor γ ; RAW 264.7, murine immortalized macrophages; ROS, reactive oxygen species; SMC, smooth muscle cells; SPMs, specialized pro-resolving mediators; TG, triglyceride; TNF, Tumor Necrosis Factor; VCAM-1, Vascular Cell adhesion Molecule-1.

LIST OF TABLES

Chapter I

Table I. Characterization of the oils applied to form the lipid-core of the nanocapsules....	44
Table II. Physico-chemical characteristics of the nanocapsules.....	45
Table III. Diameter and number of particles of the nanocapsules containing DHA in the Lipid core determined by NTA.....	46

LIST OF FIGURES

Introduction

Figure 1. Stages of atherosclerosis development.....	17
Figure 2. Omega 3 and 6 fatty acids.....	21
Figure 3. The proposed molecular mechanism of cardioprotection by n-3 FAs.....	22
Figure 4. The natural pathway if inflammation is resolution.....	25
Figure 5. The imbalance between lipid mediators can promote instability of atherosclerotic plaques.....	26
Figure 6. Schematic diagram of PECAM-1.....	28

Chapter I

Figure 1. Steps for the synthesis of the Anti-PECAM-1 Surface-Funcionalized Metal-Complex Multi-Wall nanocapsules.....	43
Figure 2. Characterization of the nanocapsules with antibody compared with the nanocapsules without antibody.....	46
Figure 3. Photomicrographs obtained by TEM of MLNC-DHA-a1.....	47
Figure 4. Three-dimensional CytoViva microscopy results for the nanocapsules; Cell viability quantified by Trypan exclusion assay; Flow cytometry analysis of annexin V + propidium iodide (PI).....	47
Figure 1S. Capacity of the PCL polymer to absorber the algae oil and MCT.....	50
Figure 2S. Diameter distribution of PCL and algae oil nanocapsules.....	51
Figure 3S. Radar chart for LNC-DHA, MLNC-DHA, LNC-MCT and MLNC-MCT formulations.....	52
Figure 4S. Size Distribution by Intensity and size distribution by volume.....	53
Figure 5S. Overlap of the Anti-PECAM-1 functionalized nanoparticles over the chitosan-coated nanocapsules performed at the NTA.....	54

Chapter II

Figure 1. HUVECs viability.....	78
Figure 2. U-937 viability.....	79
Figure 3. RAW (264.7) murine macrophages viability.....	80
Figure 4. Three-dimensional CytoViva microscopy images of uptake performed in RAW 264.7 murine macrophages.....	81
Figure 5. Flow cytometric analysis to quantify cytokines and polarization in cells obtained from the bone marrow.....	82
Figure 6. Summary of the strategy proposed in this study.....	83
S. Figure 1. HUVEC viability, necrosis, apoptosis and late apoptosis as estimated by flow cytometry after 48 h of treatment.....	84
S. Figure 2. HUVEC viability, necrosis, apoptosis and late apoptosis as estimated by flow cytometry after 72 h of treatment.....	85
S. Figure 3. U-937 viability, necrosis, apoptosis and late apoptosis as estimated by flow cytometry after 48 h of treatment.....	86
S. Figure 4. U-937 viability, necrosis, apoptosis and late apoptosis as estimated by flow cytometry after 72 h of treatment.....	87
S. Figure 5. RAW 264.7 murine macrophages viability, necrosis, apoptosis and late apoptosis as estimated by flow cytometry after 48 h of treatment.....	88
S. Figure 6. RAW 264.7 murine macrophages viability, necrosis, apoptosis and late apoptosis as estimated by flow cytometry after 72 h of treatment.....	89

SUMMARY

INTRODUCTION	14
REVIEW OF LITERATURE	16
Atherosclerosis: genesis and progression.....	16
Platelet Endothelial Cell Adhesion Molecule-1 (PECAM-1) and atherosclerosis.....	18
The anti-inflammatory effects of Docosahexaenoic acid (DHA).....	20
Resolving the unresolved may contribute to decrease atherosclerosis.....	23
Nanotechnology applied for bioactive compounds delivery.....	27
OBJECTIVE	30
DESCRIPTION OF CHAPTERS	30
REFERENCES	31
CHAPTER I: Docosahexaenoic acid nanoencapsulated with anti-PECAM-1 as co-therapy for atherosclerosis regression	40
Introduction.....	42
Materials and methods.....	42
Results.....	44
Discussion.....	46
Conclusion.....	48
References.....	48
Supplementary figures.....	50
CHAPTER II: Effect of anti-PECAM-1 vectorized nanocapsules containing docosahexaenoic acid on macrophages polarization	55
Introduction.....	62
Materials and methods.....	64
Results.....	67
Discussion.....	69
Conclusion.....	72
References.....	73

Figures..... 78

Supplementary figures..... 84

FINAL COMMENTS..... 90

ATTACHMENTS..... 91

1. INTRODUCTION

Cardiovascular diseases (CVDs), manifested mainly as coronary heart disease, angina, acute myocardial infarction and stroke, are the world's leading cause of death, and atherosclerosis is the main process involved in etiology of these conditions (REN et al., 2021). According to Benjamin et al. (2019), 121.5 million people have been diagnosed with CVDs worldwide, and, according to WHO (2021), more than 17 million people die annually from these diseases.

Atherosclerosis is an inflammatory condition involved in CVD initiation and progression. Among the risk factors for its development, the most well-known are age, sex, obesity, smoking, sedentary lifestyle, hypertension, diabetes mellitus, high plasma cholesterol concentrations and oxidative stress (MIGLIACCIO et al., 2021). In addition, because atherosclerosis has been recognized as an inflammatory disease, inflammatory biomarkers have also been considered as predictors of cardiovascular risk, especially C-reactive protein (CRP) and cytokines such as interleukins (IL) and Tumor Necrosis Factor (TNF- α) (LIBBY, 2021). However, previous and current pharmacological strategies applied to reduce inflammation in cardiovascular contexts have increased the susceptibility of patients to infections due to their non-targeted systemic approach (ADAY & RIDKER, 2018).

Diet also plays a fundamental role in the development of CVDs, especially the consumption of fat, cholesterol, and compounds that can exert anti- or pro-inflammatory effects. Therefore, there is great interest in bioactive compounds that could contribute to atherosclerotic risk reduction. Among these, numerous health claims for omega 3 fatty acids (n3FA), specifically eicosapentaenoic and docosahexaenoic acids (EPA and DHA), have been reviewed and approved by the Food and Drug Administration (FDA, 2003). Several studies have demonstrated that consumption or supplementation with n3FA can reduce pro-inflammatory molecules, including IL-6, Intracellular Adhesion Molecule-1 (ICAM-1),

Vascular Cell adhesion Molecule-1 (VCAM-1), and CRP, as well as increase in anti-inflammatory molecules, such as adiponectin and IL-10 (GROSSO et al., 2022; THOTA et al., 2018; CALDER, 2012). The mechanisms by which n3-FA decreases inflammation are mainly through their association with cell surface G-protein coupled receptor 120, activation of transcription factor Peroxisome proliferator-activated receptor γ (PPAR γ) that suppress Nuclear factor kappa-light-chain-enhancer of activated B cells (NF- κ B), reducing the NLRP3 inflammasome, promoting the synthesis of less inflammatory 3 and 5-series eicosanoids and by acting as a substrate to synthesize specialized pro-resolving mediators (SPMs) (GROSSO et al., 2022). In addition, n3FA decrease plasma triglyceride (TG) levels through the reduction of liver enzymes, which are responsible for synthesizing TGs and acting as agonists of transcription factors, such as PPAR- α , that increase fatty acid oxidation (DJURICIC & CALDER, 2021; SHEMESH & ZAFRIR, 2019; SHIBABAW, 2021).

Chronic inflammation associated with atherosclerosis is a consequence of innate and adaptive immune system activation, which occurs at beginning of endothelial injury and remains until plaque rupture (ROY et al., 2022). Among the immune cells, macrophages are reported to play an essential role in atherosclerosis progression (MOORE et al., 2013). Some studies have shown that a higher proportion of M1 phenotype macrophages compared to M2 phenotype ones is associated with more vulnerable plaques, thus more likely to rupture. In addition, previous studies have found that n3FA, particularly DHA, can promote a switch from M1 to M2 macrophages (KAWANO et al., 2019; CHANG et al., 2015).

Thus, it was hypothesized that it is possible to develop novel and targeted strategy, such as a surface-functionalized metal-complex multi-wall nanocapsules containing algae oil (MLNC-DHA-a1) as a DHA source. Applying anti-PECAM-1 to the nanocapsules can direct them to the inflamed endothelium since PECAM-1 increases the permeability between endothelial cells during the atherosclerotic process. Once they arrive at the target tissue, the nanocapsules would be recognized and phagocytosed by immune cells as Damage-

associated molecular pattern (DAMPs). Finally, once inside the immune cell phagosomes and lysosomes, the nanocapsules would deliver DHA to be used as a substrate for the synthesis of oxylipins, which have the ability to switch the macrophage phenotype from M1 to M2. Thus, this nanocapsule could, potentially contribute to the healing or stabilization of atherosclerotic plaques.

2. REVIEW OF LITERATURE

2.1. Atherosclerosis: genesis and progression

Atherosclerosis is a public health problem of great relevance, and its associated complications, such as acute myocardial infarction, stroke and peripheral arterial disease, are the main causes of morbidity and mortality worldwide (XIA et al., 2017). Atherosclerosis presents a slowly progressive development that affects the intimate layer of the arteries, being recognized as a chronic inflammatory and metabolic process, characterized by the formation of plaques containing a cholesterol-rich nucleus, surrounded by a fibrous material (KRISHNAN-SIVADOSS et al., 2021).

The atherosclerosis pathogenesis may be divided into three phases: initiation, progression and complications (LIBBY, 2021). The process can be initiated mainly in arterial regions with altered blood flow. The blood flow disturbance leads to pro-inflammatory activation of endothelial cells, which alters the integrity of the endothelial barrier, produces reactive species and facilitates the infiltration of molecules (CHISTIYAKOV et al., 2017). According to Libby et al. (2019), the low-density lipoprotein (LDL) excess is one of the main factors involved in atherosclerotic disease. Inside the intima, LDL can be oxidized forming oxidized LDL (oxLDL), the main determinant of disease initiation and progression (TURPIN et al., 2021). The presence of oxLDL stimulates the innate and adaptive immune response (LIBBY; RIDKER & HANSSON, 2009). The stimulus of the innate response promotes the

recruitment of monocytes and other leukocytes, which bind to endothelial cells, and infiltrate into the intimate layer of the vascular wall (**Figure 1**).

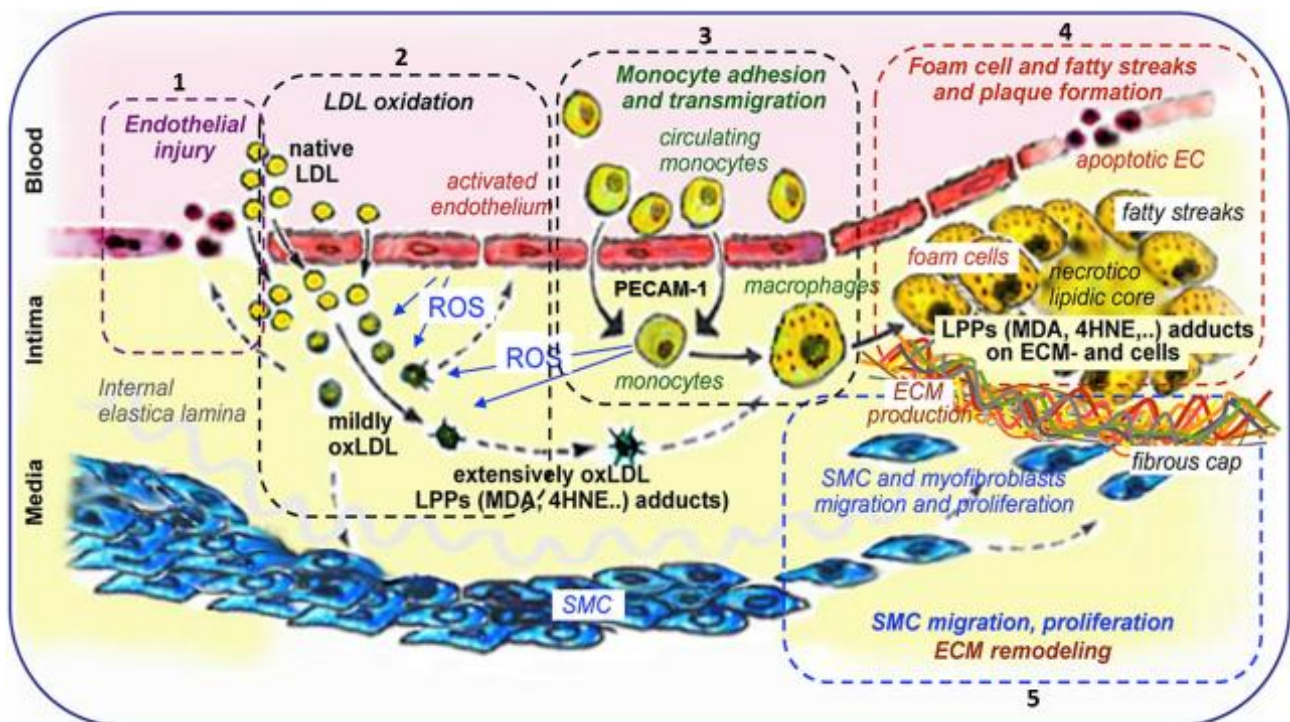


Figure 1: Stages of atherosclerosis development. 1. Damage to endothelial tissue altering membrane permeability; 2. Production of reactive oxygen species (ROS) due to the endothelial injury, infiltration and oxidation of LDL molecules; 3. Infiltration of monocytes attracted by chemokines; 4. oxLDL molecules are phagocytosed by macrophages leading to foam cell formation; 5. Migration and proliferation of smooth muscle cells (SMC) with the formation of the fibrous layer around the atherosclerotic lesion. Adapted from Salvayre & Camaré (2016).

Monocytes differentiate in macrophages, phagocyte oxLDL molecules and generate foam cells. These foam and endothelial cells, release a variety of pro-inflammatory cytokines, chemokines, adhesion molecules, such as Interleukin-1 (IL-1), Interleukin-6 (IL-6), monocyte chemoattractant protein-1 (MCP-1), Tumor necrosis factor-alpha (TNF- α), Platelet Endothelial Cell Adhesion Molecule-1 (PECAM-1) and intercellular adhesion

molecule- 1(ICAM-1) that promote the recruitment of additional monocytes, which in turn, increases macrophage proliferation, contributing to the spread and expansion of the atherosclerotic lesion (KARUNAKARAN & RAYNER, 2016). In view of this persistent inflammatory stimulus and other cytotoxic factors, several injured cells become apoptotic. At the beginning of the atherosclerotic lesion, apoptotic cells are efficiently phagocytosed by neighboring macrophages to limit the overall lesion, in a process known as efferocytosis (YURDAGUL, 2018). However, according to the plaques progress, efferocytosis begins to be deficient, resulting in the accumulation of secondary necrotic cells and the formation of a potentially inflammatory necrotic nucleus (OTSUKA et al., 2015). The presence of large necrotic nuclei is a marker of advanced atherosclerotic disease and has been associated with heart attack and stroke (YURDAGUL et al., 2018).

In addition, the secretion of growth factors stimulates the migration of SMC from the middle layer to the intima, where they secrete extracellular matrix, leading to the formation of fibrous layer around the atherosclerotic plaque (SALVAYRE & CAMARÉ, 2016). Therefore, abnormalities of blood flow and excess circulating lipids generate stress on the vessel wall and trigger an inflammatory cascade, which results in a vicious cycle in the progression of the atherosclerotic plaque (LI et al., 2022).

2.2. Platelet Endothelial Cell Adhesion Molecule-1 (PECAM-1) and atherosclerosis

During abnormal events, such as atherosclerosis, several Cell Adhesion Molecules (CAM) are expressed on the surface of endothelial cells (BAKER et al., 2018). Such molecules are essential for the progression of atherosclerotic plaque, as they promote the recruitment and infiltration of immune system cells, contributing to the development of the lesion (PATEL et al., 2020). The main adhesion molecules involved in this process are selectins, integrins, VCAM-1, ICAM-1, junctional adhesion molecules and immunoglobulins such as PECAM-1 (MALIK et al., 2015).

PECAM-1 or CD31 is a transmembrane glycoprotein of the immunoglobulin family, expressed on the surface of many cells present in the injured sites, such as monocytes, lymphocytes, platelets and endothelial cells (DING, 2008). According to Caligiuri (2020), the pro-atherosclerotic effect of PECAM-1 is related to its participation in a mechanical stimulatory complex in endothelial cells. In this complex, PECAM-1 activates NF- κ B molecules in response to oxidative stress, inducing the expression of more PECAM-1 molecules, which in turn, contribute to the recruitment of inflammatory cells to the site of injury. According to Stevens (2008), PECAM-1 is related to the maintenance of endothelial integrity and the trans-endothelial migration of leukocytes. In this sense, PECAM-1 has been the subject of studies that focus on its role as an adhesion molecule, in order to recruit drug-carrying particles or nutraceuticals targeted to the vascular endothelium (SHUVAEV *et al.*, 2013).

In this perspective, Hood *et al.* (2014) evaluated the effect of antioxidant enzyme-carrying nanoparticles on oxidative stress and inflammation in the pulmonary vascular endothelium. In this study, C57BL/6 mice received intratracheal dose of 1 mg/kg of lipopolysaccharide (LPS) to induce acute lung damage. Then, a controlled release of catalase and superoxide dismutase in the pulmonary vasculature of the animals was performed applying anti-PECAM-1 monoclonal antibodies on the surface of the nanoparticles. As firstly hypothesized, it was observed an accumulation of the nanocapsules in the pulmonary vasculature. Then, it was found that the nanoparticles protected endothelial cells from apoptosis, decreased pulmonary edema and leukocyte infiltration. Thus, this study indicates that the use of anti-PECAM-1 antibodies on the surface of nanoparticles could be effective for the infiltration and target-specific controlled release of drugs and nutraceuticals.

Moreover, Dan *et al.* (2013) evaluated the flow across the blood-brain barrier, bio-distribution and affinity of nanoparticles super-paramagnetized with iron oxide and vectorized with anti-PECAM-1 using *in vitro* and *in vivo* models, and observed a high binding

affinity between nanoparticles and cellular receptors (PECAM-1), using Sprague Dawley rats. High concentrations of vectorized nanoparticles were observed in the lungs and brain of the animals. Thus, this study also suggested that the use of the anti-PECAM-1 antibody would be an effective strategy to be applied to functionalize nanocapsules. In another study, Tietjen et al. (2017) demonstrated that conjugation of anti-PECAM-1 antibodies on the surface of polymeric nanocapsules was effective to reach the vascular endothelium of inflamed pre-transplanted human kidney. These results reinforce the hypothesis that the vectorization of nanoparticles with anti-PECAM-1 would be an interesting strategy for targeting n3FA to the inflamed vascular endothelium.

2.3. The anti-inflammatory effects of Docosahexaenoic acid (DHA)

The anti-inflammatory effects of marine omega 3 fatty acids, including the docosahexaenoic acid (DHA), occurs via different mechanisms, including inhibition of leucocyte chemotaxis, adhesion molecule expression and leucocyte-endothelial adhesive interactions, disruption of lipid rafts, inhibition of activation of pro-inflammatory transcription factor (NFkB), activation of anti-inflammatory transcription factor PPAR γ and binding to the G protein coupled receptor (GPR120) (CALDER, 2012; CALDER 2013). However, the most documented mechanism to explain the anti-inflammatory effect of n3FA is related to their enzymatic oxidation by cyclooxygenases (COX), lipoxygenases (LOX) and cytochrome P 450 (CYTP450), generating bioactive oxylipins (WASSERMAN et al., 2020).

Omega 3 fatty acids partially replace the omega 6 arachidonic fatty acid (ARA, C20:4 n-6 FA) in the membranes of cells involved in the inflammatory responses, decreasing the availability of substrate to produce potent pro-inflammatory eicosanoids, such as prostaglandin E2 (PGE2) and leukotriene B4 (LTB4), and increasing the synthesis of specialized pro-resolving mediators (SPMs) responsible to end the inflammatory process

(CALDER, 2013; CALDER 2019). **Figure 2** compares the eicosanoids pathways according to the precursor fatty acid.

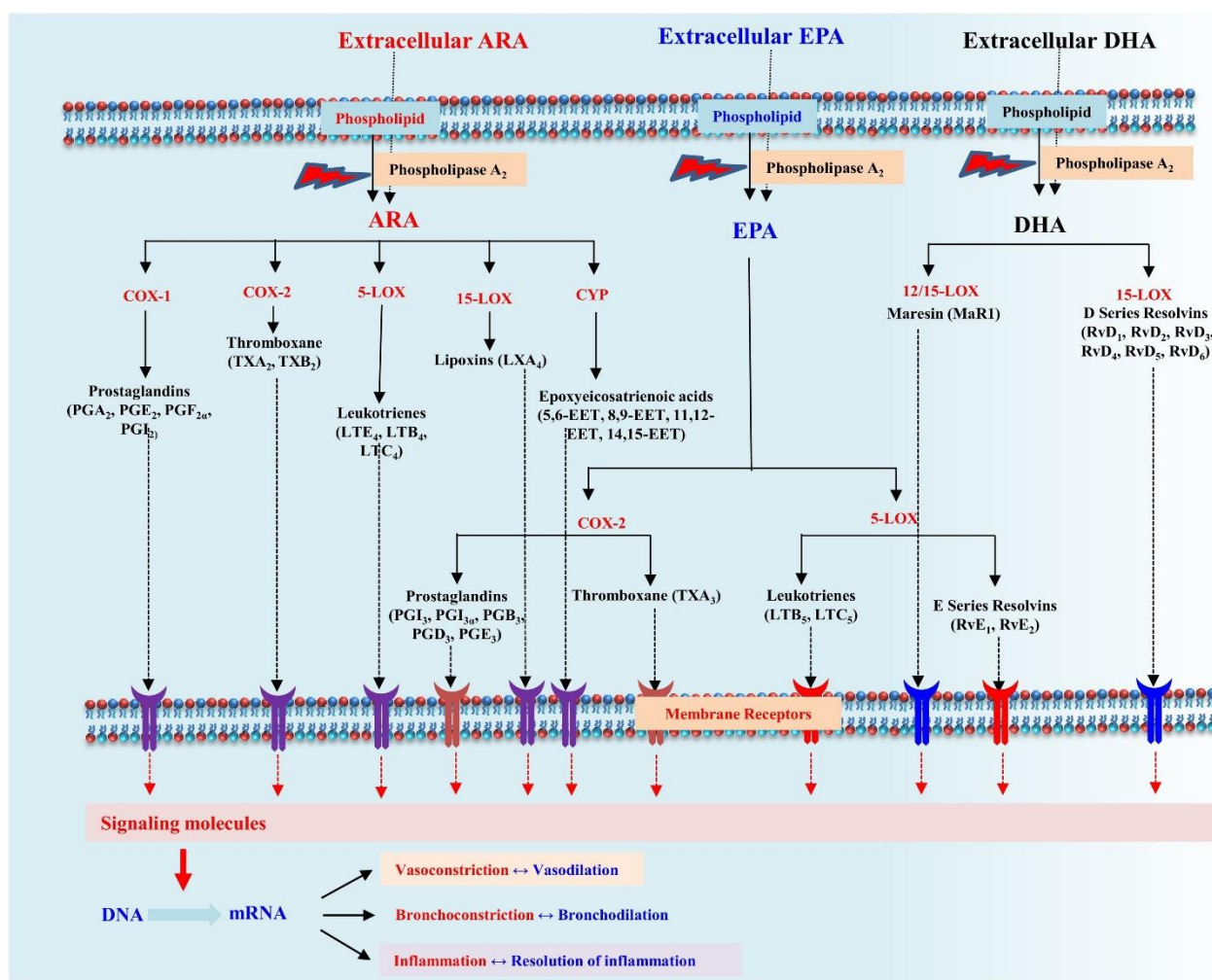


Figure 2: Omega 3 and omega 6 fatty acids – derived oxylipins. Production of eicosanoids from arachidonic acid (ARA; n-6 PUFAs), eicosapentaenoic acid (EPA; n-3 PUFAs) and docosahexaenoic acid (DHA; n-3 PUFAs). Adapted from Saini & Keun (2018).

Free ARA acts a substrate for COX, LOX or cytochrome P450 enzymes, leading to the synthesis of 2 and 4-series of prostaglandins, thromboxanes, leukotrienes, hydroxyl eicosatrienoic and epoxyeicosatrienoic acids (CALDER, 2013). The same occurs when EPA and DHA are the fatty acids precursors, but instead of 2,4-series, they are substrate to the 3,5-series synthesis, being these later eicosainoids less biologically active than those produced from ARA (CALDER, 2013). Among the SPMs, resolvins produced from EPA (E-

series) and DHA (D-series) and protectins produced from DHA, are pro-resolving molecules that inhibit the transendothelial migration of neutrophils and the production of IL-1 β and TNF α (CALDER, 2013). In *in vitro* assays, both EPA and DHA, inhibit T cell proliferation and the production of IL-2 (CALDER, 2013). Resolvins are under development as pharmaceutical agents, making EPA and DHA regarded as pro-drugs (CALDER, 2013). In a study performed in human atherosclerotic plaques, Friedman et al. (2016) observed that the levels of SPMs, particularly resolving D1 derived from DHA, and the ratio of SPMs to pro-inflammatory LTB $_4$ were lower in the vulnerable regions of the plaque. Besides eicosanoids synthesis, EPA and DHA exerts an anti-inflammatory effect by other mechanisms as summarized in **Figure 3**.

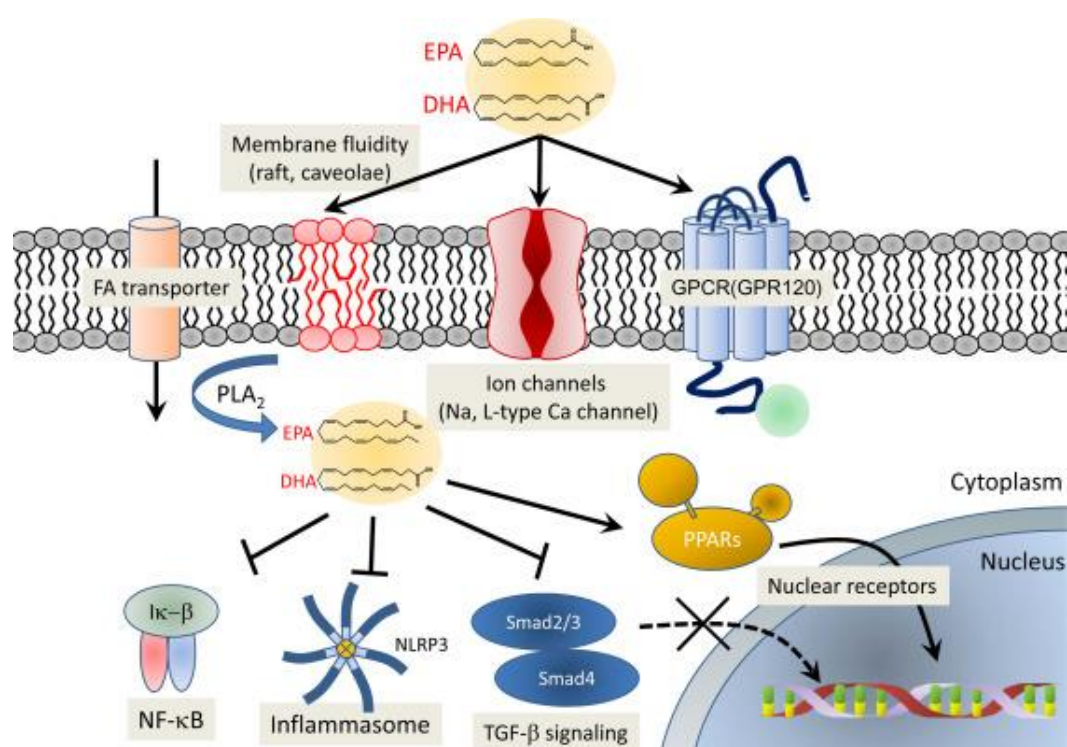


Figure 3: The proposed molecular mechanism of cardioprotection attributed to n3FA. EPA and DHA modulate cell membrane when incorporated in the bilayer phospholipidic and control membrane ion channels to prevent lethal arrhythmia. They also exert anti-inflammatory and anti-fibrotic effects by modifying NFκB signaling, the NLRP3 inflammasome, PPARα/γ, GPR120 and TGF-β signaling (Adapted from Endo & Arita, 2016).

Particularly regarding to DHA, it has been reported that DHA induces PPAR γ , decreasing the production of inflammatory cytokines (CALDER, 2013). In addition, the ability of DHA to inhibit responsiveness of macrophages to endotoxin, seems to occur via GRP120 (CALDER, 2013). According to the ComparED Study, DHA was more effective than EPA in modulating specific markers of inflammation and some blood lipids (ALLAIRE et al., 2016).

The CANTOS study, applied an antibody to neutralize IL-1 β , and showed 30% reduction in cardiovascular mortality (RIDCKER et al., 2018), demonstrating the effectiveness of targeting inflammation in atherosclerosis and the role of inflammasome pathway for further interventions. However, in the same study, patients treated with monoclonal IL-1 β antibody were more susceptible to infections. Thus, future studies should aim to develop anti-inflammatory or pro-resolving therapies that cause less perturbation of host defense (LIBBY & EVERETT, 2019). In this way, more directed attempts to block advanced plaque macrophage inflammation and rupture could be achieved by innovative drug delivery systems, such as arterial wall target nanoparticles (MOORE & TABAS, 2011).

2.3 Resolving the unresolved may contribute to decrease atherosclerosis

Inflammation is an essential mechanism of the immune system (VON-HEGEDUS et al., 2020), that protect the organism against damage caused by pathogens-associated molecular patterns (PAMPs) or DAMPs. The inflammatory process, as part of the immune response, can be acute or chronic, depending on type of stimulus and the capacity of the cells to signalize the inflammation resolution, leading to the tissue repair (FULLERTON et al., 2016).

In the acute phase of inflammation, lipid mediators formed from the fatty acids that are esterifying the phospholipids that compose the cell's membrane or delivered by lipid droplets or lysosomes in the cytoplasm, are released by immune cells at the site of injury (BRENNAN et al., 2021). At the first moment, polymorphonuclear neutrophils (PMNs) achieve the target tissue to exert the first line defense (SERHAN, 2007). Then, the cells of the damage tissue express cytokines, chemokines, growth factors and adhesion molecules, as a signal to attract monocytes to the site of the inflammation, where these myeloid cells undergo differentiation to macrophages, amplifying the inflammatory processes and promoting the phagocytosis of PAMPs and DAMPs (KASIKARA et al., 2018). However, during this process, macrophages also initiate the synthesis of molecules able to resolve the inflammation leading to the removal of apoptotic cells and consequent tissue healing (HALADE et al., 2022; SPITE et al., 2014). Specialized pro-resolution mediators (SPMs) are fatty acids derived oxylipins associated to the inflammation resolution (JOFFRE et al., 2020). The increase of SPMs has been also associated to the macrophage phenotype change, from pro-inflammatory M1 to pro-resolving M2 (RAHMAN et al., 2017). The classification of macrophage types was widely described by Gordon et al. (2010) and Mantovani et al. (2012), and include several types such as M1, M2a, b and c (NOVAK, 2013).

Although the natural inflammatory process follows a cycle with beginning and end, when uncontrolled or inappropriately activated, acute inflammation progresses to chronic inflammation, promoting fibrosis and organ dysfunction (DAVID & LÓPEZ-VALEZ, 2021), as illustrated in **Figure 4**.

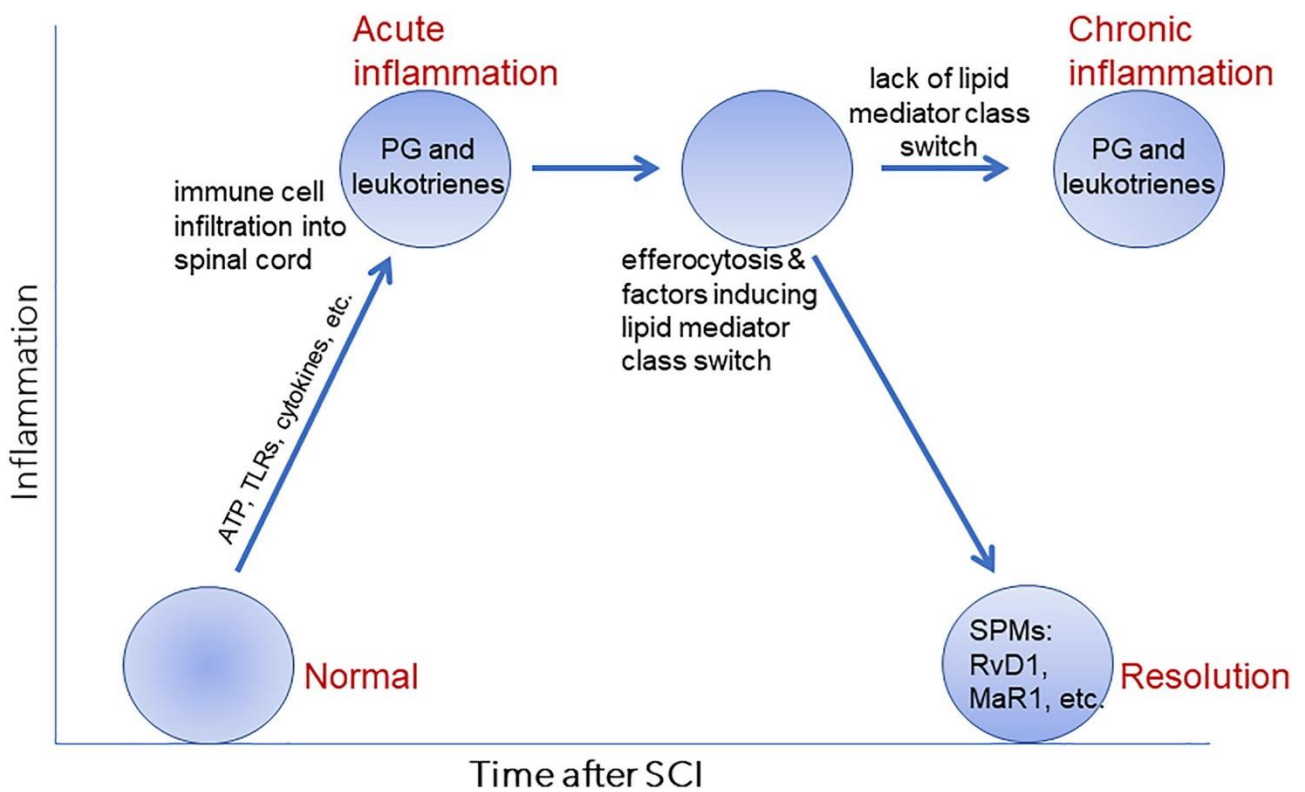


Figure 4: The natural pathway of inflammation is resolution. After an inflammatory stimulus, the natural pathway of inflammation is resolution, from a change in the class of lipid mediators and an increase in efferocytosis. However, failure to change the class of mediators can result in chronic inflammation. Adapted from David & López-Vales (2021).

Atherosclerosis is a chronic inflammatory disease, it means, an unresolved inflammatory condition. Atherosclerotic plaques are mainly formed by macrophages (HU et al., 2021). Regression of the plaques are characterized by a reduced expression of genes that encode markers of M1 macrophages and an increased expression of genes encoding markers of M2 macrophages (RAHMAN et al., 2017). Therefore, an imbalance between SPMs and pro-inflammatory oxylipins is a feature of advanced atherosclerotic plaques (KASIKARA et al., 2018). It has been reported that human atherosclerotic plaques, characterized by thin fibrous caps and large necrotic nuclei, had low levels of resolving D1 and high levels of the pro-inflammatory mediator Leukotriene B4 (KASIKARA et al. 2018),

while the opposite was observed in the more stable plaques (FREDMAN et al., 2016).

Figure 5 illustrates the imbalance of lipid mediators and its consequence in atherosclerotic plaques.

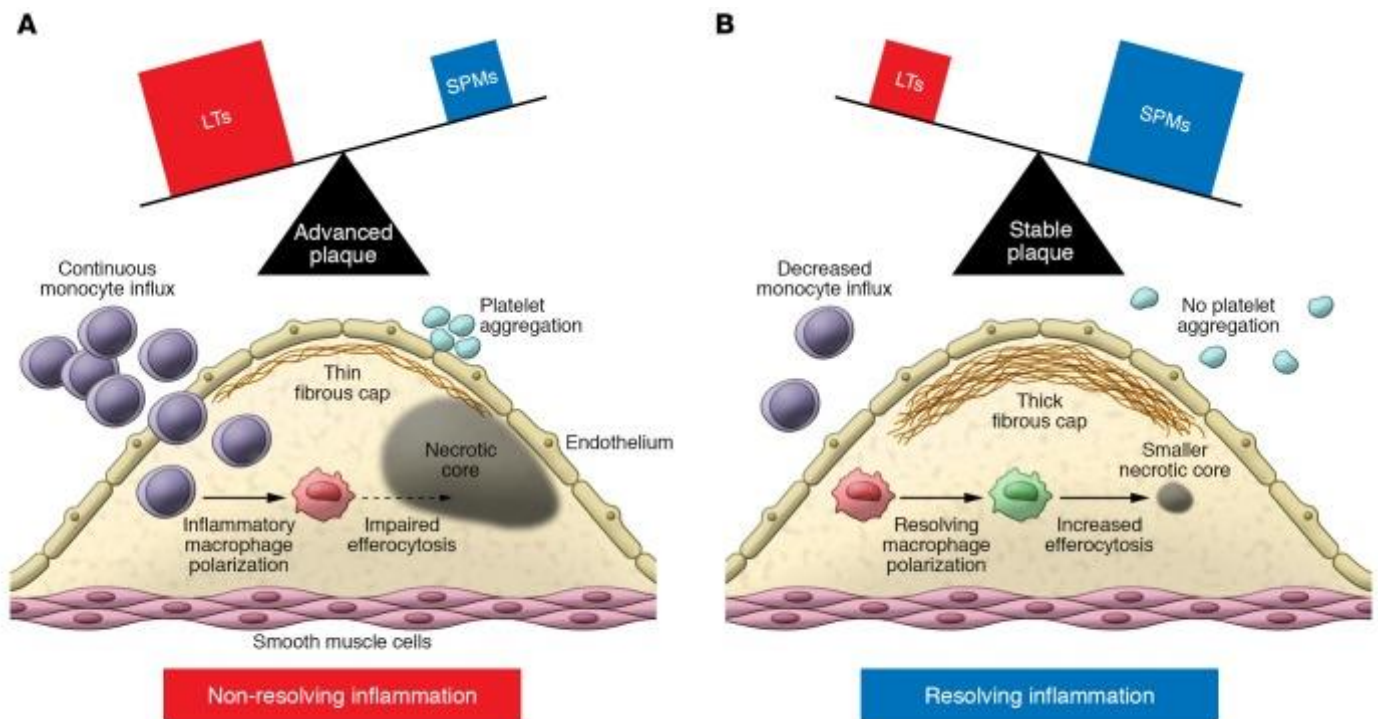


Figure 5: The imbalance between lipid mediators can promote instability of atherosclerotic plaques. In an environment where the amount of leukotrienes is greater than the amount of SPMs (A), unresolved inflammation is observed, resulting in the unstable atherosclerotic plaques. But when the amount of SPMs is greater than leukotrienes, the atherosclerotic plaque tends to be stable, where there is greater polarization of M2 macrophages, increased efferocytosis and resolution of inflammation. Adapted from Kasikara et al. (2018).

Therefore, providing substrates to increase the amount of SPMs at the site of atherosclerotic lesion may be promising for the treatment of cardiovascular diseases, both for stabilization and regression of atherosclerotic plaques.

2.4 Nanotechnology applied for bioactive compounds delivery

Nanotechnology has been applied as a very important and effective tool in several areas of science. The delivery and controlled release of drugs and bioactive compounds can be considered a frontier between science and technology, involving a multidisciplinary scientific approach and contributing significantly for human health (GALISTEO-GONZÁLEZ et al., 2018).

In the same way that it has been done with drugs, bioactive compounds could be incorporated into nanocarriers and driven to the target tissue by the functionalization of the carrier surface. This functionalization can be achieved by linkers that promote recognition and specific cell binding, increasing the specificity of the treatment (OLIVEIRA et al., 2018). In this context, functionalized nanocarriers can accumulate in specific tissues or organs due to a variety of factors, such as barrier permeability or tissue damage, delivering the bioactive compound in its original structure to the target cells (SONVICO et al., 2018).

Regarding the functionalization, the conjugation of bioactive compounds in carriers with antibodies, that bind specifically to receptors exposed on the endothelial surface, is a possible pathway for this important pharmaceutical goal (BHOWMICK et al., 2012). Among the specific targets, the PECAM-1 represents an interesting option. PECAM-1 has a molecular mass of 130 kDa being about 40% carbohydrate (**Figure 6**), that confers lectin-like properties (LERTKIAMONJKOL et al., 2016).

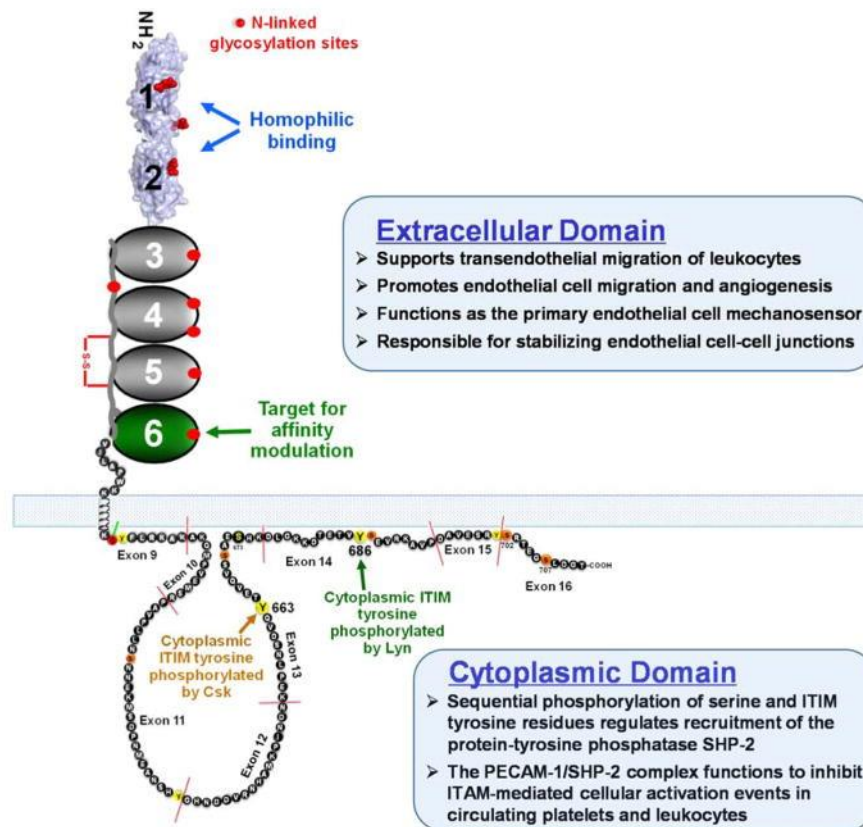


Figure 6: Schematic diagram of PECAM-1 (Adapted from Paddock et al., 2016).

Studies using antibodies specific for PECAM-1 inhibited tumor-induced angiogenesis *in vivo* (CAO et al., 2002; ZHOU et al., 1999). It has been also reported the ability of PECAM-1 to maintain vascular integrity during inflammation-induced activation, contributing to the endothelial cell permeability barrier (LERTKIAMONJKOL et al., 2016).

According to Moore & Tabas (2011), therapy directed at the arterial wall in general and macrophages in particular, could be additive or synergistic with realistic goals of apoB-LP lowering. Local delivery of pro-efferocytic therapies, as target nanoparticles, may prove be highly effective and could have a superior safety profile (KOJIMA et al., 2017). Friedman et al. (2015) administrated a collagen IV-target nanoparticles containing Ac2-26 peptide, a mimic of the pro-resolving annexin A1, to fat-fed LDL^{r(-/-)} mice and observed a suppression of oxidative stress and a decrease of necrosis in the plaques.

Thus, considering that an inflammatory environment adversely influences the prognosis and treatment of patients with atherosclerosis, the administration of anti-inflammatory bioactive compounds, such as docosahexaenoic acid (DHA) as part of a vectorized nanocapsule, seems to be an interesting strategy.

3. OBJECTIVE

The objective of this study was to develop a nanocapsule vectorized with anti-Pecam-1 containing richer DHA algae oil within its lipid nucleus and evaluate its safety and *in vitro* anti-inflammatory effects in macrophages.

4. DESCRIPTION OF CHAPTERS

This study was divided into two chapters. Chapter one brings the overcome of our first challenge that was to develop a stable nanocapsule containing algae oil within its lipid core. This first chapter was published in the “*European Journal of Pharmaceutics and Biopharmaceutics*” and describe the synthesis, characterization and preliminary toxicity evaluation of nanoparticles. In the second chapter, the functionalized nanocapsules had their toxicity evaluated in three cell’s models (HUVEC, U-937 and RAW 264.7) and their internalization and anti-inflammatory effects determined in macrophages. This second part was already submitted to publication.

REFERENCES

ADAY, Aaron W.; RIDKER, Paul M. Antiinflammatory therapy in clinical care: the CANTOS trial and beyond. **Frontiers in cardiovascular medicine**, v. 5, p. 62, 2018.

ALLAIRE, Janie et al. Randomized, crossover, head-to-head comparison of EPA and DHA supplementation to reduce inflammation markers in men and women: the Comparing EPA to DHA Study. **Am J Clin Nutr**, v. 104, n. 2, p. 280-7, 2016.

ANTONOW, Michelli B. et al. Arginylglycylaspartic acid-surface-functionalized doxorubicin-loaded lipid-core nanocapsules as a strategy to target alpha (V) beta (3) integrin expressed on tumor cells. **Nanomaterials**, v. 8, n. 1, p. 2, 2017.

BAKER, Ella J. et al. Omega-3 fatty acids and leukocyte-endothelium adhesion: Novel anti-atherosclerotic actions. **Molecular Aspects of Medicine**, v. 64, p. 169-181, 2018.

BENJAMIN, Emelia J. et al. Heart disease and stroke statistics—2019 update: a report from the American Heart Association. **Circulation**, v. 139, n. 10, p. e56-e528, 2019.

BHOWMICK, Tridib et al. Effect of flow on endothelial endocytosis of nanocarriers targeted to ICAM-1. **Journal of Controlled Release**, v. 157, n. 3, p. 485-492, 2012.

BRENNAN, Eoin et al. Pro-resolving lipid mediators: Regulators of inflammation, metabolism and kidney function. **Nature Reviews Nephrology**, v. 17, n. 11, p. 725-739, 2021.

CALDER, Philip C. Is increasing microbiota diversity a novel anti-inflammatory action of marine n-3 fatty acids?. **The Journal of Nutrition**, v. 149, n. 7, p. 1102-1104, 2019.

CALDER, Philip C. Mechanisms of action of (n-3) fatty acids. **The Journal of nutrition**, v. 142, n. 3, p. 592S-599S, 2012.

CALDER, Philip C. Omega-3 polyunsaturated fatty acids and inflammatory processes: nutrition or pharmacology?. **British journal of clinical pharmacology**, v. 75, n. 3, p. 645-662, 2013.

CALIGIURI, Giuseppina. CD31 as a therapeutic target in atherosclerosis. **Circulation Research**, v. 126, n. 9, p. 1178-1189, 2020.

CAO, Gaoyuan et al. Involvement of human PECAM-1 in angiogenesis and in vitro endothelial cell migration. **American Journal of Physiology-Cell Physiology**, v. 282, n. 5, p. C1181-C1190, 2002.

CHANG, Hae Y. et al. Docosahexaenoic acid induces M2 macrophage polarization through peroxisome proliferator-activated receptor γ activation. **Life sciences**, v. 120, p. 39-47, 2015.

CHISTIakov, Dimitry A. et al. Paraonase and atherosclerosis-related cardiovascular diseases. **Biochimie**, v. 132, p. 19-27, 2017.

DAVID, Samuel; LÓPEZ-VALES, Rubén. Bioactive lipid mediators in the initiation and resolution of inflammation after spinal cord injury. **Neuroscience**, v. 466, p. 273-297, 2021.

DING, Bi-Sen et al. Prophylactic thrombolysis by thrombin-activated latent prourokinase targeted to PECAM-1 in the pulmonary vasculature. **Blood, The Journal of the American Society of Hematology**, v. 111, n. 4, p. 1999-2006, 2008.

DJURICIC, Ivana; CALDER, Philip C. Beneficial outcomes of omega-6 and omega-3 polyunsaturated fatty acids on human health: an update for 2021. **Nutrients**, v. 13, n. 7, p. 2421, 2021.

FREDMAN, Gabrielle et al. An imbalance between specialized pro-resolving lipid mediators and pro-inflammatory leukotrienes promotes instability of atherosclerotic plaques. **Nature communications**, v. 7, n. 1, p. 1-11, 2016.

FREDMAN, Gabrielle et al. Targeted nanoparticles containing the proresolving peptide Ac2-26 protect against advanced atherosclerosis in hypercholesterolemic mice. **Science translational medicine**, v. 7, n. 275, p. 275ra20-275ra20, 2015.

FREDMAN, Gabrielle; MACNAMARA, Katherine C. Atherosclerosis is a major human killer and non-resolving inflammation is a prime suspect. **Cardiovascular Research**, v. 117, n. 13, p. 2563-2574, 2021.

FULLERTON, James N.; GILROY, Derek W. Resolution of inflammation: a new therapeutic frontier. **Nature reviews Drug discovery**, v. 15, n. 8, p. 551-567, 2016.

GALISTEO-GONZÁLEZ, F. et al. Albumin-covered lipid nanocapsules exhibit enhanced uptake performance by breast-tumor cells. **Colloids and Surfaces B: Biointerfaces**, v. 165, p. 103-110, 2018.

GORDON, Siamon; MARTINEZ, Fernando O. Alternative activation of macrophages: mechanism and functions. **Immunity**, v. 32, n. 5, p. 593-604, 2010.

GROSSO, Giuseppe et al. Anti-Inflammatory Nutrients and Obesity-Associated Metabolic-Inflammation: State of the Art and Future Direction. **Nutrients**, v. 14, n. 6, p. 1137, 2022.

HALADE, Ganesh V.; LEE, Dae H. Inflammation and resolution signaling in cardiac repair and heart failure. **EBioMedicine**, v. 79, p. 103992, 2022.

HU, Dan et al. Targeting macrophages in atherosclerosis. **Current Pharmaceutical Biotechnology**, v. 22, n. 15, p. 2008-2018, 2021.

JOFFRE, Corinne et al. N-3 polyunsaturated fatty acids and their derivatives reduce neuroinflammation during aging. **Nutrients**, v. 12, n. 3, p. 647, 2020.

KARUNAKARAN, Denuja; RAYNER, Katey J. Macrophage miRNAs in atherosclerosis. **Biochimica et Biophysica Acta (BBA)-Molecular and Cell Biology of Lipids**, v. 1861, n. 12, p. 2087-2093, 2016.

KASIKARA, Canan et al. The role of non-resolving inflammation in atherosclerosis. **The Journal of clinical investigation**, v. 128, n. 7, p. 2713-2723, 2018.

KAWANO, Aki et al. Docosahexaenoic acid enhances M2 macrophage polarization via the p38 signaling pathway and autophagy. **Journal of cellular biochemistry**, v. 120, n. 8, p. 12604-12617, 2019.

KOJIMA, Yoko; WEISSMAN, Irving L.; LEEPER, Nicholas J. The role of efferocytosis in atherosclerosis. **Circulation**, v. 135, n. 5, p. 476-489, 2017.

KRISHNAN-SIVADOSS, Indumathi et al. Heat shock protein 60 and cardiovascular diseases: An intricate love-hate story. **Medicinal Research Reviews**, v. 41, n. 1, p. 29-71, 2021.

LERTKIATMONGKOL, Panida et al. Endothelial functions of PECAM-1 (CD31). **Current opinion in hematology**, v. 23, n. 3, p. 253, 2016.

LI, Min et al. Programmed cell death in atherosclerosis and vascular calcification. **Cell Death & Disease**, v. 13, n. 5, p. 1-13, 2022.

LIBBY, Peter et al. Inflammation in atherosclerosis: from pathophysiology to practice. **Journal of the American college of cardiology**, v. 54, n. 23, p. 2129-2138, 2009.

LIBBY, Peter. Inflammation during the life cycle of the atherosclerotic plaque. **Cardiovascular Research**, v. 117, n. 13, p. 2525-2536, 2021.

LIBBY, Peter. Inflammation in atherosclerosis—no longer a theory. **Clinical chemistry**, v. 67, n. 1, p. 131-142, 2021.

LIBBY, Peter; EVERETT, Brendan M. Novel antiatherosclerotic therapies. **Arteriosclerosis, thrombosis, and vascular biology**, v. 39, n. 4, p. 538-545, 2019.

MALIK, Ihtzaz A. et al. Role of PECAM-1 in radiation-induced liver inflammation. **Journal of cellular and molecular medicine**, v. 19, n. 10, p. 2441-2452, 2015.

MANTOVANI, Antonio S. et al. Macrophage plasticity and polarization: in vivo veritas. **The Journal of clinical investigation**, v. 122, n. 3, p. 787-795, 2012.

MIGLIACCIO, Silvia et al. Environmental Contaminants Acting as Endocrine Disruptors Modulate Atherogenic Processes: New Risk Factors for Cardiovascular Diseases in Women?. **Biomolecules**, v. 12, n. 1, p. 44, 2021.

MOORE, Kathryn J.; TABAS, Ira. The cellular biology of macrophages in atherosclerosis. **Cell**, v. 145, n. 3, p. 341, 2011.

MOORE, Kathryn J.; SHEEDY, Frederick J.; FISHER, Edward A. Macrophages in atherosclerosis: a dynamic balance. **Nature Reviews Immunology**, v. 13, n. 10, p. 709-721, 2013.

NOVAK, Margaret L.; KOH, Timothy J. Macrophage phenotypes during tissue repair. **Journal of leukocyte biology**, v. 93, n. 6, p. 875-881, 2013.

OTSUKA, Fumiya et al. Natural progression of atherosclerosis from pathologic intimal thickening to late fibroatheroma in human coronary arteries: a pathology study. **Atherosclerosis**, v. 241, n. 2, p. 772-782, 2015.

OLIVEIRA, Jessica F. A. et al. Dual functionalization of nanoparticles for generating corona-free and noncytotoxic silica nanoparticles. **ACS Applied Materials & Interfaces**, v. 10, n. 49, p. 41917-41923, 2018.

PADDOCK, Cathy et al. Structural basis for PECAM-1 homophilic binding. **Blood, The Journal of the American Society of Hematology**, v. 127, n. 8, p. 1052-1061, 2016.

PATEL, Ravi B. et al. Circulating Vascular Cell Adhesion Molecule-1 and Incident Heart Failure: The Multi-Ethnic Study of Atherosclerosis (MESA). **Journal of the American Heart Association**, v. 9, n. 22, p. e019390, 2020.

RAHMAN, Karishma et al. Inflammatory Ly6C hi monocytes and their conversion to M2 macrophages drive atherosclerosis regression. **The Journal of clinical investigation**, v. 127, n. 8, p. 2904-2915, 2017.

REN, Jun et al. Endoplasmic reticulum stress and unfolded protein response in cardiovascular diseases. **Nature Reviews Cardiology**, v. 18, n. 7, p. 499-521, 2021.

RIDKER, Paul M. et al. Inhibition of interleukin-1 β by canakinumab and cardiovascular outcomes in patients with chronic kidney disease. **Journal of the American College of Cardiology**, v. 71, n. 21, p. 2405-2414, 2018.

ROY, Payel; ORECCHIONI, Marco; LEY, Klaus. How the immune system shapes atherosclerosis: roles of innate and adaptive immunity. **Nature reviews Immunology**, v. 22, n. 4, p. 251-265, 2022.

SALVAYRE, Robert; NEGRE-SALVAYRE, Anne; CAMARÉ, Caroline. Oxidative theory of atherosclerosis and antioxidants. **Biochimie**, v. 125, p. 281-296, 2016.

SERHAN, Charles N. Resolution phase of inflammation: novel endogenous anti-inflammatory and proresolving lipid mediators and pathways. **Annu. Rev. Immunol.**, v. 25, p. 101-137, 2007.

SHEMESH, Elad; ZAFRIR, Barak. Hypertriglyceridemia-related pancreatitis in patients with type 2 diabetes: links and risks. **Diabetes, metabolic syndrome and obesity: targets and therapy**, v. 12, p. 2041, 2019.

SHIBABAW, Tewodros. Omega-3 polyunsaturated fatty acids: anti-inflammatory and anti-hypertriglyceridemia mechanisms in cardiovascular disease. **Molecular and Cellular Biochemistry**, v. 476, n. 2, p. 993-1003, 2021.

SHUVAEV, Vladimir V. et al. Anti-inflammatory effect of targeted delivery of SOD to endothelium: mechanism, synergism with NO donors and protective effects in vitro and in vivo. **PLoS One**, v. 8, n. 10, p. e77002, 2013.

SONVICO, Fabio et al. Surface-modified nanocarriers for nose-to-brain delivery: from bioadhesion to targeting. **Pharmaceutics**, v. 10, n. 1, p. 34, 2018.

SPITE, Matthew; CLÀRIA, Joan; SERHAN, Charles N. Resolvins, specialized proresolving lipid mediators, and their potential roles in metabolic diseases. **Cell metabolism**, v. 19, n. 1, p. 21-36, 2014.

STEVENS, Hazel Y. et al. PECAM-1 is a critical mediator of atherosclerosis. **Disease models & mechanisms**, v. 1, n. 2-3, p. 175-181, 2008.

THOTA, Rohith N. et al. Science behind the cardio-metabolic benefits of omega-3 polyunsaturated fatty acids: Biochemical effects vs. clinical outcomes. **Food & function**, v. 9, n. 7, p. 3576-3596, 2018.

TURPIN, Chloé et al. Erythrocytes: Central actors in multiple scenes of atherosclerosis. **International Journal of Molecular Sciences**, v. 22, n. 11, p. 5843, 2021.

VELLIDO-PEREZ, J. A. et al. Novel emulsions-based technological approaches for the protection of omega-3 polyunsaturated fatty acids against oxidation processes—A comprehensive review. **Food Structure**, v. 27, p. 100175, 2021.

VON-HEGEDUS, Johannes H. et al. Toll-like receptor signaling induces a temporal switch towards a resolving lipid profile in monocyte-derived macrophages. **Biochimica et Biophysica Acta (BBA)-Molecular and Cell Biology of Lipids**, v. 1865, n. 9, p. 158740, 2020.

XIA, Xiao-Dan et al. Myocardin: a novel player in atherosclerosis. **Atherosclerosis**, v. 257, p. 266-278, 2017.

YURDAGUL, Arif J. R. et al. Mechanisms and consequences of defective efferocytosis in atherosclerosis. **Frontiers in cardiovascular medicine**, v. 4, p. 86, 2018.

ZHOU, Zhao et al. Antibody against murine PECAM-1 inhibits tumor angiogenesis in mice. **Angiogenesis**, v. 3, n. 2, p. 181-188, 1999.

WASSERMAN, Aaron H.; VENKATESAN, Manigandan; AGUIRRE, Aitor. Bioactive lipid signaling in cardiovascular disease, development, and regeneration. **Cells**, v. 9, n. 6, p. 1391, 2020.

CHAPTER I: DOCOSAHEXAENOIC ACID NANOENCAPSULATED WITH ANTI-PECAM-1 AS CO-THERAPY FOR ATHEROSCLEROSIS REGRESSION

<https://doi.org/10.1016/j.ejpb.2020.12.016>

Contents lists available at [ScienceDirect](https://www.sciencedirect.com)

European Journal of Pharmaceutics and Biopharmaceutics

journal homepage: www.elsevier.com/locate/ejpb

Docosahexaenoic acid nanoencapsulated with anti-PECAM-1 as co-therapy for atherosclerosis regression

Matheus de Castro Leão^a, Adriana Raffin Pohlmann^b, Aline de Cristo Soares Alves^b, Sandra Helena Poliselli Farsky^d, Mayara Klimuk Uchiyama^e, Koiti Araki^e, Silvana Sandri^d, Silvia Stanisquaski Guterres^c, Inar Alves Castro^{a,*}

^a LADAF, Department of Food and Experimental Nutrition, Faculty of Pharmaceutical Sciences, University of São Paulo, São Paulo, Brazil

^b Department of Organic Chemistry, Institute of Chemistry, Federal University of Rio Grande do Sul, Porto Alegre, RS, Brazil

^c Department of Production and Drugs Control, Pharmaceutical Faculty, Federal University of Rio Grande do Sul, Porto Alegre, RS, Brazil

^d Department of Clinical & Toxicological Analyses, School of Pharmaceutical Sciences, University of São Paulo, Grande do Sul, Porto Alegre, RS, Brazil

^e Department of Fundamental Chemistry, Institute of Chemistry, University of São Paulo, Brazil

ARTICLE INFO

Keywords:

Atherosclerosis

DHA

Anti-PECAM-1

Nanocapsule

Omega 3 fatty acids

Tissue target

CD31

ABSTRACT

Atherosclerosis is a non-resolving inflammatory condition that underlies major cardiovascular diseases. Recent clinical trial using an anti-inflammatory drug has shown a reduction of cardiovascular mortality, but increased the susceptibility to infections. For this reason, tissue target anti-inflammatory therapies can represent a better option to regress atherosclerotic plaques. Docosahexaenoic acid (DHA) is a natural omega 3 fatty acid component of algae oil and acts as a precursor of several anti-inflammatory compounds, such as the specialized proresolving lipid mediators (SPMs). During the atherosclerosis process, the inflammatory condition of the endothelium leads to the higher expression of adhesion molecules, such as Endothelial Cell Adhesion Molecule Plate 1 (PECAM-1 or CD31), as part of the innate immune response. Thus, the objective of this study was to develop lipid-core nanocapsules with DHA constituting the nucleus and anti-PECAM-1 on their surface and drive this structure to the inflamed endothelium. Nanocapsules were prepared by interfacial deposition of pre-formed polymer method. Zinc-II was added to bind anti-PECAM-1 to the nanocapsule surface by forming an organo-metallic complex. Swelling experiment showed that the algae oil act as non-solvent for the polymer (weight constant weight for 60 days, $p > 0.428$) indicating an adequate material to produce kinetically stable lipid-core nanocapsules (LNC). Five formulations were synthesized: Lipid-core nanocapsules containing DHA (LNC-DHA) or containing Medium-chain triglycerides (LNC-MCT), multi-wall nanocapsules containing DHA (MLNC-DHA) or containing MCT (MLNC-MCT) and the surface-functionalized (anti-PECAM-1) metal-complex multi-wall nanocapsules containing DHA (MCMN-DHA-a1). All formulations showed homogeneous macroscopic aspects without aggregation. The mean size of the nanocapsules measured by laser diffraction did not show difference among the samples ($p = 0.241$). Multi-wall nanocapsules (MLNC) showed a slight increase in the mean diameter and polydispersity index (PDI) measured by DLS, lower pH and an inversion in the zeta-potential (ζP) compared to LNCs. Conjugation test for anti-PECAM-1 showed 94.80% of efficiency. The mean diameter of the formulation had slightly increased from 160 nm (LNC-DHA) and 162 nm (MLNC-DHA) to 164 nm (MCMN-DHA-a1) indicating that the surface functionalization did not induce aggregation of the nanocapsules. Biological assays showed that the MCMN-DHA-a1 were uptaken by the HUVEC cells and did not decrease their viability. The surface-functionalized (anti-PECAM-1) metal-complex multi-wall nanocapsules containing DHA (MCMN-DHA-a1) can be considered adequate for pharmaceutical approaches.

* Corresponding author at: LADAF (www.ladaf.com.br). Department of Food and Experimental Nutrition, Faculty of Pharmaceutical Sciences, University of São Paulo, Av. Lineu Prestes, 580, B14, 05508-900 São Paulo, Brazil.

E-mail address: inar@usp.br (I. Alves Castro).

<https://doi.org/10.1016/j.ejpb.2020.12.016>

Received 14 July 2020; Received in revised form 26 November 2020; Accepted 15 December 2020

Available online 6 January 2021

0939-6411/© 2020 Elsevier B.V. All rights reserved.

1. Introduction

Nanotechnology has been applied as an important and effective tool in several areas of science. The delivery and controlled release of drugs and bioactive compounds can be considered a frontier between science and technology, involving a multidisciplinary scientific approach and contributing for human health [1]. Nanotechnology can not only improve the efficacy of a drug but also to protect against its adverse effects [2]. Drugs and bioactive compounds can also be incorporated into nanocarriers and driven to the target tissue by the functionalization of the carrier surface [3]. This surface functionalization can be achieved by ligands that promote recognition and specific cell binding, increasing the specificity of the treatment [4]. In this context, functionalized nanocarriers can accumulate in specific tissues due to a variety of factors, such as barrier permeability, tissue damage and pH of the medium, delivering bioactive compounds present in their original structure to the target cells [5].

Omega 3 fatty acids, such as eicosapentaenoic (EPA) and docosahexaenoic (DHA) acids promote cardiovascular protection by different mechanisms, including anti-inflammatory action [6,7]. The consumption of EPA and DHA increases the synthesis of less inflammatory eicosanoids, decreases the synthesis of cytokines via Nuclear factor kappa B (NFκB) and promotes the inflammation resolution through resolvins and protectins [7–9]. In addition, it has been shown that non-enzymatic oxidized metabolite of DHA, 4(RS)-4-F_{4t}-neuroprostane was able to protect I/R cardiac injuries by regulating the mitochondrial homeostasis [10]. Although the reduction of inflammation has been proved to improve cardiovascular protection, as observed in a recent study [11], the systemic aspect can increase the susceptibility to infections. For this reason, anti-inflammatory target molecules could be more efficient to treat some chronic diseases, such as atherosclerosis. Actually, studies about targeting structures to atherosclerosis lesion date to middle eighties [12]. However, despite three decades of advances in terms of multitudes of ligands, nanocarriers, and methodologies for their conjugation and assembly, the translational approach is still incipient because of the high complexity of physiological mechanisms involved in the pathologies, side effects due to enhanced local concentration or harmful interactions of delivery systems with target cells and host defense, among other limitations [13–15].

The Platelet-Endothelial Cell Adhesion Molecule – 1 (PECAM-1 or CD31) is located in the cell junction, being expressed on the surface of several cells involved in the development of atherosclerotic lesions in the injured sites [16,17]. It is a multifunctional cell adhesion molecule involved in numerous physiologic processes [18]. According to Privratsky et al. [19], the pro-atherosclerotic effect of PECAM-1 is related to its participation in a stimulatory complex in endothelial cells. In this complex, PECAM-1 activates NFκB molecules in response to oxidative stress, inducing the expression of more PECAM-1 molecules, which in turn contribute to the recruitment of inflammatory cells to the lesion site. In opposite, PECAM-1 is also related to the maintenance of endothelial integrity and to the extravasation of cells from the blood compartment to adjacent arteries and tissues [20]. In this context, PECAM-1 has been considered a target of several studies that evaluate its role as adhesion molecule in order to recruit drug-bearing particles able to promote stabilizing or regression effects on atherosclerotic lesions [21].

Previous studies have achieved success to deliver anti-inflammatory or anti-oxidant molecules to the endothelium by target nano carriers [22–25]. Considering that an inflammatory environment adversely influences the prognosis and treatment of patients with atherosclerosis, the delivery of anti-inflammatory bioactive compound, such as docosahexaenoic acid (DHA) to the inflamed endothelium, can be an interesting strategy. Thus, our objective was to develop a stable anti-PECAM-1 antibody surface-functionalized nanocapsule containing DHA as algae oil in the core. The nanocapsules were physically characterized and their preliminary biological effects analyzed in human

umbilical vein endothelial cells (HUVEC).

2. Materials and methods

2.1. Materials

Poly(ϵ -caprolactone) (PCL, Mw = 14,000 g mol⁻¹), sorbitan monostearate (SM, Span 60®), zinc acetate, low molecular weight chitosan (Mw: 50,000–190,000 g mol⁻¹, deacetylation degree: 75–85%, viscosity: 20,000 cP) and Polysorbate 80 (Tween 80®) were purchased from Sigma-Aldrich Co. (Saint Louis, MO, USA). Lipoid® S75 (LPS75) soybean phosphatidylcholine 75% pure was obtained from Gerbras Química Farmacêutica Ltda. (Diadema, Brazil). Algae oil (DHASCO) was generously donated by Sorocaps Indústria Farmacêutica Ltda (Sorocaba, Brazil), while MCT was purchased from Nutrimed Ind. Ltda (São Paulo, Brazil). Anti-CD31 antibody (500 μ L, primary antibodies, rabbit, standard, ICC/IF, IHC-FoFr, IHC-Fr, IHC-P, WB) was purchased from Biologend (San Diego, CA, USA). All aqueous solutions were prepared using deionized water obtained from a Millipore Direct-Q® system (Merck Millipore, Darmstadt, Germany). The solvents and reagents were HPLC grade.

2.2. Methods

2.2.1. Characterization of the oils applied in the lipid-core of the nanocapsules

Algae oil and MCT were characterized according to the fatty acids composition [26], using a gas chromatography equipped with a G3243A MS detector (Agilent 7890 A GC System, Agilent Technologies Inc., Santa Clara, USA). The oxidative stability of the original algae oil and MCT was measured by the concentration of hydroperoxides [27] and expressed as mEq O₂/kg oil. Malondialdehyde (MDA) concentration was determined, using a HPLC system (Agilent Technologies 1200 Series), with a Phenomenex reverse-phase C18 analytical column (250 mm \times 4.6 mm, 5 μ m) and a LC8-D8 pre-column (Phenomenex AJ0 – 1287), being fluorometrically quantified at excitation of 515 nm and emission of 553 nm [28]. A standard curve was prepared using Tetraethoxypropane and results were expressed as mg/Kg oil. The tocopherol content was also determined using a high performance liquid chromatography [29] and the results expressed as mg/Kg oil.

2.2.2. Synthesis of the anti-PECAM-1-Surface-Functionalized Metal-Complex Multi-Wall nanocapsules (MCMN)

The effect of algae oil on PCL films was determined using the swelling test [30]. It was conducted, in parallel, the PCL swelling in MCT to comparative purposes. PCL solution were prepared by dissolving 3.0 g of the PCL in 30 mL of chloroform, maintaining the solution under magnetic stirring at 40 °C for 30 min. After solubilization, the solution was stored for 5 days at room temperature for complete evaporation of the solvent. The films were trimmed, weighed and completely immersed in 2 mL of algae oil or MCT, separately. After 0, 3, 7, 11, 30 and 60 days of immersion, the films were carefully removed from the oil, dried with filter paper and weighed in an analytical balance. After this initial test, the nanocapsules were prepared by interfacial deposition of pre-formed polymer method [31], as schematized in Fig. 1. To prepare the organic solution (A), SM (0.040 g), PCL (0.100 g) and algae oil or MCT (120 μ L) were dissolved in acetone (25 mL). Another organic solution (B), was prepared mixing 5 mL of ethanol with LPS75 (0.090 g). Both organic solutions A and B were kept under magnetic stirring at 40 °C for 1 h. Then, solution B was added to solution A and kept under agitation at 40 °C for 1 h. A new aqueous solution (C) was prepared mixing distilled water (60 mL) with 0.080 g of nonionic surfactant Tween 80 for 1 h at 40 °C. After, the final organic solution (A + B) was injected into the aqueous solution (C) and stirred for 10 min. The new solution (D) was transferred to a rotary evaporator under reduced pressure and concentrated at 40 °C. The final volume of this formulation (lipid-core

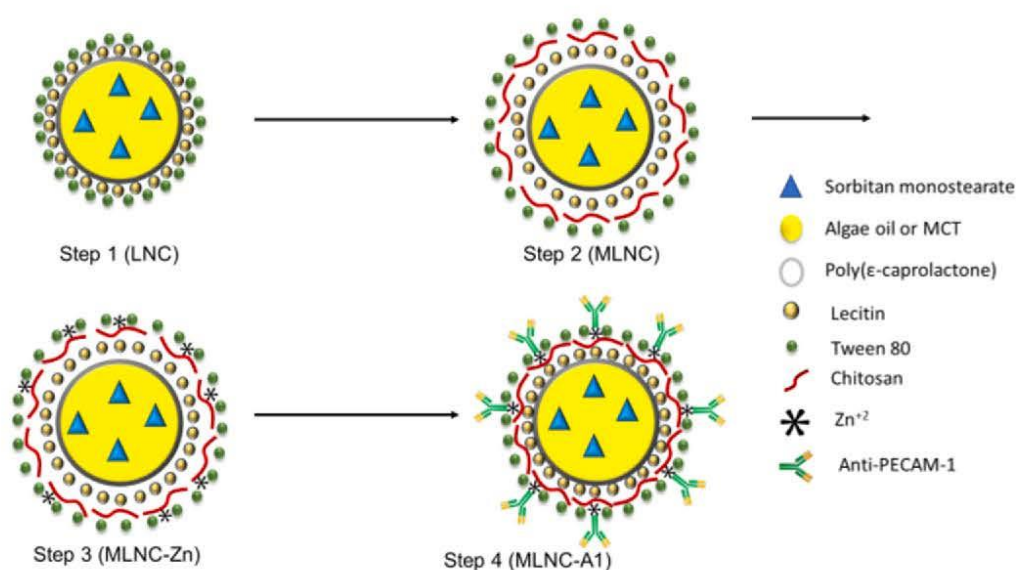


Fig. 1. Steps for the synthesis of the Anti-PECAM-1 Surface-Functionalized Metal-Complex Multi-Wall Nanocapsules. LNC: Lipid Core nanocapsule; MLNC: Multi-wall Lipid Core Nanocapsule; MLNC-Zn: Multi-wall metal complex Lipid Core Nanocapsule, and MLNC-a1: Multi-wall metal complex lipid core with Anti-PECAM-1 nanocapsule.

nanocapsules in aqueous dispersion, LNC) was transferred to a volumetric flask and adjusted to 10 mL using ultrapure water (Fig. 1, Step 1). After 24 h, 500 μL of a filtered (0.45 μm , Millipore, Merck Millipore, Darmstadt, Germany) chitosan aqueous solution (0.3%) was manually pipetted (1 drop every 10 s) in 4.5 mL of the solution D and the reaction was kept under magnetic stirring for 2 h (Fig. 1, Step 2). After, a zinc-II solution (E) was prepared by dissolving 28 mg of zinc acetate in ultrapure water (10 mL). Then, in an amber flask, 25 μL of solution E was added into 775 μL of the chitosan-coated lipid-core nanocapsules solution under magnetic stirring at 500 rpm (Fig. 1, Step 3). After 40 s, 200 μL of anti-PECAM-1 solution was added into the same solution under magnetic stirring (Fig. 1, Step 4). The complex “anti-PECAM-1-Zn-chitosan-coated lipid-core nanocapsules” was kept under agitation (500 rpm) for 20 min at room temperature (20 $^{\circ}\text{C}$). The theoretical concentration of anti-PECAM-1 in the formulation was 200 $\mu\text{g mL}^{-1}$. In the complete assay, five samples were prepared: LNC-DHA; MLNC-DHA; LNC-MCT; MLNC-MCT. Three replicates were prepared of each formulation.

2.2.3. Physicochemical characterization of the nanocapsules

2.2.3.1. Laser diffraction. The particle size distribution of the formulations was measured by laser diffraction (LD) using a Mastersizer® 2000 (Malvern Instrumens Ltd., UK) in the size range from 0.02 to 2000 μm . Each sample was inserted into the dispersion unit containing of 100 to 200 mL of distilled water, sufficient to achieve obscuration between 1 and 8%. The Mie theory was used to determine the volume-weighted mean diameter [Eq. (1)]:

$$D_{4,3} = \frac{\sum d_i^4}{\sum d_i^3} \quad (1)$$

where i is an index of the population and d_i is the particle diameter of the population i . The polydispersity was calculated as SPAN based on the particle size distribution curve (Eq. (2)). The narrower the distribution the smaller the polydispersity.

$$SPAN = \frac{d(0.9) - d(0.1)}{d(0.5)} \quad (2)$$

where $d(0.1)$, $d(0.5)$ and $d(0.9)$ are the diameters at the percentiles 10, 50 and 90 of the cumulative size distribution based on the volume of

particles. The specific surface area (SSA) was determined by the Mastersizer software considering the density of 1 g cm^{-3} for the nanocapsules.

2.2.3.2. Photon correlation spectroscopy (PCS). The particle size distribution curve, mean hydrodynamic diameter and polydispersity index (PDI) of all formulations were determined by photon correlation spectroscopy (PCS) using a Zetasizer® Nano ZS (Malvern Instrumens Ltd., UK). Each sample was diluted (500x) in ultrapure water (MilliQ®) filtered (Millipore®, 0,45 μm).

Zeta Potential (ζP)

The zeta potential of all formulations was determined by electrophoretic mobility determined (Zetasizer® Nano ZS, Malvern Instrumens Ltd., UK). Each sample was diluted (500x) in a previously filtered (Millipore®, 0,45 μm) 10 mmol L^{-1} NaCl aqueous solution.

2.2.3.3. Nanocapsule Tracking analysis (NTA). The size distribution measurement and the concentration of the formulations containing DHA were determined by NTA (NanoSight LM10 & NTA 2.0 Analytical Software, NanoSight Ltd). The latter also provided visual information of the light scattered by the particle in solution. The video images of the light scattered by the particle in Brownian motion were followed in real-time in a CCD camera [31]. The formulations were diluted 10,000 times in ultrapure water and each video clip was captured over 60 s. NTA 2.0 Analytical Software (NanoSight®) was used for calculations.

2.2.3.4. pH measurements. The pH value of the formulations was measured in a potentiometer (DM-22, Digimed, Brazil) calibrated with phosphate buffer (pH 4.01 and pH 6.86) in each sample without previous dilution. The measurements were obtained with sensitivity $\geq 99\%$.

2.2.3.5. Transmission electron microscopy (TEM). The formulations were submitted to morphological analysis through a transmission electron microscope operating at 80 kV. Nanocapsule samples (100 μL) were diluted in water (1:10, v/v), and 10 μL of the dilution was deposited on copper grids (400 mesh) coated with carbon films. Subsequently, a negative contrast (2% uranyl acetate solution) was added to the grid and kept in a vacuum desiccator for 24 h. Photomicrographs were later performed by trained technicians.

2.2.3.6. Quantification of anti-PECAM-1 bound to the nanocapsules. The

yield of anti-PECAM-1 complexation on the nanocapsule surface was determined by an indirect method. The non-bound fraction of anti-PECAM-1 in the formulations was quantified by a colorimetric method (QuantiPro™ BCA Assay Kit, Sigma-Aldrich, St. Louis, MO, USA). According to the manufacturer's instructions, a calibration curve was prepared using dilutions of bovine serum albumin (BSA) and anti-PECAM-1 from 3 to 27 $\mu\text{g mL}^{-1}$. The absorbance of the reaction product was recorded on a plate reader at 562 nm (Spectramax, Molecular Devices, Sunnyvale, CA, USA) where the correlation index was 0.9917. To isolate the non-bound fraction of anti-PECAM-1, the MLNC-DHA-A1 formulation was placed in ultrafiltration-centrifugation units (100 kDa; Merck KGaA), and centrifuged at 1,840 $\times\text{g}$ during 5 min (Sigma® 1–14; SIGMA Laborzentrifugen GmbH, Germany). The ultrafiltrate was evaluated using the colorimetric method and the antibody concentration determined using the calibration curve.

2.2.4. Biological assays

2.2.4.1. Human umbilical vein endothelial cells. Human umbilical vein endothelial cells (HUVEC), kindly donated by Professor Ana Campa of the Department of Clinical and Toxicological Analysis (Faculty of Pharmaceutical Sciences, University of São Paulo, Brazil) were cultured in Roswell Park Memorial Institute 1640 (RPMI 1640; Gibco) containing 10% of fetal bovine serum (Gibco, CA) and 1% penicillin and streptomycin solution (Gibco). Cells were maintained at 37 °C under 5% CO_2 atmosphere. Before the experiments, the HUVEC cells were characterized by endothelial markers such as the platelet endothelial cell adhesion molecule and von Willebrand factor.

2.2.4.2. In vitro uptake cell. The internalization of LNC-DHA, MLNC-DHA and MLNC-DHA-a1 by HUVECs was evaluated by enhanced dark-field hyperspectral microscopy. HUVECs (8×10^4 cells) were seeded in extra clean dust-free Nexterion® Glass D coverslips (#D263T; Schott, New York, NY, USA) present in 6-well plates (Corning, NY, USA). After adherence, cells were incubated with medium containing LNC-DHA (1.4×10^{11} nanoparticles/mL); MLNC-DHA (1.4×10^{11} nanoparticles/mL) or MLNC-DHA-a1 ($1.65 \mu\text{g/mL}$ of a 1.4×10^{11} nanoparticles/mL) for 18 h at 37 °C under 5% CO_2 atmosphere. A control group was maintained in the presence of culture medium (vehicle). Immediately after the incubation and washing four times with 5% FBS-PBS, the coverslip was placed on extra clean dust-free Nexterion® Glass B slides containing 10 μL of 5% FBS-PBS, and HUVECs were imaged using a CytoViva Ultra Resolution Imaging System (CytoViva, Inc., Auburn, AL, USA). It was mounted on an Olympus BX51 microscope ($\times 1,500$ magnification; Olympus Corporation, Tokyo, Japan) equipped with fluorite 100 \times oil iris 0.6–1.30 numerical aperture (NA) objective and a 75 W Xe light source. Optical images were taken using a Q-imaging Retiga EXi CCD camera (Olympus Corporation, Center Valley, PA, USA) and Dage XL CCD digital camera with Image Processing Software (Dage®; DAGE-MTI of MC, Inc., Michigan City, IN, USA).

2.2.4.3. Cell viability

2.2.4.3.1. Trypan exclusion assay. HUVEC cells were plated into 24-well microtiter plates (Corning, NY, USA) at a density of 2.5×10^4 cells per well. After 24 h, cells were treated with LNC-DHA (0.14; 1.4 and 2.9×10^{11} nanoparticles/mL); MLNC-DHA (0.14; 1.4 and 2.9×10^{11} nanoparticles/mL) or MLNC-DHA-a1 (0.75; 1.65 and $3.3 \mu\text{g/mL}$ of a1; 0.14; 1.4 and 2.9×10^{11} nanoparticles/mL) and cultured for 24 h. Thereafter, cells were detached using trypsin-ethylenediaminetetraacetic acid (Vitrocell, SP, Brazil) and supernatant and cells were recovered in microtube, centrifuged at $1.400 \times\text{g}$ for 5 min and cell pellet was re-suspended with 0.4% Trypan Blue staining solution. Each experiment was performed in duplicate. Cells were counted using a Neubauer chamber. The % cell viability was calculated according to Strober [32]. The relation of viable cells was calculated

based on not treated cells.

2.2.4.3.2. Propidium iodide and Annexin V incorporation. HUVEC cells were plated into 24-well microtiter plates (Corning, costar) at a density of 2.5×10^4 cells per well. After 24 h, cells were treated with LNC-DHA (0.14; 1.4 and 2.9×10^{11} nanoparticles/mL); MLNC-DHA (0.14; 1.4 and 2.9×10^{11} nanoparticles/mL) or MLNC-DHA-a1 (0.75; 1.65 and $3.3 \mu\text{g/mL}$ of a1; 0.14; 1.4 and 2.9×10^{11} nanoparticles/mL) and cultured for 24 h. Thereafter, cells were detached, and supernatant and cells were washed twice in phosphate-buffered saline containing 1% bovine serum albumin. Cells were incubated with Annexin V (previously diluted (1:20) in Annexin V (Life Technologies, Carlsbad, USA) binding buffer (10 mM N-2-hydroxyethylpiperazine-N'-2-ethanesulfonic acid, 140 mM NaCl, 25 mM CaCl_2 , pH 7.4; BD Pharmingen, Franklin Lakes, NJ) during 20 min in the dark, at room temperature. After this, 200 μL Annexin V binding buffer and 0.5 μL propidium iodide (PI; Sigma Aldrich, San Luis, USA) were added. Data from 10,000 events were acquired in Accuri C6 flow cytometer (BD Pharmingen) and the stained cells were analyzed. Data express the percentage of apoptotic cells (AnxV +), necrotic cells (PI +), late apoptotic cells (AnxV + PI +) and viable cells (AnxV – PI –).

2.2.5. Statistical analysis

Results were compared using ANOVA followed by Tukey test or equivalent non-parametric test. Normality and homogeneity of variances were evaluated by Shapiro-Wilk test and Hartley F-max test, respectively. Values were expressed as mean \pm SEM. A p value of 0.05 was adopted to reject the null hypothesis. Calculations will be performed using software Statistica v.13 (TIBCO Software Round Road, TX, USA). Graphs were elaborated using software GraphPad Prism 7 (GraphPad Software, CA, USA).

3. Results

3.1. Characterization of the oils applied in the lipid-core of the nanocapsules

The characterization of the algae oil and MCT applied in the lipid-core of the nanocapsules is shown in Table 1. It was observed that although MCT has presented other fatty acids besides medium chain ones. Major amount was given to sum of caprylic, capric and palmitic acids (94.26%). Algae oil presented 35.13% DHA and low values of oxidative markers.

Table 1
Characterization of the oils applied to form the lipid-core of the nanocapsules.

Fatty acids (%)	Algae Oil	MTC
C8:00	–	41.00 \pm 0.51
C10:00	1.09 \pm 0.02	48.53 \pm 0.26
C12:00	5.68 \pm 0.08	ND
C14:00	16.66 \pm 0.12	ND
C14:1 n9	0.20 \pm 0.01	ND
C16:00	17.28 \pm 0.40	4.73 \pm 0.13
C16:1 n7	1.84 \pm 0.02	0.06 \pm 0.06
C18:00	2.40 \pm 0.20	2.41 \pm 0.27
C18:1 n9	18.69 \pm 0.16	2.32 \pm 0.17
C18:2 n6 (LNA)	1.02 \pm 0.11	0.53 \pm 0.02
C18:3 n6 (GLA)	ND	ND
C18:3 n3 (ALA)	ND	0.43 \pm 0.19
C22:6 n3 (DHA)	35.13 \pm 0.35	ND
Total	100.00	100.00
Hydroperoxide (mEq O₂/Kg oil)	1.36 \pm 0.06	0.25 \pm 0.04
MDA (mg/Kg oil)	32.99 \pm 3.58	ND
α-Tocopherol (mg/Kg oil)	61.59 \pm 1.17	ND
γ-Tocopherol (mg/Kg oil)	17.84 \pm 0.26	ND

ND: Not Detected.

3.2. Development of formulations

3.2.1. Polymer swelling test

In vitro polymer swelling test showed no difference on weight gain (%) of PCL films immersed in the algae oil and MCT during the time ($p < 0.832$) (Fig.S1). This result demonstrated that both oils act as non-solvent for PCL.

3.2.2. Synthesis of the anti-PECAM-1 Surface-Functionalized Metal-Complex Multi-Wall nanocapsules (MCMN).

The metal-complex multi-wall nanocapsules (Fig. 1, Step 3: MLNC-Zn) was formed by a lipid-core (sorbitan monostearate dispersed in algae oil), PCL as the first wall, polysorbate 80 and lecithin as surfactant system to stabilize the nanocapsules in the aqueous dispersion and chitosan as second wall complexed with a metal ion (zinc-II). Zinc-II was selected as metal ion in our formulation due to its biocompatibility. For comparative purposes, LNC-MCT and MLNC-MCT (containing MCT as internal phase) was also prepared. All formulations, prepared using both oils, presented homogeneous macroscopic aspects, with no visible aggregation in the storage vials.

The formulations before and after chitosan coating presented unimodal size distribution curves with diameters exclusively in the nanometric range (Fig.S2). No microaggregate was observed. Narrow size distributions were determined with mean diameters ($D_{4,3}$) ranging from 130 ± 2 nm (LNC-MCT) to 138 ± 2 nm (MLNC-DHA) (Table 2), without difference among the formulations ($p = 0.241$). MLNC-DHA formulation showed a slightly higher SPAN value compared to LNC-MCT ($p = 0.040$). Nevertheless, that formulation had the polydispersity of diameters lower than 1.2 indicating narrow size distribution. All other formulations presented SPAN values lower than 1.0 not differing from each other ($p = 0.040$) (Table 2).

Afterwards, formulations were analyzed by dynamic light scattering (DLS) to characterize their nanometric populations. D_h values ranged from 120 ± 1 (LNC-MCT) to 163 ± 5 nm (MLNC-DHA-a1). LNC-MCT nanocapsules exhibited the lowest mean values ($p < 0.001$) for this variable when compared to the other nanocapsules, while LNC-DHA showed a higher D_h than LNC-MCT. After the chitosan coating, the nanocapsules presented in general a slight increase in D_h comparing to the correspondent formulation without chitosan. The polydispersity index (PDI) indicated respectively narrow and moderate size dispersions for formulations before and after chitosan-coating ($p < 0.001$) (Table 2). Zeta potential (ζ P) was inverted after chitosan coating ($p < 0.001$) (Table 2) indicating the interfacial reaction by electrostatic interactions. LNC-DHA nanocapsule suspension had a slightly lower pH value ($p < 0.001$) when compared to LNC-MCT (Table 2). Chitosan-coated nanocapsule formulations exhibited lower values of pH when compared to the formulations before coating. The pH reduction of the formulations was expected due to the use of acetic acid to disperse chitosan before the interfacial reaction with the nanocapsules. Fig. 2 shows the comparison of LNC-DHA, MLNC-DHA and MLNC-HA-a1 formulations. MLNC-DHA and MLNC-DHA-a1 nanocapsules showed higher values of hydrodynamic mean diameter (Fig. 2A) and PDI (Fig. 2B) than LNC-DHA, while the negative ζ P showed by LNC-DHA sample was inverted after chitosan interfacial reaction (Fig. 2C).

Table 2
Physico-chemical characteristics of the nanocapsules.

Nanocapsules ¹	$D_{4,3}$ (nm)	SPAN	DLS (nm)	PDI	ZP (mV)	pH
LNC-DHA	134.33 ± 1.76	0.98 ± 0.03^{ab}	139.40 ± 1.14^a	0.10 ± 0.01^a	-13.33 ± 0.28^a	5.28 ± 0.02^b
MLNC-DHA	137.67 ± 1.76	1.13 ± 0.05^b	159.12 ± 1.25^b	0.21 ± 0.01^b	$+12.50 \pm 0.95^b$	3.94 ± 0.00^a
MLNC-DHA-a1	ND	ND	163.50 ± 5.33^b	0.21 ± 0.01^b	$+5.00 \pm 0.95^c$	ND
LNC-MCT	130.00 ± 2.00	0.86 ± 0.02^a	119.73 ± 0.71^c	0.14 ± 0.01^a	-12.67 ± 0.33^a	5.40 ± 0.02^c
MLNC-MCT	132.67 ± 3.71	0.96 ± 0.09^{ab}	133.47 ± 0.75^a	0.22 ± 0.01^b	$+13.93 \pm 0.35^b$	3.96 ± 0.01^a
<i>p</i>	0.241	0.040	< 0.001	< 0.001	< 0.001	< 0.001

ND, not determined.

¹ Values are expressed as mean \pm SEM (n = 3). Values followed by the same upperscript letter are not different ($p < 0.05$).

The laser diffraction data were plot in radar charts to compare slight variations in the mean diameter and the diameters at percentiles 10, 50 and 90 under the size distribution curves. Those charts were constructed in 8 axes using the diameters calculated by volume and by number of particles. The radar charts for LNC and MLNC formulations (Fig.S3) revealed almost superimposed profiles indicating that even though some differences in the dispersity were observed, those formulations had very near and almost superimposed size distribution profiles.

Once obtained the algae oil-containing polymeric nanocapsule formulation, the optimal antibody concentration was evaluated by DLS. The anti-PECAM-1 at 200, 300 and 400 $\mu\text{g mL}^{-1}$ concentrations was used in the interfacial reactions (Fig.S4). The DLS size distribution curves were analyzed just after preparation ($t = 0$) and 1 h after ($t = 1$ h). After preparation, DLS curves (by intensity) for the formulations prepared using anti-PECAM-1 at 200 and 300 $\mu\text{g mL}^{-1}$ showed unimodal populations, while DLS curve for the formulation prepared using anti-PECAM-1 at 400 $\mu\text{g mL}^{-1}$ showed microaggregates. After 1 h of preparation, the formulation prepared using anti-PECAM-1 at 300 $\mu\text{g mL}^{-1}$ showed microaggregates. DLS curves expressed by volume of particles were calculated to compared better the formulations just after preparation and after 1 h. The only formulation presenting stable DLS curves was that prepared at 200 $\mu\text{g mL}^{-1}$ of anti-PECAM-1. Thus, 200 $\mu\text{g mL}^{-1}$ was chosen to next steps.

3.2.3. Nanocapsule Tracking analysis (NTA); transmission electron microscopy (TEM) and quantification of anti-PECAM-1 bound to the nanocapsules

Using the Nanocapsule Tracking Analysis (NTA), mean diameters were 160 ± 2 (LNC-DHA) and 164 ± 3 (MLNC-DHA-a1), without difference among the samples ($p = 0.209$) (Table 3). MLNC-DHA-a1 showed a lower ($p < 0.001$) concentration of particles ($1.34 \times 10^{13} \pm 2.20 \times 10^{11}$ particles mL^{-1}) compared with LNC-DHA and MLNC-DHA ($p < 0.001$). A comparison between the size distributions of the diluted formulations before and after the functionalization with anti-PECAM-1 (MLNC-DHA and MLNC-DHA-a1) showed an overlap in 2D plot (diameter vs. intensity of the scattered light) (Fig.S5). TEM photomicrographs (Fig. 3) demonstrated that Anti-PECAM-1-functionalized nanocapsules (MLNC-DHA-a1) presented a spherical shape. After ultrafiltration-centrifugation, the calculated yield of anti-PECAM-1 complexation on the surface of the nanocapsules was $94.8 \pm 3.3\%$. It was estimated around 100 molecules of anti-PECAM-1/nanocapsule, based on molar mass of the antibody, the Avogadro number to calculate the number of nanocapsules and NTA data.

3.2.4. Biological assays

3.2.4.1. Nanocapsules up-take by endothelial cells and cell viability. After physicochemical properties evaluation, the ability of endothelial cells to internalize the synthesized nanocapsules was verified by CytoViva® DARKFIELD ULTRA microscopy (Fig. 4A). HUVECs were incubated with LNC-DHA, MLNC-DHA and MLNC-DHA-a1 at concentration of 1.4×10^{11} nanoparticles/mL, and with the isolated PECAM antibody as control, and cultured for 18 h. As observed in the Fig. 4A, MLNC-DHA-a1 was efficiently uptaken by endothelial cells in comparison to LNC-DHA

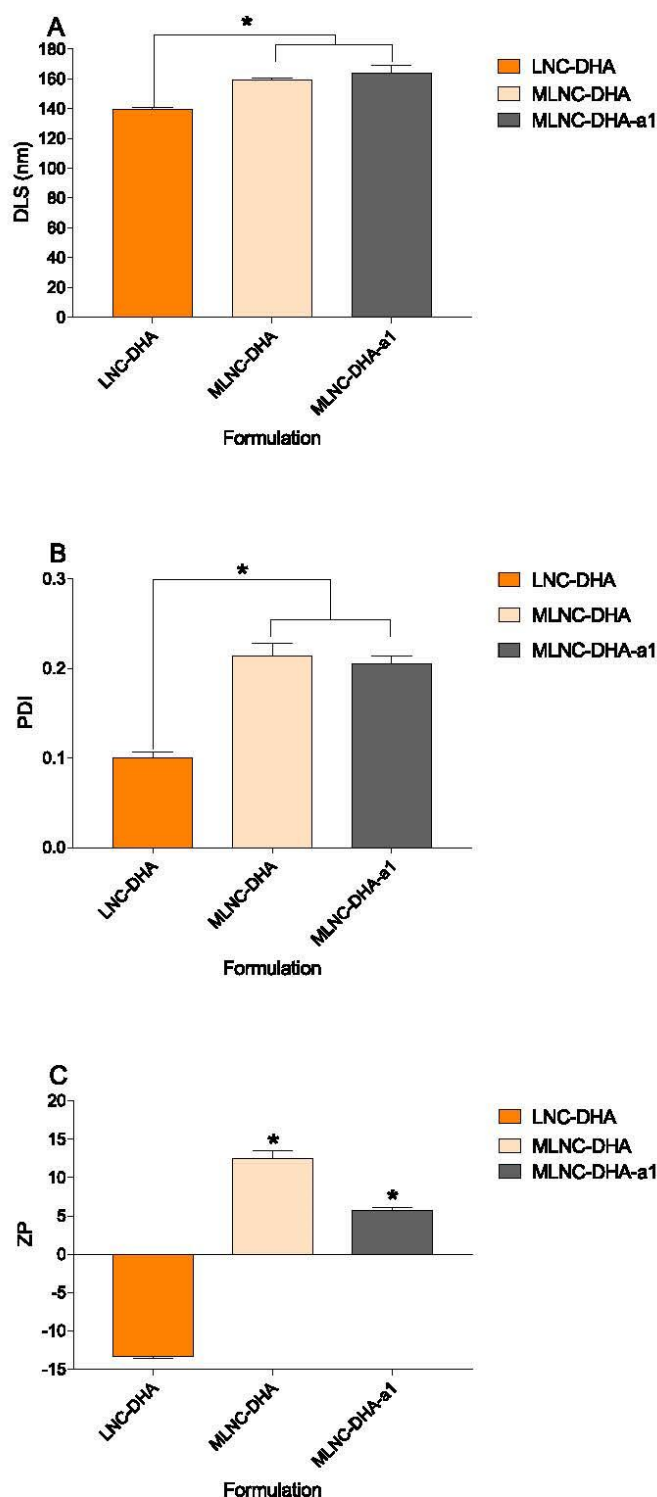


Fig. 2. Characterization of the nanocapsules with antibody compared with the nanocapsules without antibody. Values are expressed as mean \pm SEM ($n = 3$). * $p < 0.001$.

and MLNC-DHA, as expected. The MLNC-DHA-a1 was located next to nucleus as observed by the greater scattering of light, which was not observed for control nanocapsules (DHA-LNC and DHA-MLNC). The endothelial cells viability was assessed by trypan blue exclusion assay after nanocapsules treatment (Fig. 4B). It was observed that DHA-MLNC and MLNC-DHA-a1 at concentrations of 1.4 and 2.9×10^{11} nanoparticles/mL reduced the number of viable cells (Fig. 4B). Although it was observed a reduction of number of cells, the control and antibody functionalized nanocapsules at different concentrations did not alter the

Table 3

Diameter and number of particles of the nanocapsules containing DHA in the lipid core determined by NTA.

Nanocapsules ¹	Mean Diameter (nm)	Particles number
LNC-DHA	159.85 \pm 1.62	$2.30 \times 10^{13} \pm 9.75 \times 10^{11}/\text{mL}^a$
MLNC-DHA	162.31 \pm 4.91	$2.37 \times 10^{13} \pm 1.54 \times 10^{12}/\text{mL}^a$
MLNC-DHA-a1	163.77 \pm 3.51	$1.34 \times 10^{13} \pm 2.20 \times 10^{11}/\text{mL}^b$
<i>p</i>	0.209	0.001

¹ Values are expressed as mean \pm SEM ($n = 3$). Values followed by the same superscript letter are not different ($p < 0.05$).

cell viability since the number of dead cells was not significantly increased. These findings were corroborated by Annexin V and PI incorporation assay (Fig. 4C).

4. Discussion

Initially, the characterization of the oils used in the nanocapsule nucleus was performed. The algae oil applied in our study was composed by DHA (35.13%), oleic acid (18.69%), palmitic acid (17.28%), myristic acid (16.66%) and other minor fatty acids. Algae oil instead of isolated DHA was chosen due to the very low oxidative stability of the free fatty acid. In terms of lipid oxidation, algae oil presented satisfactory values of hydroperoxides, which were found within the range established by *Codex Alimentarius* of 10 mEq O_2/Kg oil [33]. The hydroperoxide concentration observed in our sample (1.36 mEq O_2/Kg oil) was lower than the value observed in the study reported by Nogueira *et al.* [34] that characterized fresh algae oil (5.56 mEq O_2/Kg oil). This better stability was due to the higher proportion of oleic acid and the lower proportion of DHA present in the algae oil applied in our study, besides the antioxidant action of the tocopherol (79.43 mg/Kg) added to the oil by the supplier.

An important aspect to be analyzed previously to the development of polymeric nanocapsules is whether the oil used in the nucleus can be a solvent for the polymer, causing swelling and dissolution [30]. Polymeric nanocapsules are formed by interfacial deposition of polymer when both phases (oil and water) act as non-solvent for the polymer [35]. Taking this aspect into account, PCL films were prepared and completely immersed in algae oil and MCT, separately, in order to verify if these oils were capable of causing some mass change in the polymer films. In this way, in the swelling experiment, the weight of PCL films was constant for 60 days indicating that the algae oil is an adequate internal phase to produce kinetically stable polymeric nanocapsules dispersed in water. Our results showed no variation in the weight of the films within 60 days, longer than 30 days found by Silva *et al.* [36], evaluating the effect of vitamin K1 on the PCL (MW = 65.000) films. All formulations presented reproducible particle size dispersion profiles among the batches with unimodal distributions at the nanometric scale, when analyzed by laser diffraction technique, corroborating with the results reported by other studies carried out using different ligands on the nanocapsule surface, in which our methods were based [31–37]. Radar charts have been proposed as an easy and useful tool to determine the differences in size distribution curves during pre-formulation studies using laser diffraction data [38]. All our formulations presented similar fingerprints, showing almost superimposable profiles. SPAN values indicated narrow dispersity without any microscopic contamination in the formulations.

Considering that the profiles obtained by the laser diffraction technique did not present micrometer populations, DLS was used to characterize the nanometric population of the formulations. Algae oil nanocapsules (LNC-DHA and MLNC-DHA) were larger in size when compared to MCT nanocapsules (LNC-MCT and MLNC-MCT). This fact can be explained by the viscosity of algae oil when compared to MCT. According to Jornada *et al.* [39], the higher viscosity of the organic phase directly influences the final average size of the nanostructure. In

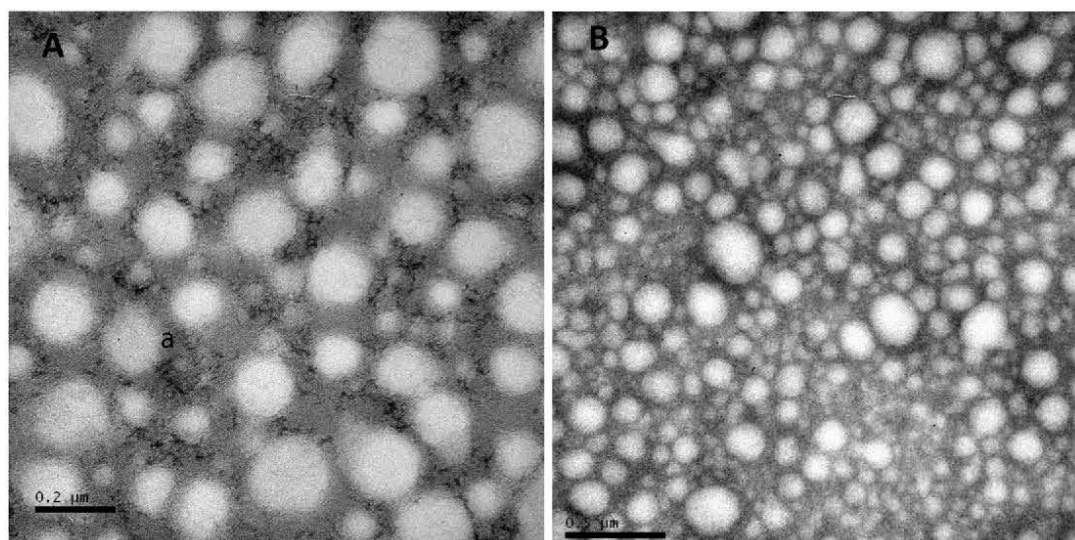


Fig. 3. Photomicrographs obtained by TEM of MLNC-DHA-a1. (A) bar = 0.2 μm ; (B) bar = 0.5 μm .

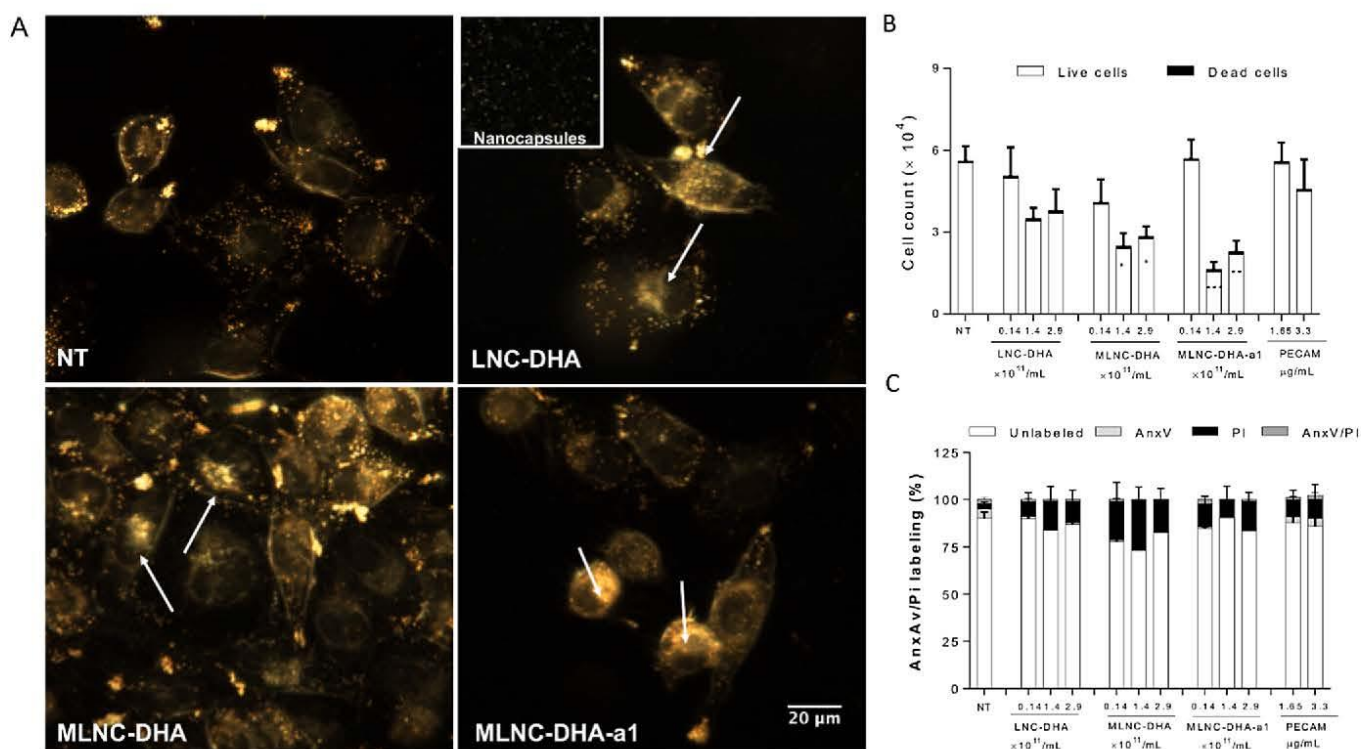


Fig. 4. Three-dimensional Cytoviva microscopy results obtained for the nanocapsules particles (A). The % cell viability quantified by Trypan exclusion assay (B); and Flow cytometry analysis of annexin V + propidium iodide (PI). Data express the percentage of apoptotic cells (AnxV +)/ necrotic cells (PI +), late apoptotic cells (AnxV + PI +) and viable cells (AnxV - PI -).

addition, the slight increase in the mean diameter observed in chitosan-coated nanocapsules, after the interfacial reaction, was also observed by Bender *et al.* [31]. Higher PDI values are usually observed to higher size nanocapsules due to their elevated heterogeneity when compared to smaller particles [40].

DLS technique was used to characterize the antibody-functionalized formulation. The hydrodynamic mean diameter was calculated by the method of Cumulants assuming that the nanocapsules have spherical shape according to the images obtained by transmission electron microscopy (Fig. 3). Moreover, the ideal antibody concentration for the optimal functionalization of the nanocapsules was assayed. After the interfacial reaction with anti-PECAM-1 tested at 200 $\mu\text{g}/\text{mL}$, the

batches of formulations showed unimodal distribution profiles, which maintained constant after 1 h. At higher concentrations (300 and 400 $\mu\text{g}/\text{mL}$), the batches of formulations showed multimodal profiles, indicating nanocapsules aggregation, corroborating the results reported by Bender *et al.* [31], in which nanocapsules aggregated with increasing phenylalanine concentrations. Zeta potential of LNC formulations was negative due to the presence of phosphatidic acid as contaminant of lecithin [37]. All absolute values of zeta potential were lower than 14 mV independent on the negative or positive coating indicating the presence of polysorbate 80 (a non-ionic surfactant) at the particle-water interface. Functionalization with anti-PECAM-1 neither change the mean diameter of chitosan-coated nanocapsules nor PDI, but it reduced

zeta potential indicating that anti-PECAM-1 was efficiently complexed on the nanocapsule surface. Stable constitutive molecules as PECAM-1 can be used as prophylactic and therapeutic delivery [13] and can be up-regulated in sites of inflammation and other vascular pathologies [17]. According to Shuvaev et al. [17], the only disadvantage of the endothelial drug delivery target by affinity ligands is its complex design. This step was overcome in our study, since it was possible to develop a stable anti-PECAM-1 surface-functionalized metal-complex multi-wall nanocapsules (MCMN) containing algae oil in the core.

This is the first study applying anti-PECAM-1 as ligand on nanocapsules containing algae oil as lipid core. Our proposal was based in previous studies that showed success to deliver different compounds to the endothelial cells using PECAM-1 as target. Dan et al. [41] was able to target anti-PECAM-1 iron oxide nanoparticles toward to the inflamed lung and brain tissues. The authors first evaluated the flux of these functionalized nanoparticles across the blood–brain barrier and their transcytosis and biodistribution using a human cortical microvascular endothelial cells (hCMEC/D3) model. Dziubla et al. [25] showed that antioxidant enzymes encapsulated into polymer nanocarrier target to PECAM-1 protected the endothelium against oxidative stress in cell culture and animal protocols. In another example, an indirect NOX inhibitor was encapsulated into immunoliposomes target to PECAM-1 and provided a significant protection against acute oxidative stress [23]. A reduction of ischemia–reperfusion injury was achieved by intravenous injected catalase conjugated with an antibody to PECAM-1 during lung transplantation [22]. In our study, the increase of DHA proportion, esterifying the phospholipids in the membranes or in a free form, can contribute to improve the cell's functionality, through its enzymatic and non-enzymatic oxidation [9,10,42], being this beneficial effect increased by nanoencapsulation [43].

Biological results showed that our nanocapsules containing algae oil as lipid core were up taken by HUVEC cells and did not significantly decrease the cell viability. Endothelial cells present in the inflamed artery are the target of our nanocapsules. It is known that the surface area ratio for desired target is really large [13], but the LDL^(-/-) animal model applied in our previous studies [44,45] fed for 6 months with a high fat diet, presents significant amount of fatty streaks in aorta, with consequent higher PECAM-1 expression in the HUVEC junctions, contributing to improve the surface area ratio for desired target. Thus, the results suggest that our anti-PECAM-1 antibody surface-functionalized nanocapsule containing algae oil can be now evaluated in other cells models and also *in vivo* using animal models. It represents a preliminary toxicological result that must be complemented by *in vivo* assays.

The success of the strategy proposed in our study depends on several factors that will be still analyzed. According to Shuvaev et al. [17], translational challenges are paramount, and different results can be achieved depending on pharmacokinetics, biodistribution, toxicity, mechanisms of delivery and other parameters of the nanocapsules that are associated to the cellular localization of ligands, ligand surface density, carrier geometry and flexibility, local infusion and interaction between drug delivery systems and humoral and cellular host defense [13–17]. Although PECAM-1 antibodies at moderate doses can be rapidly removed from the blood, the modulation of PECAM-1 by the antibody binding can potentially disturb its vascular barrier function, increasing the expression of pro-inflammatory CAMs and cytokines, as investigated by Kiseleva et al. [18]. In addition, the material applied to prepare the capsules can stimulate the innate immune system causing an inflammatory response. This configures a pharmacological limitation to the advance of drugs target delivery systems [15]. However, in our proposal, this limitation could be an advantage if our spherical nanocapsules can escape from the innate immune cells and be rapidly up taken by HUVECs, since the nanocapsules must be phagocyted by macrophages in the intima to exert their functionality, improving plaques stability. Thus, the strategy suggested in this study depends on the nanocapsules development, their capacity of escaping from immune system cells during their circulation in the blood, be internalized in the

inflamed endothelium, and finally be phagocyted by the macrophages, improving their phenotype. It is important to highlight that some beneficial effects of omega 3 fatty acids can be obtained in condition of oxidative stress [46], as present in the atherosclerosis. Despite of all complexity involved in this strategy, we showed in the present study that the first challenge was successfully overcome.

There is an agreement that atherosclerosis is a multifactorial disease of difficult control, even by changes in the life style or current drugs, such as statins [47]. It is also known that several patients with cholesterol at normal levels present a residual risk [48]. Thus, it seems essential that other factors of risk than cholesterol, such as inflammation or oxidative stress associated to innate or adapted immune system are also investigated [49]. Although the anti-PECAM-1 surface-functionalized metal-complex multi-wall nanocapsules (MCMN) containing DHA developed in our study has shown positive results, it only represents the first step of a complex strategy.

5. Conclusion

The anti-PECAM-1 surface-functionalized metal-complex multi-wall nanocapsules (MCMN) containing DHA in the lipid core were the first time successfully developed. The nanocapsules showed excellent size for application for future *in vitro* and *in vivo* studies, showing potential as a new pharmacological strategy to reduce atherosclerotic plaques.

Acknowledgements

This study was partially supported by CNPq (National Council for Scientific and Technological Development) – Process n. 166541/2017-6; PRONEX CNPq-FAPERGS (Foundation for Research of the State of Rio Grande do Sul) – Process n. 12/2014 #16/2551-0000467-6 and Fundação de Amparo à Pesquisa do Estado de São Paulo (Process 2019/21029-3).

References

- [1] F. Galisteo-González, J.A. Molina-Bolívar, S.A. Navarro, H. Boulaiz, A. Aguilera-Garrido, A. Ramírez, J.A. Marchal, Albumin-covered lipid nanocapsules exhibit enhanced uptake performance by breast-tumor cells, *Colloids Surf. B. Biointerf.* 165 (2018) 103–110, <https://doi.org/10.1016/j.colsurfb.2018.02.024>.
- [2] R. Branquinho, J. Roy, C. Farah, et al., Biodegradable Polymeric Nanocapsules Prevent Cardiotoxicity of Anti-Trypanosomal Lychnopholide, *Sci. Rep.* 7 (2017) 1–13, <https://doi.org/10.1038/srep44998>.
- [3] Q. Yi, J. Ma, K. Kang, Z. Gu, Bioreducible nanocapsules for folic acid-assisted targeting and effective tumor-specific chemotherapy, *Int. J. Nanomed.* 13 (2018) 653–667, <https://doi.org/10.2147/IJN.S149458>.
- [4] C.P. Oliveira, S.L. Büttgenbender, W.A. Prado, A. Beckenkamp, A.C. Asbahr, A. Buffon, S.S. Guterres, A.R. Pohlmann, Enhanced and selective antiproliferative activity of methotrexate-functionalized nanocapsules to human breast cancer cells (MCF-7), *Nanomat* 4 (2018) 24, <https://doi.org/10.3390/nano8010024>.
- [5] F. Sonvico, A. Clementino, F. Buttini, G. Colombo, S. Pescina, S.S. Guterres, A. R. Pohlmann, S. Nicoli, Surface-Modified nanocarriers for nose-to-brain delivery: From bioadhesion to targeting, *Pharm.* 10 (2018) E34, <https://doi.org/10.3390/pharmaceutics10010034>.
- [6] M. Arca, C. Borghi, R. Pontremoli, G.M. Ferrari, F. Colivicchi, G. Desideri, P. L. Temporelli, Hypertriglyceridemia and omega-3 fatty acids: Their often overlooked role in cardiovascular disease prevention, *Nutr. Metab. Cardiovasc. Dis.* 28 (2018) 197–205, <https://doi.org/10.1016/j.numecd.2017.11.001>.
- [7] L.B.B. Benes, N.S. Bassi, M.A. Kalot, M.H. Davidson, Evolution of omega-3 fatty acid therapy and current and future role in the management of dyslipidemia, *Cardio. Clinics* 36 (2018) 277–285, <https://doi.org/10.1161/CIR.0000000000000709>.
- [8] P.C. Calder, Marine omega-3 fatty acids and inflammatory processes: effects, mechanisms and clinical relevance, *Biochimica et Biophys. Acta (BBA)* 2015 (1851) 469–484, <https://doi.org/10.1016/j.bbailp.2014.08.010>.
- [9] Y. Adkins, D.S. Kelley, Mechanisms underlying the cardioprotective effects of omega-3 polyunsaturated fatty acids, *J. Nutritional Biochem.* 21 (9) (2010) 781–792, <https://doi.org/10.1016/j.jnutbio.2009.12.004>.
- [10] J. Roy, et al., Non-enzymatic oxidized metabolite of DHA, 4 (RS)-4-F4t-neuroprostane protects the heart against reperfusion injury, *Free Radical Biol. Med.* 102 (2017) 229–239, <https://doi.org/10.1016/j.freeradbiomed.2016.12.005>.
- [11] B.M. Everett, M.Y. Donath, A.D. Pradhan, T. Thuren, P. Pais, J.C. Nicolau, et al., Anti-inflammatory therapy with canakinumab for the prevention and management

- of diabetes, *J. Am. Coll. Cardiol.* 71 (2018) 2392–2401, <https://doi.org/10.1016/j.jacc.2018.03.002>.
- [12] A.S. Antonov, et al., Primary culture of endothelial cells from atherosclerotic human aorta: Part 1 Identification, morphological and ultrastructural characteristics of two endothelial cell subpopulations, *Atherosclerosis* 59 (1) (1986) 1–19, [https://doi.org/10.1016/0021-9150\(86\)90027-4](https://doi.org/10.1016/0021-9150(86)90027-4).
- [13] P.M. Glassman, et al., Targeting drug delivery in the vascular system: Focus on endothelium, *Adv. Drug Deliv. Rev.* (2020), <https://doi.org/10.1016/j.addr.2020.06.013>.
- [14] V.V. Shuvaev, et al., PECAM-targeted delivery of SOD inhibits endothelial inflammatory response, *FASEB J.* 25 (1) (2011) 348–357, <https://doi.org/10.1096/fj.10-169789>.
- [15] H. Parhiz, et al., Unintended effects of drug carriers: Big issues of small particles, *Adv. Drug Deliv. Rev.* 130 (2018) 90–112, <https://doi.org/10.1016/j.addr.2018.06.023>.
- [16] B.S. Ding, N. Hong, J.C. Murciano, K. Ganguly, C. Gottstein, M. Christofidou-Solomidou, V.R. Muzykantor, Prophylactic thrombolysis by thrombin-activated latent prourokinase targeted to PECAM-1 in the pulmonary vasculature, *Blood* 111 (2008) 1999–2006, <https://doi.org/10.1182/blood-2007-07-103002>.
- [17] V.V. Shuvaev, J.S. Brenner, V.R. Muzykantor, Targeted endothelial nanomedicine for common acute pathological conditions, *J. Control. Release* 219 (2015) 576–595, <https://doi.org/10.1016/j.jconrel.2015.09.055>.
- [18] R.Y. Kiseleva, et al., Vascular endothelial effects of collaborative binding to platelet/endothelial cell adhesion molecule-1 (PECAM-1), *Sci. Rep.* 8 (1) (2018) 1–10, <https://doi.org/10.1038/s41598-018-20027-7>.
- [19] J.R. Privratsky, C.M. Paddock, O. Forey, D.K. Newman, W.A. Muller, P. Newman, Relative contribution of PECAM-1 adhesion and signaling to the maintenance of vascular integrity, *J. Cell Sci.* 124 (2011) 1477–1485, <https://doi.org/10.1242/jcs.082271>.
- [20] H.Y. Stevens, B. Melchior, K.S. Bell, S. Yun, J.C. Yeh, J.A. Frangos, PECAM-1 is a critical mediator of atherosclerosis, *Dis. Models Mech.* 1 (2008) 175–181, <https://doi.org/10.1242/dmm.000547>.
- [21] V.V. Shuvaev, J. Han, S. Tliba, E. Argüiri, M. Christofidou-Solomidou, S. H. Ramirez, et al., Anti-Inflammatory Effect of Targeted Delivery of SOD to Endothelium: Mechanism, Synergism with NO Donors and Protective Effects In Vitro and In Vivo, *PLoS ONE* 8 (2013), <https://doi.org/10.1371/journal.pone.0077002>.
- [22] B.D. Kozower, et al., Immunotargeting of catalase to the pulmonary endothelium alleviates oxidative stress and reduces acute lung transplantation injury, *Nat. Biotechnol.* 21 (4) (2003) 392–398, <https://doi.org/10.1038/nbt806>.
- [23] E.D. Hood, et al., Antioxidant protection by PECAM-targeted delivery of a novel NADPH-oxidase inhibitor to the endothelium in vitro and in vivo, *J. Control. Release* 163 (2) (2012) 161–169, <https://doi.org/10.1016/j.jconrel.2012.08.031>.
- [24] M.D. Howard, et al., Nanocarriers for vascular delivery of anti-inflammatory agents, *Annu. Rev. Pharmacol. Toxicol.* 54 (2014) 205–226, <https://doi.org/10.1146/annurev-pharmtox-011613-140002>.
- [25] T.D. Dziubla, et al., Endothelial targeting of semi-permeable polymer nanocarriers for enzyme therapies, *Biomaterials* 29 (2) (2008) 215–227, <https://doi.org/10.1016/j.biomaterials.2007.09.023>.
- [26] N. Shirai, H. Suzuki, S. Wada, Direct methylation from mouse plasma and from liver and brain homogenates, *Anal. Biochem.* 343 (2005) 48–53, <https://doi.org/10.1016/j.ab.2005.04.037>.
- [27] N.C. Shanta, E.A. Decker, Rapid, Sensitive, Iron-based spectrophotometric methods for determination of peroxide values of food lipids, *J. AOAC Int.* 77 (1994) 421–424, <https://doi.org/10.1093/jaoac/77.2.421>.
- [28] Y.L. Hong, S.L. Yeh, C.Y. Chang, M. Hu, Total plasma malondialdehyde levels in 16 Taiwanese college students determined by various thiobarbituric acid tests and an improved high-performance liquid chromatography-based method, *Gin Biochem.* 33 (2000) 619–625, [https://doi.org/10.1016/s0009-9120\(00\)00177-6](https://doi.org/10.1016/s0009-9120(00)00177-6).
- [29] A. Gliszczynska-Swiglo, E. Sikorska, Simple reversed-phase liquid chromatography method for determination of tocopherols in edible plant oils, *J. Chromatogr. A.* 1048 (2004) 195–198, <https://doi.org/10.1016/j.chroma.2004.07.051>.
- [30] S.S. Guterres, V. Weiss, L.D.L. Freitas, A.R. Pohlmann, Influence of benzyl benzoate as oil core on the physicochemical properties of spray-dried powders from polymeric nanocapsules containing indomethacin, *Drug Deliv.* 7 (2000) 195–199, <https://doi.org/10.1080/107175400455119>.
- [31] E.A. Bender, M.F. Cavalcante, M.D. Adorne, L.M. Colomé, S.S. Guterres, D.S. Abdalla, A.R. Pohlmann, New strategy to surface functionalization of polymeric nanoparticles: one-pot synthesis of scFv anti-LDL(-)-functionalized nanocapsules, *Pharm. Res.* 31 (2014) 2975–2987, <https://doi.org/10.1007/s11095-014-1392-5>.
- [32] W. Strober, Trypan blue exclusion test of cell viability, *Current protocols in immunology*, 21.1 (1997), pp. A-3B. 10.1002/0471142735.ima03bs21.
- [33] Codex Alimentarius Commission. Codex alimentarius: fats, oils and related products., 8. FAO (2001). ISBN 92-5-104682-4.
- [34] M.S. Nogueira, B. Scolaro, G.L. Milne, I.A. Castro, Oxidation products from omega-3 and omega-6 fatty acids during a simulated shelf life of edible oils, *LWT* 101 (2019) 113–122, <https://doi.org/10.1016/j.lwt.2018.11.044>.
- [35] P. Couvreur, C. Dubernet, F. Puisieux, Controlled Drug Delivery with Nanoparticles: Current possibilities and future trends, *Eur. J. Pharm. Biopharm.* 41 (1995) 2–13.
- [36] A.L.M. Silva, R.V. Contri, D.S. Jornada, A.R. Pohlmann, S.S. Guterres, Vitamin K1-loaded lipid-core nanocapsules: physicochemical characterization and in vitro skin permeation, *Skin Res. Tech.* 19 (2013) 223–230, <https://doi.org/10.1111/j.1600-0846.2012.00631.x>.
- [37] M.F. Cavalcante, S.M. Kazuma, E.A. Bender, M.D. Adorne, M. Ullian, M.M. Veras, et al., A nanoformulation containing a scFv reactive to electronegative LDL inhibits atherosclerosis in LDL receptor knockout mice, *Eur. J. Pharm. Biopharm.* 107 (2016) 120–129, <https://doi.org/10.1016/j.ejpb.2016.07.002>.
- [38] M.D. Bianchin, I.C. Küllkamp-Guerreiro, C.P. de Oliveira, R.V. Contri, S.S. Guterres, A.R. Pohlmann, Radar charts based on particle sizing as an approach to establish the fingerprints of polymeric nanoparticles in aqueous formulations, *J. Drug Delivery Sci. Technol.* 30 (2015) 180–189, <https://doi.org/10.1016/j.jddst.2015.10.015>.
- [39] D.S. Jornada, A.F. Luana, K. Bueno, J. Gerent, C.L. Petzhold, R.C. Beck, S. S. Guterres, A.R. Pohlmann, Lipid-core nanocapsules: mechanism of self-assembly, control of size and loading capacity, *Soft Matter*. 8 (2012) 6646–6655, <https://doi.org/10.1039/C2SM25754H>.
- [40] P.M.S. Souza, F.A. Lobo, A.H. Rosa, L.F. Fraceto, Desenvolvimento de nanocápsulas de poli-ε-caprolactona contendo o herbicida atrazina, *Quim. Nova* 35 (2012) 132–137, <https://doi.org/10.1590/S0100-40422012000100024>.
- [41] M. Dan, D.B. Cochran, R.A. Yokel, T.D. Dziubla, Binding, transcytosis and biodistribution of anti-PECAM-1 iron oxide nanoparticles for brain-targeted delivery, *PLoS ONE* 8 (2013) 81051, <https://doi.org/10.1371/journal.pone.0081051>.
- [42] J.M. Galano, et al., Biological activities of non-enzymatic oxygenated metabolites of polyunsaturated fatty acids (NEO-PUFAs) derived from EPA and DHA: New anti-arrhythmic compounds? *Mol. Aspects Med.* 64 (2018) 161–168, <https://doi.org/10.1016/j.mam.2018.03.003>.
- [43] J. Roy, et al., Polymeric nanocapsules prevent oxidation of core-loaded molecules: evidence based on the effects of docosahexaenoic acid and neuroprostane on breast cancer cells proliferation, *J. Exp. Clin. Cancer Res.* 34 (1) (2015) 155, <https://doi.org/10.1186/s13046-015-0273-z>.
- [44] L.N. Chassot, B. Scolaro, G.G. Roschel, B. Cogliati, M.F. Cavalcanti, D.S.P. Abdalla, I.A. Castro, Comparison between red wine and isolated trans-resveratrol on the prevention and regression of atherosclerosis in LDLr (-/-) mice, *J. Nutritional Biochem.* 61 (2018) 48–55, <https://doi.org/10.1016/j.jnutbio.2018.07.014>.
- [45] M. S. Nogueira, M. C. Kessuane, A. A. B. Lobo Ladd, F. V. Lobo Ladd, Effect of long-term ingestion of weakly oxidised flaxseed oil on biomarkers of oxidative stress in LDL-receptor knockout mice, 116 (2016), pp. 258–269. 10.1017/S0007114516001513.
- [46] J. Roy, J.-Y. Le Guennec, Cardioprotective effects of omega 3 fatty acids: origin of the variability, *J. Muscle Res Cell Motil.* 38 (1), pp.25–30. 10.1007/s10974-016-9459-z.
- [47] J.M. Kim, W.S. Lee, J. Kim, Therapeutic strategy for atherosclerosis based on bone-vascular axis hypothesis, *Pharmacol. Ther.* 206 (2020), 107436, <https://doi.org/10.1016/j.pharmthera.2019.107436>.
- [48] A.W. Aday, P.M. Ridker, Targeting residual inflammatory risk: a shifting paradigm for atherosclerotic disease, *Front. Cardiovas. Med.* 6 (2019) 16, <https://doi.org/10.3389/fcvm.2019.00016>.
- [49] R.I. Jaén, et al., Innate Immune Receptors, Key Actors in Cardiovascular Diseases, *JACC Basic Translation Sci.* 5 (7) (2020) 735–749, <https://doi.org/10.1016/j.jacbs.2020.03.015>.

Supplementary Figures

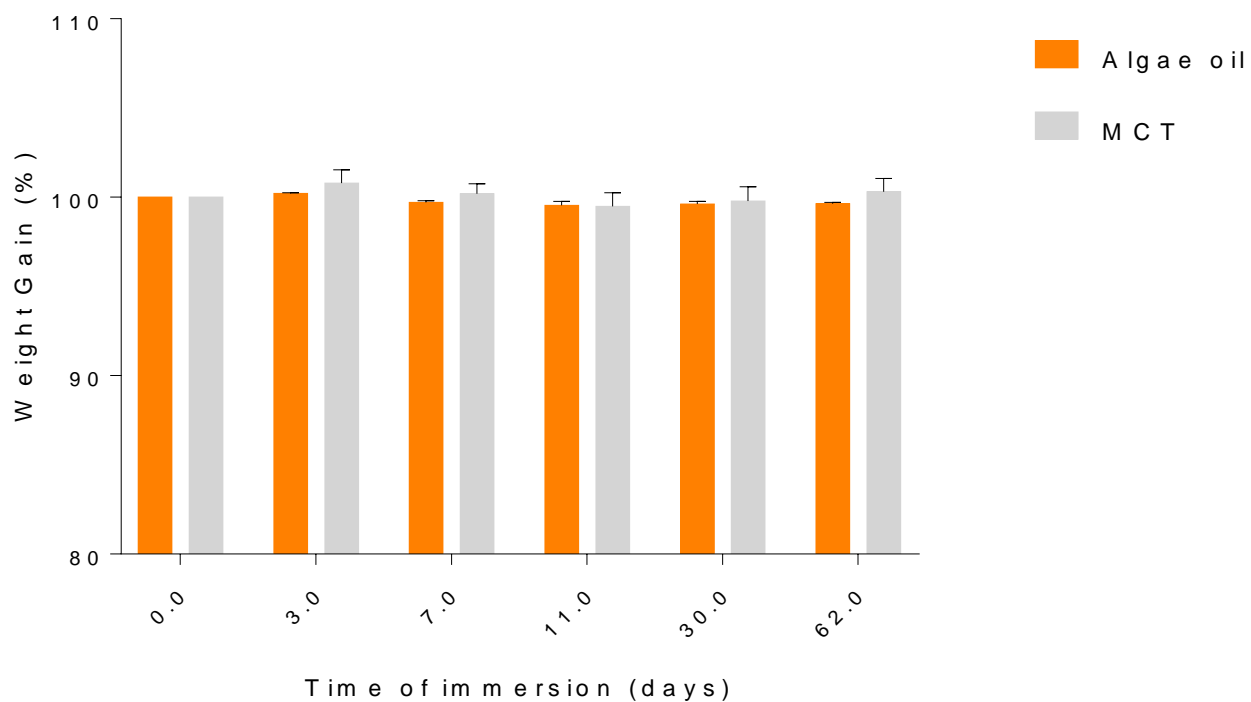


Figure 1S. Capacity of the PCL polymer to absorb the algae oil and MCT. Values are expressed as mean \pm SEM. (n=3)

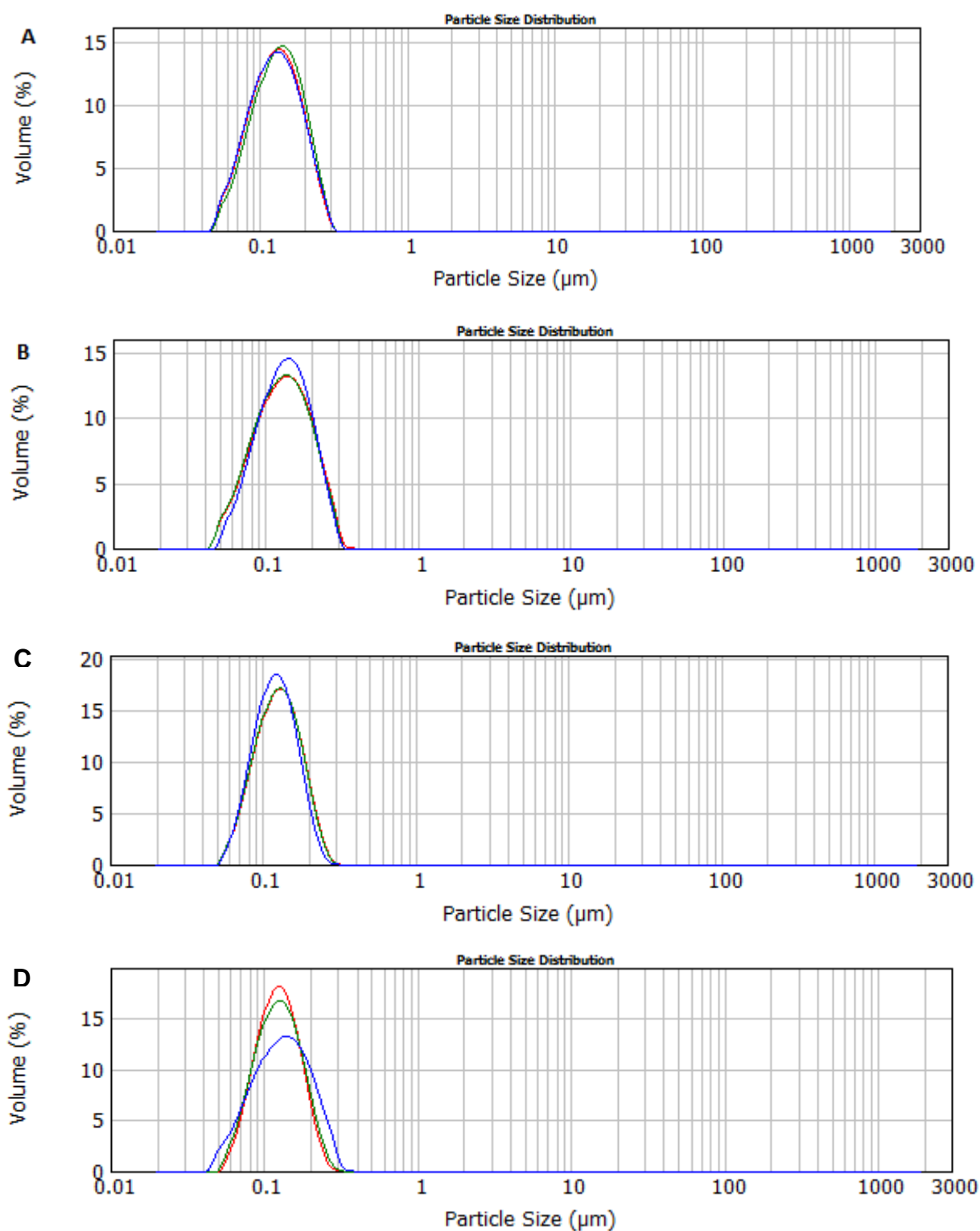


Figure 2S. Diameter distribution of PCL and algae oil nanocapsules: LNC-DHA (A), MLNC-DHA (B), LNC-MCT (C), MLNC-MCT (D), determined by Laser diffraction.

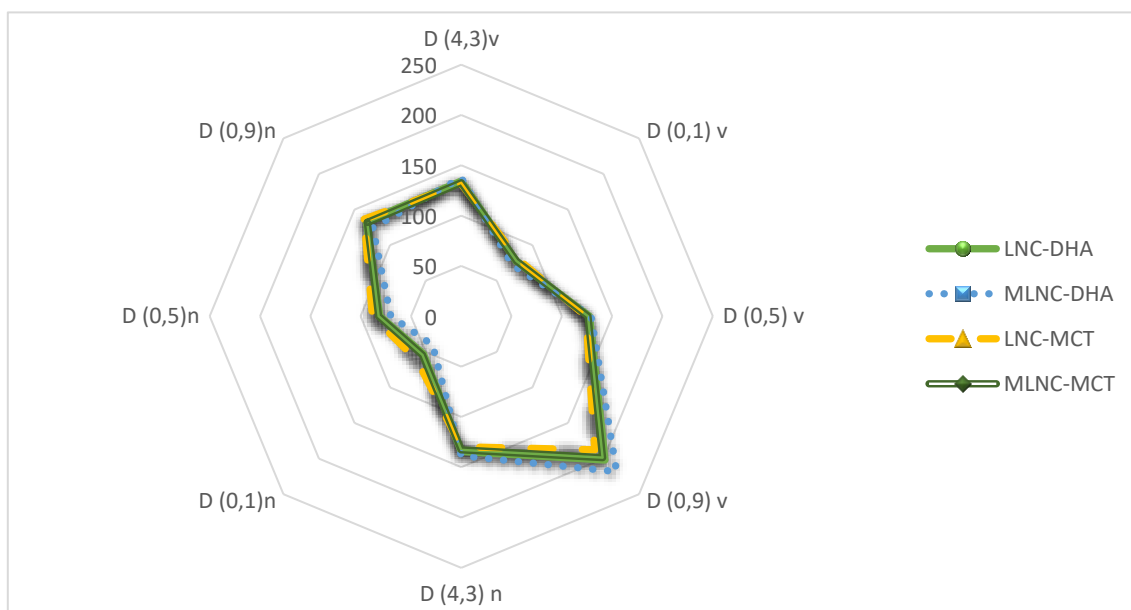
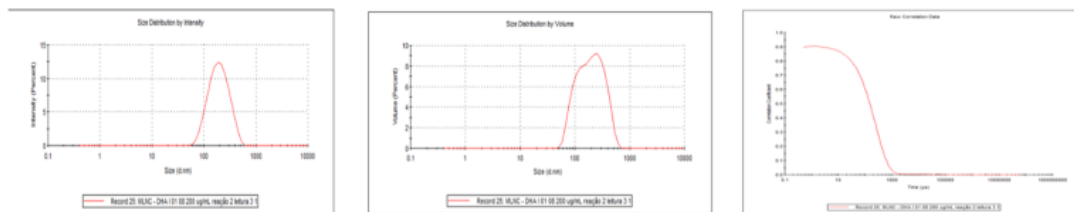
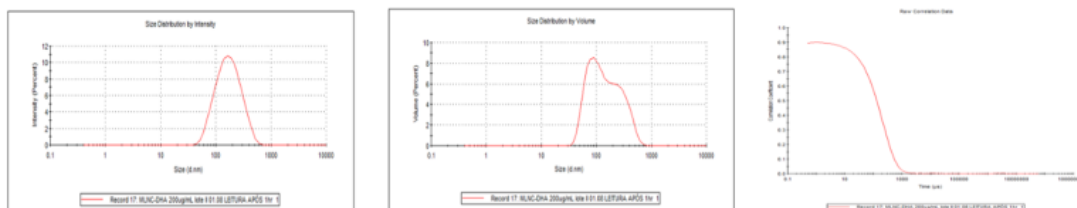


Figure 3S. Radar chart for LNC-DHA, MLNC-DHA, LNC-MCT and MLNC-MCT formulations. [axes: 1, volume-weighted mean diameter by volume of particles, $D(4.3)v$; 2, diameter at percentile 10 under the distribution curve by volume, $D(0.1)v$; 3, diameter at percentile 50 under the distribution curve by volume, $D(0.5)v$; 4, diameter at percentile 90 under the distribution curve by volume, $D(0.9)v$; 5, volume-weighted mean diameter by number of particles, $D(4.3)n$; 6, diameter at percentile 10 under the distribution curve by number, $D(0.1)n$; 7, the diameter at percentile 50 under the distribution curve by number, $D(0.5)n$ and 8, diameter at percentile 90 under the distribution curve by number, $D(0.9)n$.

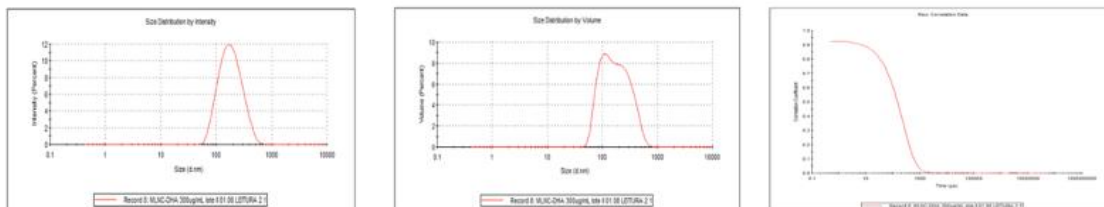
MLNC-DHA-a1 200 μ g/mL T-0



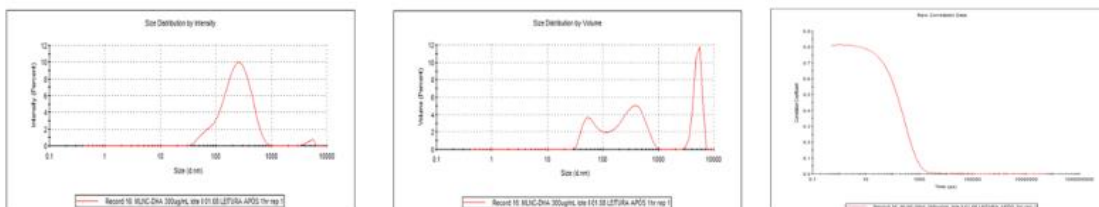
MLNC-DHA-a1 200 μ g/mL 1 hour after



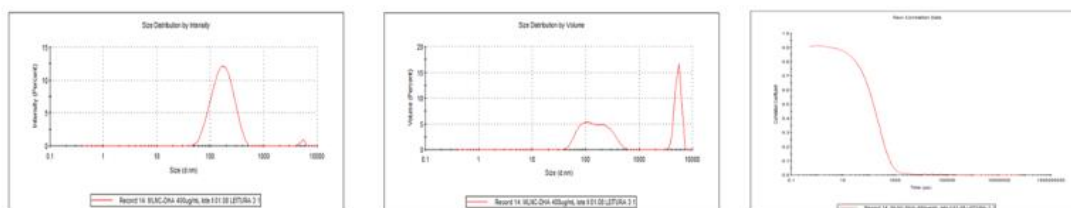
MLNC-DHA-a1 300 μ g/mL T-0



MLNC-DHA-a1 300 μ g/mL 1 hour after



MLNC-DHA-a1 400 μ g/mL T-0



MLNC-DHA-a1 400 μ g/mL 1 hour after

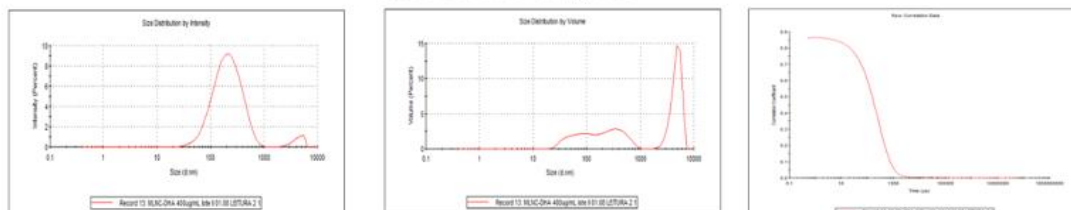


Figure 4S. Size Distribution by Intensity and size distribution by volume.

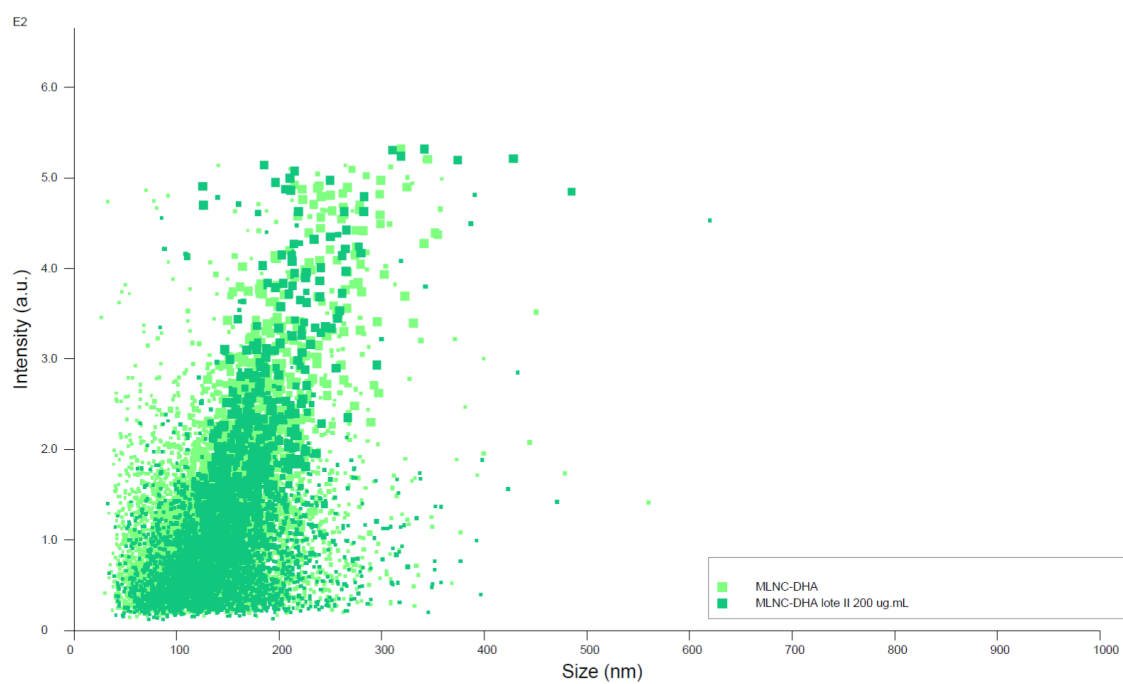


Figure 5S. Overlap of the Anti-PECAM-1 functionalized nanoparticles over the chitosan-coated nanocapsules performed at the NTA.

**CHAPTER II: EFFECT OF ANTI-PECAM-1 VECTORIZED NANOCAPSULES CONTAINING
DOCOSAHEXAENOIC ACID ON MACROPHAGES POLARIZATION**

European Journal of Pharmaceutics and Biopharmaceutics

Effect of anti-PECAM-1 vectorized nanocapsules containing docosahexaenoic acid on macrophages polarization.

--Manuscript Draft--

Manuscript Number:	
Article Type:	Research Paper
Keywords:	atherosclerosis; Nanocapsules; DHA; macrophages; inflammation; polarization
Corresponding Author:	Inar Castro Universidade de Sao Paulo BRAZIL
First Author:	Inar Castro
Order of Authors:	Inar Castro Matheus de Castro Leão Isabella di Piazza Milena Fronza Broering Sandra Helena Poiselli Farsky Mayara Klimuk Uchiyama Koiti Araki Adriana Raffin Pohlmann Silvia Stanisçuaski Guterres
Abstract:	It has been shown that atherosclerotic plaques healing or stabilization depends on various factors, including the type of immune cells present in the atheroma. The presence of pro-resolving M2 macrophages instead of pro-inflammatory M1 macrophages has been associated to wound healing and more stable plaques. Omega 3 fatty acids, such as docosahexanoic acid (DHA; C22:6 n3) could promote the switch of M1 to M2 macrophages. Thus, the objective of this study was firstly to evaluate the toxicity of lipid-core nanocapsules containing DHA (LNC-DHA), multi-wall nanocapsules containing DHA (MLNC-DHA) and the surface-functionalized (anti-PECAM-1) metal-complex multi-wall nanocapsules containing DHA (MLNC-DHA-a1) in HUVEC, U937 and RAW 264.7 cells; and after to determine the effect of these nanocapsules on macrophages uptake and polarization. Cells were exposed to three concentrations: 0.14x10 ¹¹ , 0.75 x10 ¹¹ and 1.40x10 ¹¹ nanocapsules/mL during 24, 48 and 72h, being the cell viability determined by flow cytometry. The uptake of MLNC-DHA and MLNC-DHA-a1 nanocapsules by RAW 264.7 macrophages and their polarization were determined at 0.75x10 ¹¹ nanocapsules/mL. Cell viability was not changed according to the type of cells after 24, 48 and 72h, suggesting absence of toxicity in the three concentrations evaluated in this study. It was observed that both MLNC-DHA and MLNC-DHA-a1 nanocapsules decreased the concentration of Tumor necrosis factor-alpha (TNFα) (p=0.02) compared with non-treated group (NT), with no changes in Interleukin-10 (IL-10) (p=0.29). The nanocapsules also showed an increase of M2 (F4/80+ CD206) phenotype % (p<0.01) without M1 (F4/80+ CD80) alteration (p=0.25). This result suggests that DHA richer algae oil, as part of the lipid core of the nanocapsules, did not reduce cells viability and improved the macrophage phenotype, being a potential therapy to heal or stabilize atherosclerotic plaques.
Suggested Reviewers:	Cécile Gladinea University of Clermont Auvergne cecile.gladinea@inra.fr Clermont Université, Centre INRA Auvergne Rhône Alpes Vladimir Muzykantova University of Pennsylvania muzykant@pennmedicine.upenn.edu University of Pennsylvania David Masson University of Burgundy david.masson@chu-dijon.fr

	<p>Ichiro Manabe Chiba University manabe-ky@umin.ac.jp Department of Disease Biology and Molecular Medicine, Graduate School of Medicine, Chiba University</p>
	<p>Katsuhito Fujii The University of Tokyo fujii-ky@umin.ac.jp Department of Cardiovascular Medicine, the University of Tokyo</p>
Opposed Reviewers:	

Cover Letter

At.

Prof. Professor Thomas Rades

Editor-in-Chief, *European Journal of Pharmaceutics and Biopharmaceutics*

University of Copenhagen Faculty of Health and Medical Sciences, 2200, København Denmark

August 08th, 2022

Dear Prof. Rades,

We are pleased to submit our manuscript entitled "**Effect of anti-PECAM-1 vectorized nanocapsules containing docosahexaenoic acid on macrophages polarization**" for publication in the *European Journal of Pharmaceutics and Biopharmaceutics*. It is the second part of our previous study published last year (<https://doi.org/10.1016/j.ejpb.2020.12.016>) in which the toxicity and physiological effect of a vectorized nanocapsule containing a bioactive fatty acid (DHA) was evaluated in macrophages.

Thank you in advance.

Sincerely,

Inar Alves Castro

Department of Food and Experimental Nutrition

Faculty of Pharmaceutical Sciences, University of São Paulo

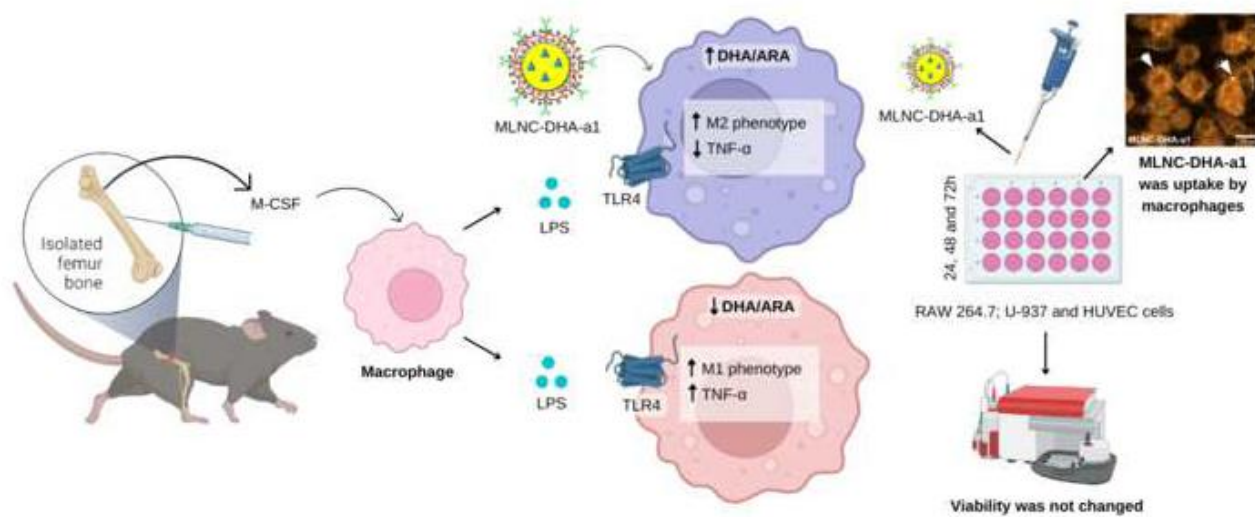
Av. Lineu Prestes, 580, B14

05508-900 São Paulo, Brazil

+55 11 3091 1481

inar@usp.br

Graphical Abstract

[Click here to access/download;Graphical Abstract;GRAPHICAL ABSTRACT .png](#)

Effect of anti-PECAM-1 vectorized nanocapsules containing docosahexaenoic acid on macrophages polarization.

Matheus de Castro Leão¹; Isabella di Piazza¹; Milena Fronza Broering²; Sandra Helena Poiselli Farsky²; Mayara Klimuk Uchiyama³; Koiti Araki³; Adriana Raffin Pohlmann⁴; Silvia Stanisçuaski Guterres⁵; Inar Alves Castro^{1*}

¹LADAF. Department of Food and Experimental Nutrition, Faculty of Pharmaceutical Sciences, University of São Paulo, São Paulo-SP, Brazil. Food Research Center (FoRC), CEPID-FAPESP, Research Innovation and Dissemination Centers São Paulo Research Foundation, São Paulo 05468-140, Brazil

²Department of Clinical & Toxicological Analyses, School of Pharmaceutical Sciences, University of São Paulo, Brazil.

³Department of Fundamental Chemistry, Institute of Chemistry, University of São Paulo, Brazil.

⁴Department of Organic Chemistry; Institute of Chemistry; Federal University of Rio Grande do Sul; Porto Alegre, RS, Brazil

⁵Department of Production and Drugs Control; Pharmaceutical Faculty; Federal University of Rio Grande do Sul; Porto Alegre, RS, Brazil

***Address for correspondence:** *Inar Alves Castro: LADAF (www.ladaf.com.br). Department of Food and Experimental Nutrition, Faculty of Pharmaceutical Sciences, University of São Paulo, Av. Lineu Prestes, 580, B14 - 05508-900 São Paulo, Brazil.

Phone number: +55 11 3091 1152 **e-mail:** inar@usp.br

Abstract

1
2
3
4 It has been shown that atherosclerotic plaques healing or stabilization depends on various factors,
5 including the type of immune cells present in the atheroma. The presence of pro-resolving M2
6 macrophages instead of pro-inflammatory M1 macrophages has been associated to wound
7 healing and more stable plaques. Omega 3 fatty acids, such as docosahexanoic acid (DHA; C22:6
8 n3) could promote the switch of M1 to M2 macrophages. Thus, the objective of this study was
9 firstly to evaluate the toxicity of lipid-core nanocapsules containing DHA (LNC-DHA), multi-wall
10 nanocapsules containing DHA (MLNC-DHA) and the surface-functionalized (anti-PECAM-1)
11 metal-complex multi-wall nanocapsules containing DHA (MLNC-DHA-a1) in HUVEC, U937 and
12 RAW 264.7 cells; and after to determine the effect of these nanocapsules on macrophages uptake
13 and polarization. Cells were exposed to three concentrations: 0.14×10^{11} , 0.75×10^{11} and 1.40×10^{11}
14 nanocapsules/mL during 24, 48 and 72h, being the cell viability determined by flow cytometry.
15 The uptake of MLNC-DHA and MLNC-DHA-a1 nanocapsules by RAW 264.7 macrophages and
16 their polarization were determined at 0.75×10^{11} nanocapsules/mL. Cell viability was not changed
17 according to the type of cells after 24, 48 and 72h, suggesting absence of toxicity in the three
18 concentrations evaluated in this study. It was observed that both MLNC-DHA and MLNC-DHA-
19 a1 nanocapsules decreased the concentration of Tumor necrosis factor-alpha (TNF α) ($p=0.02$)
20 compared with non-treated group (NT), with no changes in Interleukin-10 (IL-10) ($p=0.29$). The
21 nanocapsules also showed an increase of M2 (F4/80⁺ CD206) phenotype % ($p<0.01$) without M1
22 (F4/80⁺ CD80) alteration ($p=0.25$). This result suggests that DHA richer algae oil, as part of the
23 lipid core of the nanocapsules, did not reduce cells viability and improved the macrophage
24 phenotype, being a potential therapy to heal or stabilize atherosclerotic plaques.
25
26
27
28
29
30
31
32
33
34
35
36
37
38
39
40
41
42
43
44
45
46
47
48
49
50
51
52
53
54
55
56
57
58
59
60
61
62
63
64
65

Key words: atherosclerosis, nanocapsules, DHA, macrophages, inflammation, polarization

1.Introduction

1
2
3
4 Although recent and important pharmacological advances have contributed to reduce
5 mortality and morbidity caused by cardiovascular diseases (CVDs), the ischemic events such as
6 myocardium infarction and stroke are still responsible for the majority of deaths, estimated in 17.9
7 million people each year [1]. In fact, this number can even become higher due to the still unknown
8 consequences of SARS-Cov-2 infection in the endothelial dysfunction, strictly involved in the
9 atherosclerotic lesions [2]. For this reason, in addition to the prevention strategies recommended
10 in the guidelines, such as the consumption of a healthy diet, physical activity, smoking cessation
11 and hypolipidemic drugs prescription [3], new strategies aiming to regress or improve the stability
12 of the already present atherosclerotic plaques must be searched in order to reduce CVD mortality.
13
14
15
16
17
18
19
20
21

22 Atherosclerosis is a non-resolving inflammatory condition that underlies the ischemic
23 events [4,5]. The chronic inflammation of the intima arterial occurs by different stimulus, including
24 hypertension and excess of circulating apolipoprotein B-containing lipoproteins, especially low-
25 density-lipoproteins (LDL) that enter the intima by passive filtration and transcytosis. As
26 consequence, endothelial cells express adhesion molecules, such as intercellular adhesion
27 molecule-1 (ICAM-1), vascular cell adhesion molecule-1 (VCAM-1), e-selectins and
28 platelet/endothelial cell adhesion molecule-1 (PECAM-1) to attract and infiltrate the myeloid cells
29 in the inflammation site [5,6,7,8]. After infiltration, growth factors as Macrophage Colony-
30 Stimulating Factor- 1(CSF-1) promote the maturation of monocytes into tissue macrophages,
31 that in turn, take up modified or aggregated LDL particles, as part of the normal immune response
32 [7,9]. However, different from the acute inflammation, there is no resolution in the atherosclerosis
33 condition because, in general, the stimulus that depends on lifestyle choices, does not stop. The
34 continuous uptake of LDL particles by the macrophages, associated to a pro-inflammatory
35 microenvironment, cause a dysfunction of these lipid-load cells, that can suffer apoptosis followed
36 by secondary necrosis, leading to the formation of fatty streaks and plaques [10,11]. The plaques,
37 in turn, can suffer erosion or even rupture, provoking ischemic insults such as myocardium
38 infarction and stroke, or can be healed or stabilized depending on factors that include the
39 phenotype of macrophages that take part of the plaque composition [7,9,12,13].
40
41
42
43
44
45
46
47
48
49
50
51
52
53
54
55
56
57
58
59
60
61
62
63
64

1
2
3
4
5
6
7
8
9
10
11
12
13
14
15
16
17
18
19
20
21
22
23
24
25
26
27
28
29
30
31
32
33
34
35
36
37
38
39
40
41
42
43
44
45
46
47
48
49
50
51
52
53
54
55
56
57
58
59
60
61
62
63
64

Monocytes derived macrophages present in the intima layer have been classified in different subtypes, according to their phenotype and consequent physiological function. M1, M(Hb), Mhem, M2, Mox and M4 macrophages have been found in atherosclerotic lesions [14,15]. Among them, M1 macrophages are characterized as pro-inflammatory and part of Th1 cells response, while M2 macrophages are triggered by Th2 cells and have pro-resolving effects [12,13]. It is supposed that M2 macrophages can contribute to reduce the plaque size and risk of rupture, because it exerts a better efferocytosis, reducing the secondary necrosis and increasing the cholesterol efflux by high-density-lipoprotein (HDL). As consequence, there is a decrease of production and secretion of reactive oxygen species (ROS), pro-inflammatory cytokines, chemokines, tissue factors and metalloproteinases [13,15]. Thus, modulation of macrophage phenotypes might be a new strategy for the pharmacological treatment aiming to heal or stabilize the atherosclerotic plaques [14,15].

Omega 3 fatty acids, such as EPA (eicosapentaenoic acid) and DHA (docosahexaenoic acid) are substrate to the synthesis of less-inflammatory and pro-resolution oxylipins in different cells, including macrophages [16]. Some *in vitro* and *in vivo* studies have reported that omega 3 fatty acids can induce M2 macrophage polarization by different mechanisms [17,18,19,20]. Based on the fact that DHA can switch the M1 to M2 macrophage, and that this later phenotype has been associated to the plaque healing, we raised the hypothesis that a direct supply of DHA to the macrophages by a drug delivery system could contribute to reduce the foam cells, leading to a plaque stabilization or healing. In a previous study [21], anti-PECAM-1-surface-functionalized metal-complex multi-wall nanocapsules containing DHA richer algae oil in their core (MLNC-DHA-a1) were developed, showed 94.80% of conjugation efficiency and did not show significant toxicity toward HUVECs. The metal complex multi-wall nanocapsules are prepared by self-assembly of a polyester, sorbitan monostearate and oils (in general triacylglycerols) stabilized with lecithin and polysorbate 80, followed by chitosan coating, interfacial complexation using metal ions, such as zinc(II), iron(II) or gold(III), and a ligand [21,22,23,24]. On basis on that positive preliminary result, the objective of this study was firstly evaluate the toxicity of lipid-core nanocapsules containing DHA (LNC-DHA), multi-wall nanocapsules containing DHA (MLNC-DHA) and the surface-functionalized (anti-PECAM-1) metal-complex multi-wall nanocapsules containing DHA (MLNC-

DHA-a1) in HUVEC, U937 and RAW 264.7 cells, and then determine the *in vitro* effect of these nanocapsules on macrophages polarization.

2. Materials and methods

Lipid-core nanocapsules containing DHA (**LNC-DHA**), multi-wall nanocapsules containing DHA (**MLNC-DHA**) and the surface-functionalized (anti-PECAM-1) metal-complex multi-wall nanocapsules containing DHA (**MLNC-DHA-a1**) were prepared and characterized as described in our previous study [21].

2.2. Methods

2.2.1. Cell culture

Human umbilical vein endothelial cells (HUVECs) were kindly donated by Professor Ana Campa of the Department of Clinical and Toxicological Analysis (Faculty of Pharmaceutical Sciences, University of São Paulo, Brazil). HUVEC cells were maintained in Roswell Park Memorial Institute (RPMI) 1640 (Gibco, Grand Island, NY, USA) containing 10% FBS and 1% antibiotic solution containing streptomycin and penicillin. RAW 264.7 (immortalized murine macrophages) and U937 cells were obtained from the Rio de Janeiro Cell Bank (BCRJ, Rio de Janeiro, RJ, Brazil) and cultured in DMEM (Gibco, Grand Island, NY, USA) high glucose (4,500 pg/mL) containing 10% FBS. Cells were kept at 37 °C under controlled CO₂ atmosphere of 5%. Cell's culture medium was replaced every 2-3 days and the cells were trypsinized with 0.01% trypsin in EDTA buffer (Vitrocell Embriolife, Campinas, SP, Brazil).

2.2.2. Cell viability

The cytotoxicity of the nanocapsules was evaluated using flow cytometer after culturing. Briefly, cells were seeded at 2.5×10^4 cells/well in 24-well microplates (Costar® Multiple Well Cell

1 Culture Plates, Corning, Glendale, Arizona, USA), and kept at 37 °C for 24h. Afterward, cells were
2 treated with LNC-DHA; MLNC-DHA and MLNC-DHA-a1 at three concentrations: 0.14, 0.75 and
3 1.40 x 10¹¹ nanoparticles/mL, and cultured for 24, 48 and 72h. Isolated anti-Pecam-1 was also
4 evaluated at concentration of 200 µg/mL. Thereafter, cells were detached, and supernatant and
5 cells were washed twice in phosphate-buffered saline containing 1% bovine serum albumin. Cells
6 were incubated with Annexin V (previously diluted (1:20) in Annexin V (Life Technologies,
7 Carlsbad, USA) binding buffer (10 mM N-2-hydroxyethylpiperazine-N'-2-ethanesulfonic acid, 140
8 mM NaCl, 25 mM CaCl₂, pH 7.4; BD Pharmingen, Franklin Lakes, NJ) during 20 min in the dark,
9 at room temperature. After this, 200 µL Annexin V binding buffer and 7AAD (1:200) were added.
10 Data from 10,000 events were acquired in Accuri C6 flow cytometer (BD Pharmingen) and the
11 stained cells were analyzed. The negative double group for AnxV-7-AAD (non-apoptotic and non-
12 necrotic) marking were plotted to quantify the cell viability (AnxV-, 7-ADD -), single marking with
13 AnxV represented cells in apoptosis (AnxV+, 7-ADD -), single marking with 7-AAD indicated cells
14 in necrosis (AnxV-, 7-ADD+), while the double group positive for AnxV-7-AAD denoted the group
15 of cells in late apoptosis AnxV+, 7-ADD+). Results of triplicates were expressed as percentage
16 (%).

2.2.3. Real time up take of the nanocapsules by RAW 264.7 macrophages

34 The uptake of nanocapsules by macrophages was determined by enhanced dark-field
35 hyperspectral microscopy (CytoViva®) as described by Sandri et al. [25]. RAW 264.7 murine
36 macrophages (8 × 10⁴ cells) were seeded in extra clean dust-free Nexterion® Glass D coverslips
37 (#D263T; Schott, New York, NY, USA) present in 96-well plates (Corning, NY, USA). After
38 adherence, cells were incubated with medium containing MLNC-DHA and MLNC-DHA-a1 at 0.75
39 x 10¹¹ nanoparticles/mL for 4h at 37 °C under 5% CO₂ atmosphere. A non-treated group (NT)
40 was kept in DMEM 10% SFB. Immediately after incubation, cells were washed three times with
41 5% FBS-PBS, and the coverslip was placed on extra clean dust-free Nexterion® Glass B slides
42 (NexterionR Glass B; Schott, NY, EUA) containing 10 µL of 5% FBS-PBS. Then, 10 µl of cell
43 solution were set up using extra clean dust-free slides (NexterionR Glass B; Schott, NY, USA)
44 and coverslips (Nexterion Glass D #D263T; Schott). RAW 264.7 murine macrophages were
45 imaged using a CytoViva Ultra Resolution Imaging System (CytoViva, Inc., AL, USA) mounted on
46
47
48
49
50
51
52
53
54
55
56
57
58
59
60
61
62
63
64
65

1 an Olympus BX51 microscope (x1,500 magnification; Olympus Corporation, Tokyo, Japan)
2 equipped with fluorite 100 × oil iris 0.6–1.30 numerical aperture (NA) objective and a 75 W Xe
3 light source. Optical images were take using a Dage XL CCD digital camera with Image
4 Processing Software (Dage®; DAGE-MTI of MC, Inc., MI, USA). ImageJ software, version 2.1.0/
5 1.53c (2010 - 2022), was used to place the scale bars. One hundred cells from representative
6 photomicrographs were randomly chosen for this measurement and for each treatment.
7
8
9
10
11
12

13 **2.2.4. Macrophages polarization**

14
15
16
17
18 The experiment was performed according to the method previously established by Ying
19 et al. [26]. Initially, C57Bl/6 mice were anesthetized and euthanized to collect the left and right
20 femurs for medullary washes collection, using an icy PBS solution containing 2% Fetal Bovine
21 Serum (FBS). All animal experiments were conducted under the guidelines of the National
22 Institutes of Health and were approved by the Institutional Animal Care and Use Committee of
23 FCF/USP. Then the bone marrow pool was resuspended using 21G needles to dissociate the
24 cells and pass them through a 70 µm cell strainer for removal of other tissues. The cells were
25 washed with NH₄Cl 0.8% solution and incubated in ice for red cell removal. After centrifugation
26 for 5 min, 500 x g at 4 °C, the cells were resuspended with BMDM medium, composed of IMDM
27 (Iscove Modified Dulbecco Media), 20% L929 cell culture rich in monocyte growth factor (M-CSF)
28 and 10% of FBS. The cells were counted and plated at the concentration of 5 x10⁵ cells/well in
29 24-well plate and maintained in BMDM medium for 7 days for cell differentiation. After this period,
30 and considering that this time provides 90% of macrophages differentiation, naive cells were
31 exposed to *Escherichia coli* (LPS) 100 ng/mL and maintained for 24h to generate the M1-
32 inflammatory phenotype macrophage. Treatments were performed with dexamethasone (500
33 ng/mL), MLNC-DHA (0.75 x 10¹¹ particles/mL) or MLNC-DHA-a1 (0.75 x 10¹¹ particles/mL
34 containing 200 µg/mL of Anti-PECAM-1). After 48 h, the supernatant was removed and cytokines
35 were analyzed by ELISA assay according to the manufacturer's instructions. Single cell
36 suspensions were prepared at 2 X 10⁷ cells/mL in staining buffer (10% FCS in PBS) and pre-
37 incubated with 1 µg of the 2.4G2 antibodies for 5-10 min on ice prior to staining. About 50 µL of
38 cell suspension (equal to 10⁶ cells) were dispensed into each tube or well along with a previously
39
40
41
42
43
44
45
46
47
48
49
50
51
52
53
54
55
56
57
58
59
60
61
62
63
64
65

1 determined optimal concentration of cell surface specific antibody against F4/80⁺ CD80 and
2 F4/80⁺ CD206 for differentiation of M1 and M2 macrophages respectively, in 50 μ L of staining
3 buffer. Cell surface expression of these maturation markers was measured on a BD opteia™ kits
4 (BD Biosciences). The collected events were analyzed with FlowJo v7.6 (Treestar).
5
6
7
8
9

10 11 12 **2.2.6. Statistical analysis**

13
14
15
16 Data were presented as mean \pm SEM. Treatments were compared using one-way
17 ANOVA and Tukey HSD post-test or non-parametric Kruskal-Wallis ANOVA by Ranks, followed
18 by Multiple Comparisons (2-tailed). A *p* value of 0.05 was adopted to reject the null hypothesis.
19
20 Calculations will be performed using software Statistica v.13 (TIBCO Software Round Road, TX,
21 USA). Graphs were elaborated using R Studio software (Wickham, 2016).
22
23
24
25
26
27

28 **3. Results**

29 30 31 **3.1. Cell viability**

32
33
34
35
36 In a previous study, anti-PECAM-1-surface-functionalized metal-complex multi-wall
37 nanocapsules containing DHA as algae oil in their core (MLNC-DHA-a1) were for the first time
38 developed, and their uptake and toxicity evaluated in HUVECs at three concentrations: from to
39 0.14 x 10¹¹ to 2.90 x 10¹¹ nanoparticles/mL for 24h. It was observed that MLNC-DHA-a1 was
40 efficiently internalized by endothelial cells, without reduction of the number of viable cells when
41 compared with not treated cells and analyzed by Flow cytometry analysis of annexin V +
42 propidium iodide (PI) [21]. However, due to the use of immune cells in the sequence of this initial
43 study, we opted to reduce the nanocapsules concentration (0.14 x 10¹¹ to 1.40 x 10¹¹
44 nanoparticles/mL) to evaluate the toxicity in three types of cells, including again HUVEC, added
45 now of RAW 237 and U937 cells. **Figure 1** shows the HUVEC viability when incubated with three
46 concentrations of nanocapsules LNC-DHA, MLNC-DHA and MLNC-DHA-a1(**Fig. 1A**) for 24h
47 compared with non-treated cells (NT) and also with isolated anti-PECAM-1. The viability ranged
48
49
50
51
52
53
54
55
56
57
58
59
60
61
62
63
64
65

1 from $82.14 \pm 7.69\%$ to $91.34 \pm 2.93\%$ after 24h, without difference from NT $88.87 \pm 5.09\%$ ($p=$
2 0.73). No difference was observed among the treatments and NT in all concentrations
3 investigated in this study (**Fig.1B**). Similar results were observed after 48h and 72h
4
5 **(Supplementary Figure 1)**.

6
7
8 It was also important to evaluate the toxicity of the nanocapsules towards the monocytes,
9 since the final objective would be to change the macrophages phenotype. **Figure 2** presents the
10 cells viability of U937 cells incubated with three concentrations of each type of nanocapsules:
11 LNC-DHA, MLNC-DHA and MLNC-DHA-a1 (**Fig. 2A**) for 24h. As observed to HUVEC, the mean
12 U937 cells viability ranged from $95.08 \pm 1.34\%$ to $96.89 \pm 1.38\%$ at 24h, without difference from
13 control $95.24 \pm 0.72\%$ ($p=0.96$). No difference was observed among the treatments and NT in all
14 concentrations investigated in this study, neither (**Fig.2B**). Similar results were observed after 48h
15 and 72h (**Supplementary Figure 2**).

16
17
18 Finally, the toxicity of the nanocapsules was determined using RAW 264.7 murine
19 macrophages (**Figure 3**). Results showed that the viability of the 264.7 murine macrophages
20 incubated with three concentrations of nanocapsules for 24h (**Fig.3A**), ranged from $52.36 \pm$
21 17.62% to $83.33 \pm 1.59\%$, did not differ among themselves or when compared with NT ($74.33 \pm$
22 9.29%) ($p=0.39$) (**Fig. 3B**). The same behavior was observed after 48 h and 72 h (**Supplementary**
23 **Figure 3**). Since nanocapsules did not show toxicity toward HUVEC, U937 and RAW 264.7 cells,
24 the uptake of LNC-DHA, MLNC-DHA and MLNC-DHA-a1 was evaluated at the concentration of
25 0.75×10^{11} nanocapsules/mL, including a non-treated sample (NT). **Figure 4** shows that all
26 nanocapsules were internalized as a damage-associated molecular pattern (DAMP) by the RAW
27 264.7 macrophages, according to the strategy proposed in our hypothesis. **Figure 5** confirmed
28 that after MLNC-DHA and MLNC-DHA-a1 uptake, there was a reduction of TNF- α compared with
29 NT cells ($p = 0.0187$), while no difference was observed to IL-10 ($p=0.29$). Regarding to the
30 macrophages polarization, the treatments with dexamethasone or with the nanocapsules did not
31 change M1 phenotype ($p=0.25$), while the MLNC-DHA-a1 enhanced ($p < 0.01$) and MLNC-DHA
32 showed a strong trend to increase ($p=0.06$) M2 phenotype compared with NT cells, suggesting
33 the beneficial effect of our nanocapsule towards macrophages switch phenotype.
34
35
36
37
38
39
40
41
42
43
44
45
46
47
48
49
50
51
52
53
54
55
56
57
58
59
60
61
62
63
64
65

4. Discussion

1
2
3
4 This study takes part of a project that proposed the development of a surface-
5 functionalized (anti-PECAM-1) metal-complex multi-wall nanocapsules containing algae oil as
6 DHA source (MLNC-DHA-a1). The idea was to apply anti-PECAM-1 to drive the nanocapsules to
7 the inflamed endothelium. Once arrived at the target tissue, the nanocapsules would be
8 recognized and phagocytosed by immune cells as DAMPs. Finally, inside the immune cells
9 phagosomes and lysosomes, the nanocapsules would deliver DHA to be used as substrate to the
10 synthesis of oxylipins, able to switch the phenotype from M1 to M2, contributing in this way to
11 heal or stabilize the atherosclerotic plaques, as summarized in **Figure 6**.

12
13
14
15
16
17
18
19
20 Therefore, as the first challenge, the nanocapsules could not show adverse effects to
21 endothelial cells, monocytes or macrophages. Our data showed that lipid-core nanocapsules
22 containing DHA (LNC-DHA), multi-wall nanocapsules containing DHA (MLNC-DHA) and the
23 surface-functionalized (anti-PECAM-1) metal-complex multi-wall nanocapsules containing DHA
24 (MLNC-DHA-a1) did not present any toxicity when evaluated at three concentrations (0.14, 0.75
25 and 1.40×10^{11} nanocapsules/mL) in HUVEC, U937 and RAW 264.7 cells, after 24, 48 and 72h.

26
27
28
29
30
31
32 In fact, nanocapsules efficiency regarding to toxicity and ability to be phagocytosed by
33 immune system cells, is a very complex subject that depend on many aspects, including carrier
34 components, excipients, impurities, therapeutic content, shape, size, elasticity and surface
35 chemistry and charge [27]. Our results showed that the nanocapsules had no toxicity using an *in*
36 *vitro* assay. The nanocapsules were composed by poly(ϵ -caprolactone), sorbitan monostearate,
37 zinc acetate, low molecular weight chitosan and polysorbate 80, as previously described [21].
38 These materials have been widely applied to synthesize nanoparticles without reported toxicity
39 even using animal models [22,23,28]. Moreover, lipid-core nanocapsules (LNC) containing poly(ϵ -
40 caprolactone) were evaluated in Wistar rats at concentration of 115×10^{12} nanocapsules/mL/Kg
41 and showed no indications of cardiotoxicity [29]. Regarding to Anti-PECAM-1, only modest or
42 non-significant effects in response to antibodies to PECAM-1 were observed using a combination
43 of *in vitro* and *in vivo* techniques and employing human and mouse endothelial cells under
44 physiologic and pathologic conditions [30]. Considering that PECAM is normally expressed by
45 endothelium, it is expected that an anti-PECAM-1 was well tolerate, as reported before [31]. Our
46
47
48
49
50
51
52
53
54
55
56
57
58
59
60
61
62
63
64
65

1 results confirmed that the material applied to build the capsule wall and the anti-PECAM-1 applied
2 in the surface as targeted carrier did not show any significant toxicity to U937 nor RAW 264.7
3 cells. Moreover, the algae oil (DHASCO®, DSM) containing 35.13 ± 0.35 g/100g of DHA [21] used
4 to compose the lipid core was not sterilized or depyrogenated due to its very low oxidative stability.
5 It was also the reason by which algae oil instead of pure isolated DHA was applied to synthesize
6 the MLNC-DHA nanocapsules, since DHA is even more unstable than algae oil. Thus, our results
7 signalize that although non-sterilized, the algae oil applied in our study was safe to prepare
8 nanocapsules to be evaluated in further *in vivo* animal assays. However, any extrapolation from
9 *in vitro* data to *in vivo* behavior should be done with caution [27].

10
11
12
13
14
15
16
17
18 In terms of phagocytosis and polarization, the shape and size of our nanocapsules may
19 also have contributed to their uptake by RAW macrophages. Our nanocapsules showed spherical
20 shape, size ranged from 159.12 ± 1.25 to 163.50 ± 5.33 nm and all absolute values of zeta
21 potential lower than 14 mV, independent on the negative or positive coating [21]. It has been
22 reported that non-spherical and non-electrical charged carriers may circulate longer than similarly
23 sized spheres, cationic or anionic nanoparticles, due to reduced recognition by host defense cells
24 [27,32]. The capacity of RAW macrophages of engulfing booth MLNC-DHA and MLNC-DHA-a1
25 nanocapsules, as shown in **Figure 4**, may be the result of an equilibrium between their spherical
26 shape associated to non-ionic surface charge. This combination may influence their further
27 clinical application via vascular injection.

28
29
30
31
32
33
34
35
36
37
38
39
40
41
42
43
44
45
46
47
48
49
50
51
52
53
54
55
56
57
58
59
60
61
62
63
64
65
Once engulfed by the macrophage, the lipid content of the MLNC-DHA and MLNC-DHA-
a1 nanocapsules are hydrolyzed by lysosomal lipases, delivering non-esterified fatty acids
(NEFA) that bind to fatty acids binding proteins (FABPs) to be used for metabolic or signaling
pathways, including generation of lipid mediators [33,34]. Under TLR4 activation, there is a fast
decrease of polyunsaturated fatty acids cellular content due to increased phagocytic activity,
endoplasmic reticulum enlargement and synthesis of oxylipins [34]. Thus, it is supposed that the
DHA supplied by our nanocapsules is rapidly oxidized by cyclooxygenase, 5-lipoxygenase and
cytochrome P450 (CYP), leading to the synthesis of less inflammatory oxylipins, including
Specialized Pro-Resolving Mediators [34,35]. Following the proposal of applying the
nanocapsules as DHA carriers to the inflamed endothelium, our data showed that both MLNC-

1 DHA and MLNC-DHA-a1 worked as DAMPs and were taken up by macrophages, reducing TNF α
2 concentration and promoting M2 polarization.

3
4 The immunomodulating effect of omega 3 fatty acids seems be mainly dependent on four
5 mechanisms: (1st) the suppression of Nuclear factor kappa B (NF κ B) signalling via G protein-
6 coupled receptor 120 (GPR-120) or as agonist of peroxisome proliferator-activated receptor-
7 gamma isoform (PPAR- γ), (2nd) suppression of the NLRP3 inflammasome pathway and
8 consequent IL-1 β secretion, (3rd) replacing the substrate for pro-inflammatory eicosanoid
9 synthesis and (4th) as precursors of SPMs [14,18, 20, 35, 36, 37]. All these well documented
10 mechanisms of omega 3 fatty acids contribute to reduce the systemic or tissue target
11 inflammation.
12
13
14
15
16
17
18
19

20 SPMs modulate the phenotype conversion of M1 into M2 macrophages, promoting
21 apoptosis and efferocytosis of inflammatory cells and may play a role in the resolution of
22 inflammation during plaque healing [12]. A supplementation composed by omega-3 fatty acids,
23 vitamin D3 and resveratrol was associated to an increased rate of macrophage polarization to the
24 M1-M2 type but only in patients with Apo E ϵ 3/ ϵ ϵ allele, while the *in vitro* stimulation by RvD1 was
25 effective in both groups, ϵ 3/ ϵ ϵ and ϵ 3/ ϵ 4 alleles [17], suggesting the role of SPMs on phenotype
26 change.
27
28
29
30
31
32
33

34 Based on fact that omega 3 fatty acids could decrease the levels of TNF α and NF κ B in
35 various dystrophic muscles, *mdx* mice treated with omega 3 fatty acids by gavage during 16 days,
36 showed a reduction of metalloproteinase MM9 gene expression, followed by an improvement of
37 muscle environment for repair, being these beneficial results associated to an increase of pro-
38 regenerative M2 macrophages and a decrease of M1 macrophages, when compared with mineral
39 oil supplementation [19]. Chang et al. [20] incubated murine macrophage RAW 264.7 with DHA
40 (20 μ M) for 24h and observed that DHA increased the efferocytic activity through M2 polarization,
41 and pro-resolving effect appeared to be mediated by PPAR γ activation. In another study, mice
42 were treated with omega 3 fatty acids (1.5 mg/g bw) via feeding needle 5 days before be subjected
43 to pressure overload to induce cardiac hypertrophy. The authors applied anti-iNOS and anti-
44 CD163 antibodies to evaluate M1 and M2 macrophages, respectively; and observed a higher
45 anti-CD163/anti-iNOS positive cell number ratio in the omega 3 fatty acids treated group
46 compared with vehicle [38]. *In vitro* assays, using transgenic *fat-1* mice fed a high-fat diet for 10
47
48
49
50
51
52
53
54
55
56
57
58
59
60
61
62
63
64

1 weeks, indicated that omega 3 fatty acids stimulates M2 and suppressed M1 polarization also in
2 adipocyte, being this result followed of a reduction of TNF α , IL-6 and MCP-1 [18]. This fact is
3 important because there is evidence that macrophage polarization in surrounding epicardial
4 adipose tissue, could influence the progression of coronary atherosclerosis in humans [14].
5

6
7 In our study, it was not observed difference of M1 percentage as measured using F4/80+
8 CD80 marker (**Fig. 5C**) nor regarding to IL-10 concentrations, found typically in lower levels in M1
9 phenotype (**Fig. 5B**) [14,15]. In addition, dexamethasone did work as control of the assay, since
10 no difference was observed to all markers when compared with LPS group. Dexamethasone is
11 potent immunosuppressant that inhibits the cytokine production induced by bacterial
12 lipopolysaccharides [39]. Thus, although the nanocapsules results are optimistic, more assays
13 should be carried out to confirm this expectative.
14

15
16 Taking into account the strong M2 polarization showed by MLNC-DHA-a1 (7.04%)
17 compared with LPS (0.30%), as measured using F4/80+ CD206 marker (**Fig. 5D**), followed by
18 reduced secretion of TNF α (**Fig. 5A**) observed to both MLNC-DHA and MLNC-DHA-a1, our
19 results suggest that DHA present in the algae oil that composed the lipid core of the nanocapsules
20 has potential to reduce the inflammatory microenvironment and improve macrophage
21 functionality. This is the first biological study in which a surface-functionalized (anti-PECAM-1)
22 metal-complex multi-wall nanocapsules containing algae oil as DHA source (MLNC-DHA-a1) was
23 evaluated in terms of capacity of modulate the macrophages phenotype. According to Chinetti-
24 Gbaguidi et al. [14], macrophage phenotypes should be characterized on the basis of cell surface
25 marker expression combined with functional studies. Thus, in the next steps of this project, other
26 cell markers and controls would be evaluated aiming to confirm the effect of our nanocapsules
27 toward M2 polarization and their potential to promote tissue repair and healing.
28
29
30
31
32
33
34
35
36
37
38
39
40
41
42
43
44
45
46
47

48 **5. Conclusion**

49
50
51
52 Our results suggest that DHA richer algae oil as part of the lipid core of the nanocapsules
53 did not reduce cells viability and improved the macrophage phenotype, being a potential therapy
54 to control chronic inflammation and heal or stabilize atherosclerotic plaques.
55
56
57
58
59
60
61
62
63
64
65

Acknowledgements

This study was supported by The State of São Paulo Research Foundation (FAPESP) (Scholarship and Research Grant 2019/21029-3 and 2021/02021-1) and National Council for Scientific and Technological Development (CNPq – Scholarship: 166541/2017-6).

References

- [01] World Health Organization. https://www.who.int/health-topics/cardiovascular-diseases#tab=tab_1. Accessed: 09 August 2022
- [02] Y. Liu, H.G. Zhang. Vigilance on New-Onset Atherosclerosis Following SARS-CoV-2 Infection. *Front. Med. (Lausanne)*, 7 (2020), pp. 629413. Doi: 10.3389/fmed.2020.629413.
- [03] D.K. Arnett, R.S. Blumenthal, M.A. Albert, A.B. Buroker, Z.D. Goldberger, E.J. Hahn, C.D. Himmelfarb, A. Khera, D. Lloyd-Jones, J.W. McEvoy, E.D. Michos, M.D. Miedema, D. Munoz, S.C. Smith, Jr., S.S. Virani, K.A. Williams, Sr., J. Yeboah, B. Ziaeian. 2019 ACC/AHA Guideline on the Primary Prevention of Cardiovascular Disease: A Report of the American College of Cardiology/American Heart Association Task Force on Clinical Practice Guidelines. *Circulation*, 140 (2019), pp. e596-e646. Doi: 10.1161/CIR.0000000000000678.
- [04] C. Kasikara, A.C. Doran, B. Cai, I. Tabas. The role of non-resolving inflammation in atherosclerosis. *J. Clin. Invest.*, 128 (2018), pp. 2713-2723. Doi: 10.1172/JCI97950.
- [05] P. Roy, M. Orecchioni, K. Ley. How the immune system shapes atherosclerosis: roles of innate and adaptive immunity. *Nat. Rev. Immunol.*, 22 (2022), pp. 251-265. Doi: 10.1038/s41577-021-00584-1.
- [06] J. Boren, M.J. Chapman, R.M. Krauss, C.J. Packard, J.F. Bentzon, C.J. Binder, M.J. Daemen, L.L. Demer, R.A. Hegele, S.J. Nicholls, B.G. Nordestgaard, G.F. Watts, E. Bruckert, S. Fazio, B.A. Ference, I. Graham, J.D. Horton, U. Landmesser, U. Laufs, L. Masana, G. Pasterkamp, F.J. Raal, K.K. Ray, H. Schunkert, M.R. Taskinen, B. van de Sluis, O. Wiklund, L. Tokgozoglul, A.L. Catapano, H.N. Ginsberg. Low-density lipoproteins cause atherosclerotic cardiovascular disease: pathophysiological, genetic, and therapeutic insights: a consensus statement from the European Atherosclerosis Society Consensus Panel. *Eur. Heart. J.*, 41 (2020), pp. 2313-2330. Doi: 10.1093/eurheartj/ehz962.

- 1 [07] M.B. Lorey, K. Öörni, P. T. Kovanen. Modified Lipoproteins Induce Arterial Wall
2 Inflammation During Atherogenesis. *Front. Cardiovasc. Med.* 9 (2022) 841545. doi:
3 10.3389/fcvm.2022.841545
4
5
6
7 [08] I. Tabas, K.J. Williams, J. Boren. Subendothelial lipoprotein retention as the initiating
8 process in atherosclerosis: update and therapeutic implications. *Circulation*, 116
9 (2007), pp. 1832-1844. Doi: 10.1161/CIRCULATIONAHA.106.676890.
10
11
12
13 [09] F.K. Swirski, M. Nahrendorf, P. Libby. Mechanisms of Myeloid Cell Modulation of
14 Atherosclerosis. *Microbiol. Spectr.*, 4 (2016), pp. Doi: 10.1128/microbiolspec.MCHD-
15 0026-2015.
16
17
18
19 [10] M.S. Gibson, N. Domingues, O.V. Vieira. Lipid and Non-lipid Factors Affecting
20 Macrophage Dysfunction and Inflammation in Atherosclerosis. *Front. Physiol.*, 9
21 (2018), pp. 654. Doi: 10.3389/fphys.2018.00654.
22
23
24
25 [11] K.J. Moore, I. Tabas. Macrophages in the pathogenesis of atherosclerosis. *Cell*, 145
26 (2011), pp. 341-355. Doi: 10.1016/j.cell.2011.04.005.
27
28
29
30 [12] R. Vergallo, F. Crea. Atherosclerotic Plaque Healing. *N. Engl. J. Med.*, 383 (2020), pp.
31 846-857. Doi: 10.1056/NEJMra2000317.
32
33
34
35 [13] I. Tabas, K. E. Bornfeldt. Macrophage Phenotype and Function in Different Stages of
36 Atherosclerosis. *Circ Res*, 118 (2016), pp.653-657. doi:
37 10.1161/CIRCRESAHA.115.306256.
38
39 [14] G. Chinetti-Gbaguidi, S. Colin, B. Staels. Macrophage subsets in atherosclerosis. *Nat.*
40 *Ver. Cardiol.*, 12 (2015), pp. 10-17. Doi: 10.1038/nrcardio.2014.173.
41
42
43
44 [15] M. de Gaetano, D. Crean, M. Barry, O. Belton. M1- and M2-Type Macrophage
45 Responses Are Predictive of Adverse Outcomes in Human Atherosclerosis. *Front.*
46 *Immunol.*, 7 (2016), pp. 275. Doi: 10.3389/fimmu.2016.00275.
47
48
49
50 [16] R. Bosviel, L. Jourard-Cubizolles, G. Chinetti-Gbaguidi, D. Bayle, C. Copin, N.
51 Hennuyer, I. Duplan, B. Staels, G. Zanoni, A. Porta, L. Balas, J.M. Galano, C. Oger, A.
52 Mazur, T. Durand, C. Gladine. DHA-derived oxylipins, neuroprostanes and protectins,
53 differentially and dose-dependently modulate the inflammatory response in human
54 macrophages: Putative mechanisms through PPAR activation. *Free Radic. Biol. Med.*,
55 103 (2017), pp. 146-154. Doi: 10.1016/j.freeradbiomed.2016.12.018.
56
57
58
59
60
61
62
63
64
65

- 1
2
3
4
5
6
7
8
9
10
11
12
13
14
15
16
17
18
19
20
21
22
23
24
25
26
27
28
29
30
31
32
33
34
35
36
37
38
39
40
41
42
43
44
45
46
47
48
49
50
51
52
53
54
55
56
57
58
59
60
61
62
63
64
65
- [17] S. Famenini, E.A. Rigali, H.M. Olivera-Perez, J. Dang, M.T. Chang, R. Halder, R.V. Rao, M. Pellegrini, V. Porter, D. Bredesen, M. Fiala. Increased intermediate M1-M2 macrophage polarization and improved cognition in mild cognitive impairment patients on omega-3 supplementation. *FASEB J.*, 31 (2017), pp. 148-160. Doi: 10.1096/fj.201600677RR.
- [18] M.Y.Song, J.Wang, Y.Lee, J. Lee , K.S. Kwon, E.J.Bae,B.H. Park. Enhanced M2 macrophage polarization in high n-3 polyunsaturated fatty acid transgenic mice fed a high-fat diet. *Mol Nutr Food Res*, 60(2016), pp.2481-2492. doi: 10.1002/mnfr.201600014.
- [19] S.C. de Carvalho, S.M. Hindi, A. Kumar, M.J. Marques. Effects of omega-3 on matrix metalloproteinase-9, myoblast transplantation and satellite cell activation in dystrophin-deficient muscle fibers. *Cell Tissue Res.*, 369 (2017), pp. 591-602. Doi: 10.1007/s00441-017-2640-x.
- [20] H.Y. Chang, H.N. Lee, W. Kim, Y.J. Surh. Docosahexaenoic acid induces M2 macrophage polarization through peroxisome proliferator-activated receptor gamma activation. *Life Sci.*, 120 (2015), pp. 39-47. Doi: 10.1016/j.lfs.2014.10.014.
- [21] M.C. Leao, A.R. Pohlmann, A.C.S. Alves, S.H.P. Farsky, M.K. Uchiyama, K. Araki, S. Sandri, S.S. Guterres, I.A. Castro. Docosahexaenoic acid nanoencapsulated with anti-PECAM-1 as co-therapy for atherosclerosis regression. *Eur. J. Pharm. Biopharm.*, 159 (2021), pp. 99-107. Doi: 10.1016/j.ejpb.2020.12.016.
- [22] M.F. Cavalcante, M.D. Adorne, W.M. Turato, M. Kemmerer, M.K. Uchiyama, A.C.C. Asbahr, A.C.S. Alves, S.H.P. Farsky, C. Drewes, M.C. Spatti, S.M. Kazuma, M. Boss, S.S. Guterres, K. Araki, B. Brune, D. Namgaladze, A.R. Pohlmann, D.S.P. Abdalla. scFv-Anti-LDL(-)-Metal-Complex Multi-Wall Functionalized-Nanocapsules as a Promising Tool for the Prevention of Atherosclerosis Progression. *Front. Med. (Lausanne)*, 8 (2021), pp. 652137. Doi: 10.3389/fmed.2021.652137.
- [23] C.B. Michalowski, M.D. Arbo, L. Altknecht, A.N. Ancuti, A.S.G. Abreu, L.M.R. Alencar, A.R. Pohlmann, S.C. Garcia, S.S. Guterres. Oral Treatment of Spontaneously Hypertensive Rats with Captopril-Surface Functionalized Furosemide-Loaded Multi-Wall Lipid-Core Nanocapsules. *Pharmaceutics*, 12 (2020), pp. Doi: 10.3390/pharmaceutics12010080.
- [24] A.Alves, V. Lavayen, F. Figueiró, D.R. Dallemole, A.F.Dias, R. Cé, A.M.O. Battastini, S.S.Guterres, A.R. Pohlmann. Chitosan-Coated Lipid-Core Nanocapsules Functionalized with Gold-III and Bevacizumab Induced In Vitro Cytotoxicity against C6

Cell Line and In Vivo Potent Antiangiogenic Activity. Pharm Res.,37(2020),pp.DOI: 10.1007/s11095-020-02804-0

- 1
2
3
4 [25] S. Sandri, C.B. Hebeda, R.A. Loiola, S. Calgaroto, M.K. Uchiyama, K. Araki, L.A.
5 Frank, K. Paese, S.S. Guterres, A.R. Pohlmann, S.H.P. Farsky. Direct effects of
6 poly(epsilon-caprolactone) lipid-core nanocapsules on human immune cells.
7 Nanomedicine (Lond), 14 (2019), pp. 1429-1442. Doi: 10.2217/nnm-2018-0484.
8
9
10
11 [26] W. Ying, P.S. Cheruku, F.W. Bazer, S.H. Safe, B. Zhou. Investigation of macrophage
12 polarization using bone marrow derived macrophages. J. Vis. Exp., (2013), pp. Doi:
13 10.3791/50323.
14
15
16
17 [27] H. Parhiz, M. Khoshnejad, J.W. Myerson, E. Hood, P.N. Patel, J.S. Brenner, V.R.
18 Muzykantov. Unintended effects of drug carriers: Big issues of small particles. Adv.
19 Drug. Deliv. Ver., 130 (2018), pp. 90-112. Doi: 10.1016/j.addr.2018.06.023.
20
21
22
23 [28] F.A. Bruinsmann, A.C.S. Alves, A.F. Dias, L.F.L. Silva, F. Visioli, A.R. Pohlmann, F.
24 Figueiro, F. Sonvico, S.S. Guterres. Nose-to-brain delivery of simvastatin mediated by
25 chitosan-coated lipid-core nanocapsules allows for the treatment of glioblastoma in
26 vivo. Int. J. Pharm., 616 (2022), pp. 121563. Doi: 10.1016/j.ijpharm.2022.121563.
27
28
29
30
31 [29] R.Fracasso, M. Baierle, G.Goëthel, A.Barth, F. Freitas, S.Nascimento, L.
32 Altknecht, V.Olsen, K. Paese, V. D. da Silva, I. Castro, M. Andrades, N.
33 Clausell, A. Pohlmann, S. Guterres, S.C. Garcia. Evaluation of potential acute
34 cardiotoxicity of biodegradable nanocapsules in rats by intravenous administration.
35 Toxicol Res (Camb), 5(2016),pp. 168-179. Doi: doi: 10.1039/c5tx00207a.
36
37
38
39
40 [30] R.Y. Kiseleva, C.F. Greineder, C.H. Villa, O.A. Marcos-Contreras, E.D. Hood, V.V.
41 Shuvaev, H.M. DeLisser, V.R. Muzykantov. Vascular endothelial effects of
42 collaborative binding to platelet/endothelial cell adhesion molecule-1 (PECAM-1). Sci.
43 Rep., 8 (2018), pp. 1510. Doi: 10.1038/s41598-018-20027-7.
44
45
46
47
48 [31] V. R. Muzykantov, M. Christofidou-Solomidou, I. Balyasnikova, D. W. Harshaw, L.
49 Schultz, A. B. Fisher, S. M. Albelda. Streptavidin facilitates internalization and
50 pulmonar targeting of an anti-endothelial cell antibody (platelet-endothelial cell
51 adhesion molecule 1): A strategy for vascular immunotargeting of drugs. Proceedings
52 of the National Academy of Sciences, 96(5) (1999), pp. 2379–2384. Doi:
53 10.1073/pnas.96.5.2379WHO.
54
55
56
57
58
59
60
61
62
63
64
65

- 1
2
3
4
5
6
7
8
9
10
11
12
13
14
15
16
17
18
19
20
21
22
23
24
25
26
27
28
29
30
31
32
33
34
35
36
37
38
39
40
41
42
43
44
45
46
47
48
49
50
51
52
53
54
55
56
57
58
59
60
61
62
63
64
65
- [32] P.M. Glassman, J.W. Myerson, L.T. Ferguson, R.Y. Kiseleva, V.V. Shuvaev, J.S. Brenner, V.R. Muzykantov. Targeting drug delivery in the vascular system: Focus on endothelium. *Adv. Drug Deliv. Rev.*, 157 (2020), pp. 96-117. Doi: 10.1016/j.addr.2020.06.013.
- [33] S. Schlager, N. Vujic, M. Korbelius, M. Duta-Mare, J. Dorow, C. Leopold, S. Rainer, M. Wegscheider, H. Reicher, U. Ceglarek, W. Sattler, B. Radovic, D. Kratky. Lysosomal lipid hydrolysis provides substrates for lipid mediator synthesis in murine macrophages. *Oncotarget*, 8(25) (2017), pp. 40037–40051. Doi: 10.18632/oncotarget.16673
- [34] L. Menegaut, A. Jalil, C. Thomas, D. Masson. Macrophage fatty acid metabolism and atherosclerosis: The rise of PUFAs. *Atherosclerosis*, 291 (2019), pp. 52-61. Doi: 10.1016/j.atherosclerosis.2019.10.002.
- [35] C.N. Serhan, B.D. Levy. Resolvins in inflammation: emergence of the pro-resolving superfamily of mediators. *J. Clin. Invest.*, 128 (2018), pp. 2657-2669. Doi: 10.1172/JCI97943.
- [36] Y. Yan, W. Jiang, T. Spinetti, A. Tardivel, R. Castillo, C. Bourquin, G. Guarda, Z. Tian, J. Tschopp, R. Zhou. Omega-3 fatty acids prevent inflammation and metabolic disorder through inhibition of NLRP3 inflammasome activation. *Immunity*, 38 (2013), pp. 1154-1163. Doi: 10.1016/j.immuni.2013.05.015.
- [37] P.C. Calder. Omega-3 polyunsaturated fatty acids and inflammatory processes: nutrition or pharmacology? *Br J Clin Pharmacol*, 75 (2013), pp. 645-662. Doi: 10.1111/j.1365-2125.2012.04374.x.
- [38] H. Toko, H. Morita, M. Katakura, M. Hashimoto, T. Ko, S. Bujo, Y. Adachi, K. Ueda, H. Murakami, M. Ishizuka, J. Guo, C. Zhao, T. Fujiwara, H. Hara, N. Takeda, E. Takimoto, O. Shido, M. Harada, I. Komuro. Omega-3 fatty acid prevents the development of heart failure by changing fatty acid composition in the heart. *Sci. Rep.*, 10 (2020), pp. 15553. Doi: 10.1038/s41598-020-72686-0.
- [39] T. Y. Chuang, A. J. Cheng, I. T. Chen, T. Y. Lan, I. H. Huang, C. W. Shiau, C. L. Hsu, Y. W. Liu, Z. F. Chang, P. H. Tseng, J. C., Kuo. Suppression of LPS-induced inflammatory responses by the hydroxyl groups of dexamethasone. *Oncotarget*, 8(30) (2017), pp. 49735–49748. Doi: 10.18632/oncotarget.17683.

Figure

[Click here to access/download;Figure;FIGURES + SUPP FIGURES.docx](#)

±

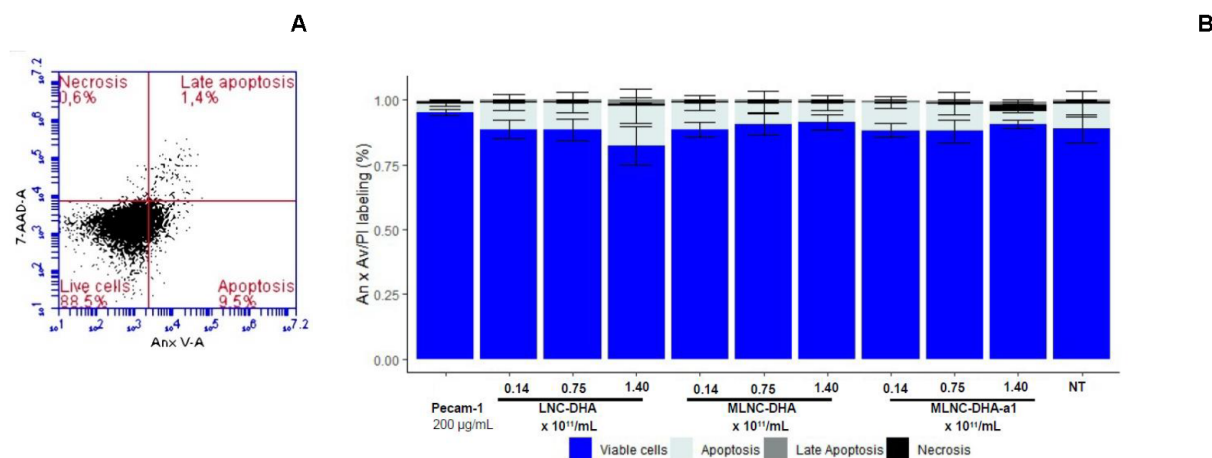


Figure 1. HUEVEC viability, necrosis, apoptosis and late apoptosis as estimated by flow cytometry after culturing incubated with LNC-DHA, MLNC-DHA and MLNC-DHA-a1 at three concentrations (0.14×10^{11} , 0.75×10^{11} and 1.40×10^{11} /mL), also incubated without any nanocapsules (NT) and isolated anti-PECAM-1 at $200 \mu\text{g/mL}$ for 24h. Fig.1A: Flow cytometry colocalization of annexin-V binding and propidium iodide uptake for quantitation of HUVEC incubated with MLNC-DHA-a1, as example. The horizontal axis depicts fluorescein-labeled annexin V; the vertical axis shows binding of propidium iodide fluorescence. Fig.1B: Proportion of HUEVEC viability, necrosis, apoptosis and late apoptosis. Vertical bars are mean \pm SEM. No difference was observed among the samples according to cell viability ($p=0.73$) necrosis ($p=0.92$), apoptosis ($p=0.51$) and late apoptosis ($p=0.94$) by Kruskal Wallis analysis.

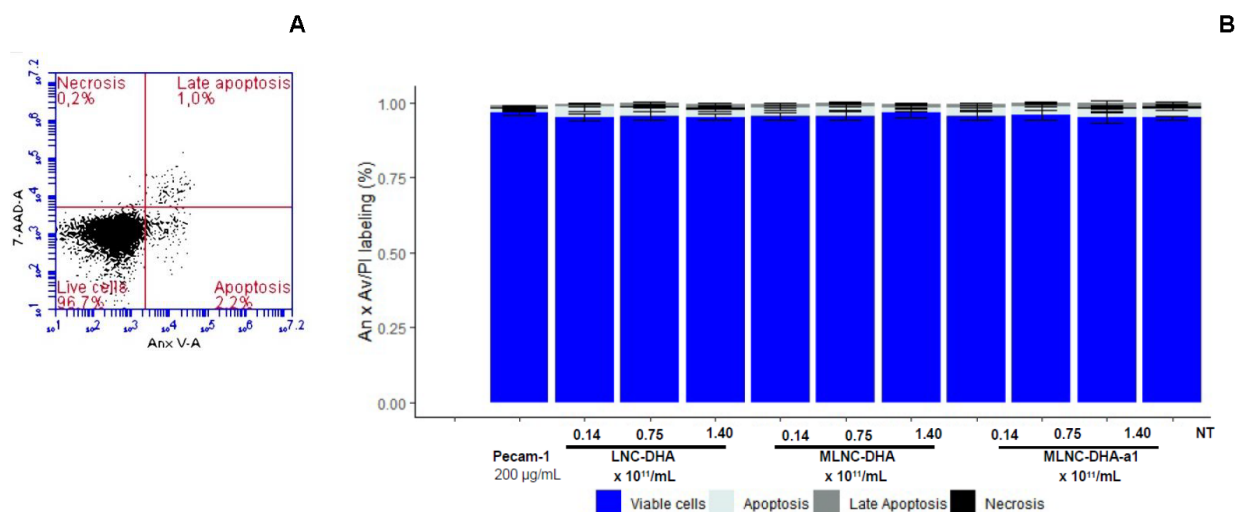


Figure 2. U937 cells viability, necrosis, apoptosis and late apoptosis as estimated by flow cytometry after culturing incubated with LNC-DHA, MLNC-DHA and MLNC-DHA-a1 at three concentrations (0.14×10^{11} , 0.75×10^{11} and 1.40×10^{11} /mL), also incubated without any nanocapsules (NT) and isolated anti-PECAM-1 at $200 \mu\text{g/mL}$ for 24h. **Fig.2A:** Flow cytometry colocalization of annexin-V binding and propidium iodide uptake for quantitation of U937 cells incubated with MLNC-DHA-a1, as example. The horizontal axis depicts fluorescein-labeled annexin V; the vertical axis shows binding of propidium iodide fluorescence. **Fig.2B:** Proportion of U937 cells viability, necrosis, apoptosis and late apoptosis. Vertical bars are mean \pm SEM. No difference was observed among the samples according to cell viability ($p=0.96$) necrosis ($p=0.87$), apoptosis ($p=0.94$) and late apoptosis ($p=0.94$) by Kruskal Wallis analysis.

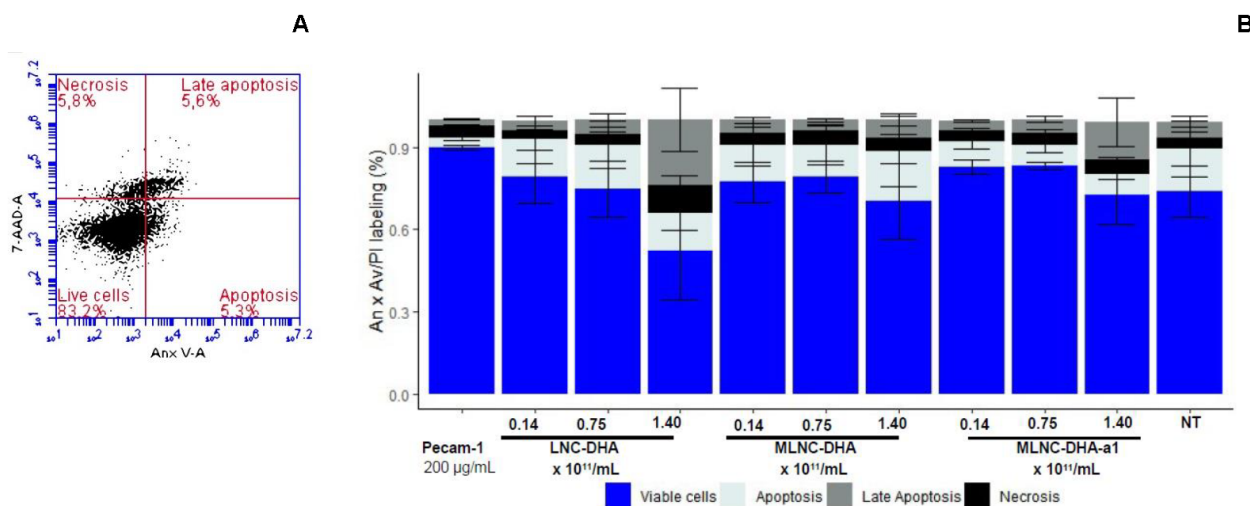


Figure 3. RAW 264.7 murine macrophages viability, necrosis, apoptosis and late apoptosis as estimated by flow cytometry after culturing incubated with LNC-DHA, MLNC-DHA and MLNC-DHA-a1 at three concentrations (0.14×10^{11} , 0.75×10^{11} and 1.40×10^{11} /mL), also incubated without any nanocapsules (NT) and isolated anti-PECAM-1 at 200 µg/mL for 24h. Fig.2A: Flow cytometry colocalization of annexin-V binding and propidium iodide uptake for quantitation of RAW 264.7 murine macrophages incubated with MLNC-DHA-a1, as example. The horizontal axis depicts fluorescein-labeled annexin V; the vertical axis shows binding of propidium iodide fluorescence. Fig.2B: Proportion of RAW 264.7 murine macrophages viability, necrosis, apoptosis and late apoptosis. Vertical bars are mean \pm SEM. No difference was observed among the samples according to cell viability ($p= 0.34$), necrosis ($p= 0.66$), apoptosis ($p= 0.75$) and late apoptosis ($p= 0.48$) by Kruskal Wallis analysis.

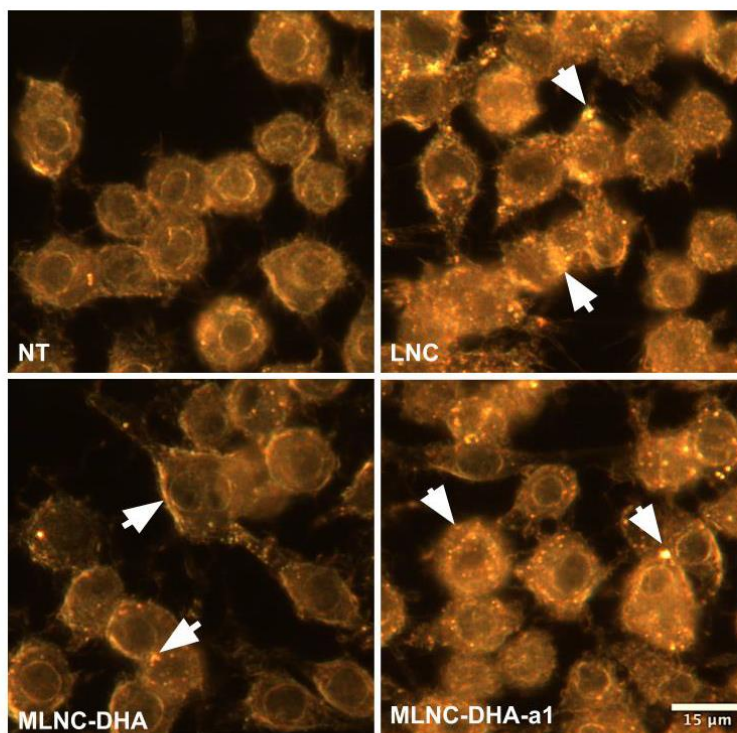


Figure 4. Three-dimensional CytoViva microscopy images of uptake performed in RAW 264.7 murine macrophages after 2 h of incubation with LNC-DHA, MLNC-DHA and MLNC-DHA-a1 at 0.75×10^{11} /mL, and also incubated without any nanocapsules (NT). Scale barr: 15 μ m.

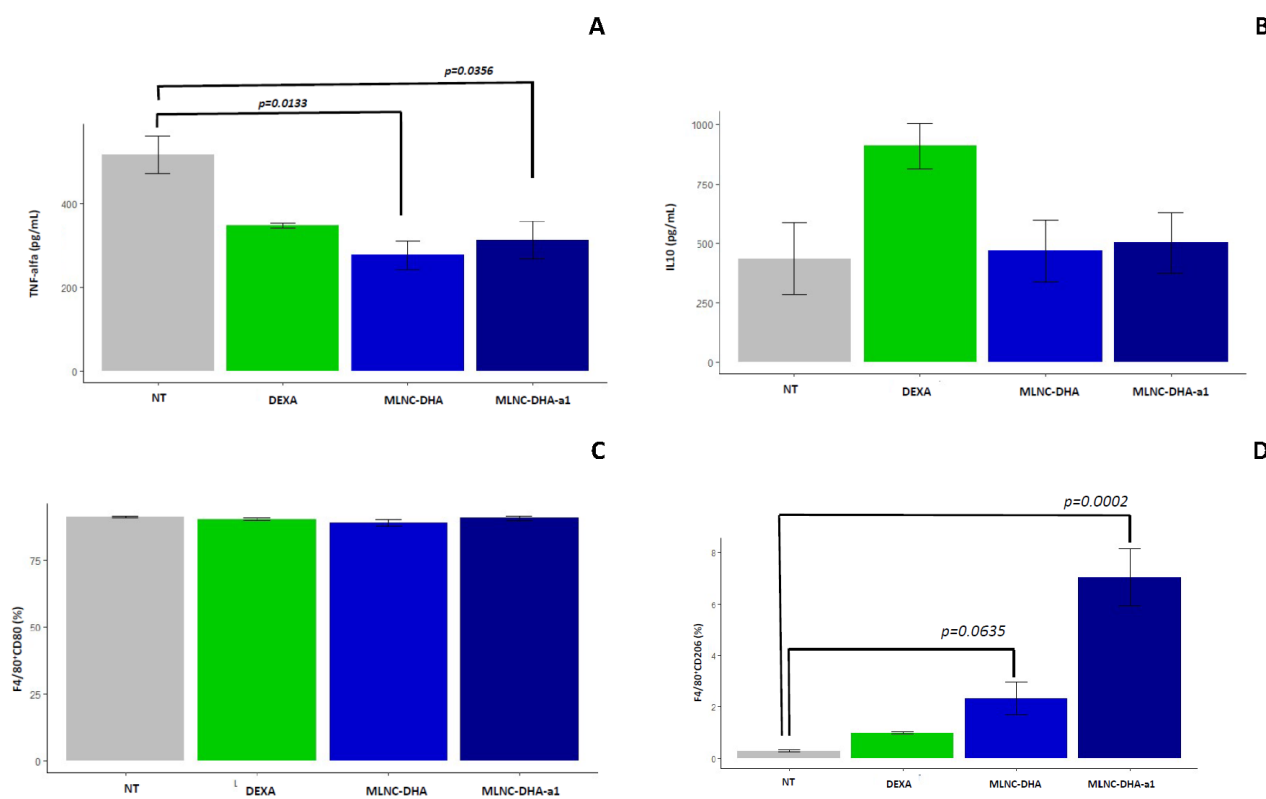


Figure 5. Flow cytometric analysis to quantify cytokines and polarization in cells obtained from the bone marrow, exposed to Escherichia coli (LPS) 100 ng/mL and maintained for 24h to provide RAW 264.7 murine macrophages. Assays were performed with dexamethasone (500 ng/mL) (DEXA), MLNC-DHA (0.75 x 10¹¹ particles/mL), MLNC-DHA-a1 (0.75 x 10¹¹ particles/mL containing 200 μ g/mL of Anti-PECAM-1 and without any treatment (NT) for 48h. **Fig 5A:** TNF α (pg/mL); $p=0.02$; **Fig.5B:** IL-10 (pg/mL); $p=0.29$; **Fig 5C:** Percentage of F4/80⁺ CD80 double positive cells (M1), ($p=0.25$) and **Fig 5D:** Percentage of F4/80⁺ and CD206 double positive cells (M2), ($p<0.01$). Vertical bars are mean \pm SEM. Treatments were compared by One-way ANOVA and Tukey HSD or equivalent non parametric Kruskal Wallis analysis.

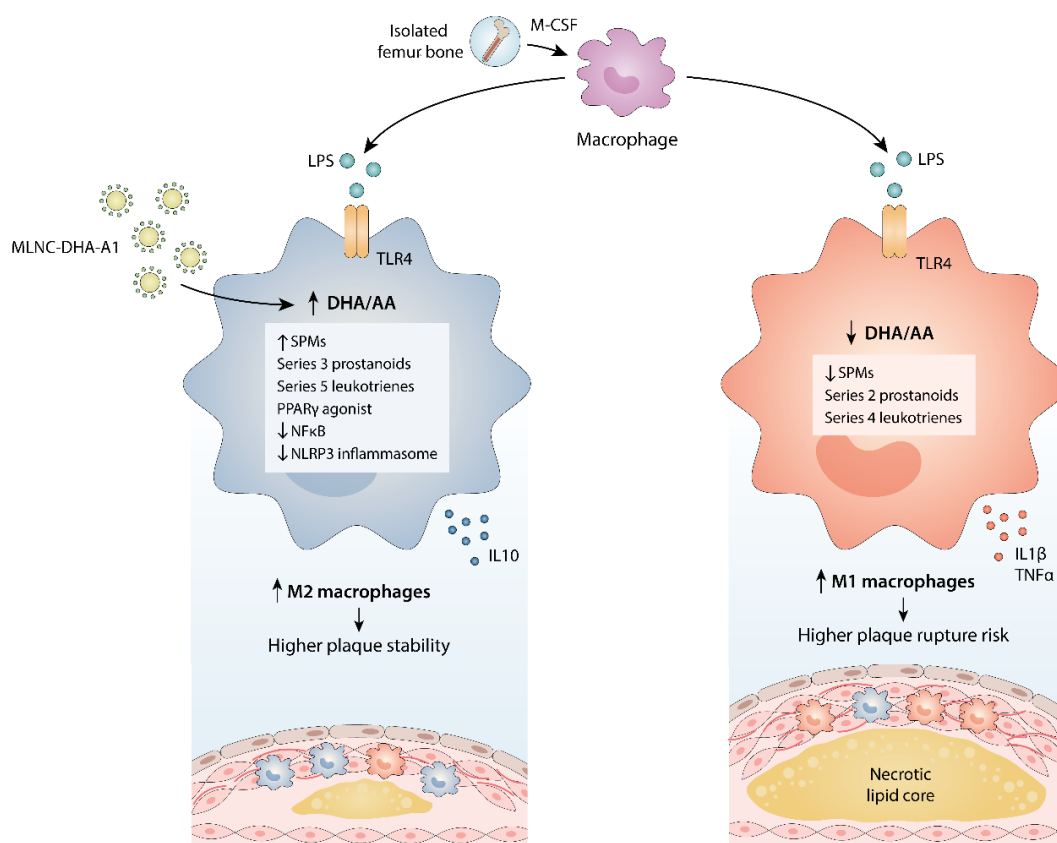
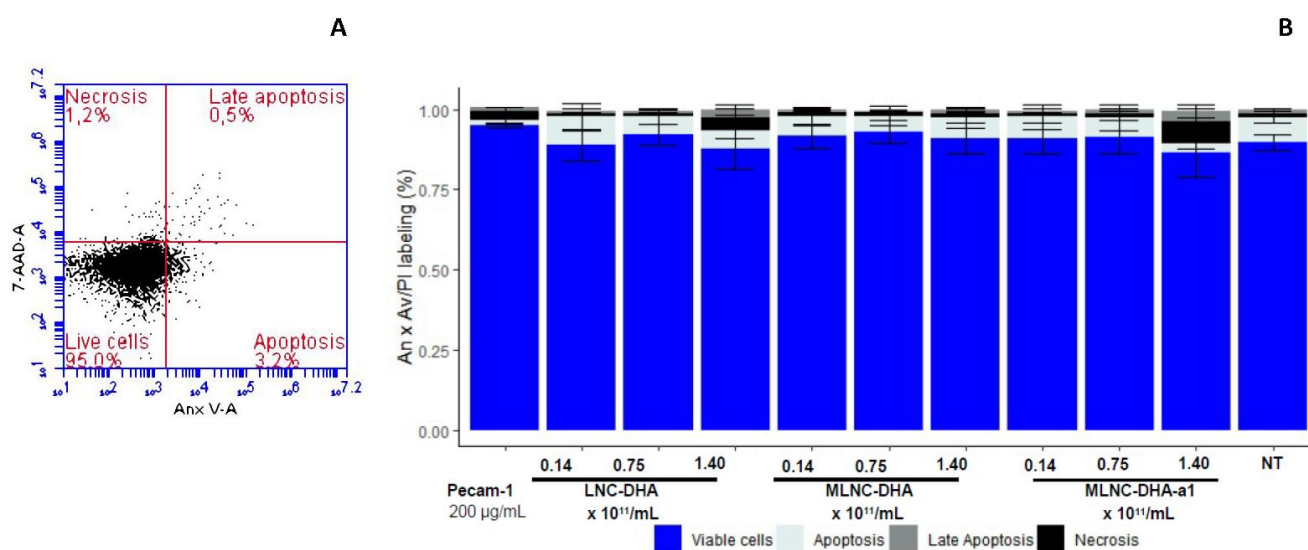
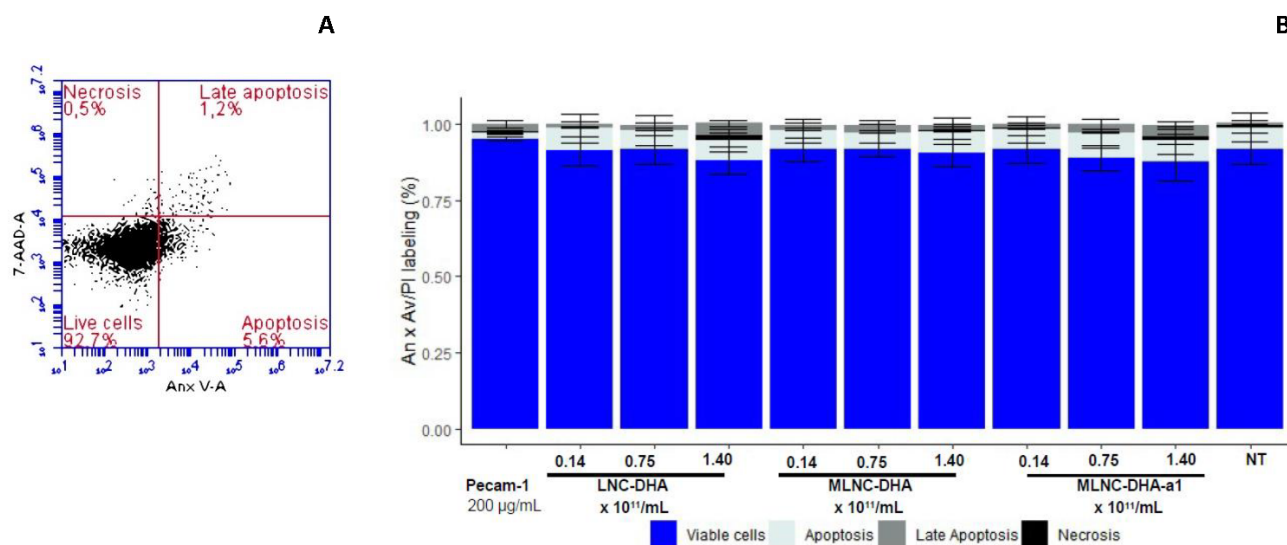


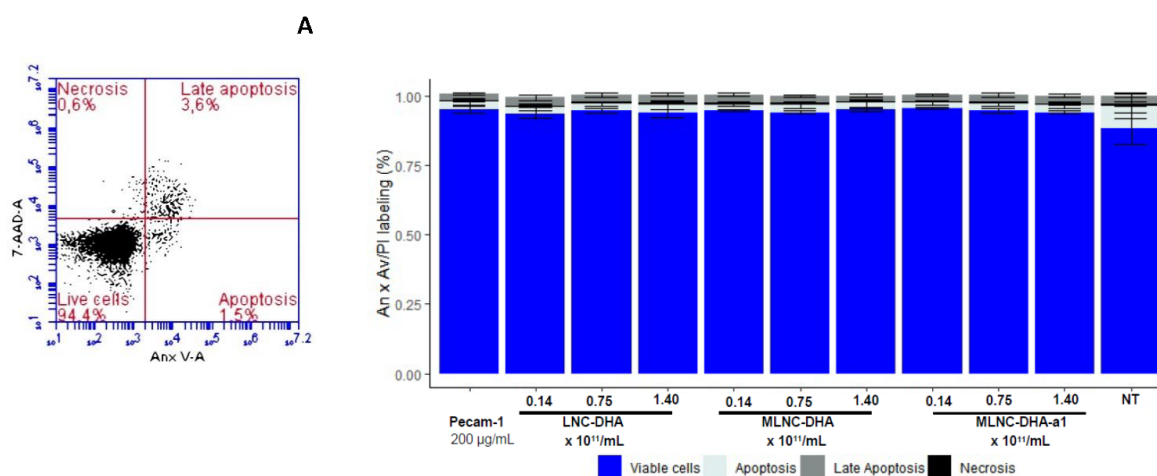
Figure 6. Summary of the strategy proposed in this study. The surface-functionalized (anti-PECAM-1) metal-complex multi-wall nanocapsules containing algae oil as DHA source (MLNC-DHA-a1) could be internalized by the macrophages, promoting a higher DHA/AA ratio inside the cell compared with non-treated samples. As consequence, MLNC-DHA-a1 supplemented cells would show an anti-inflammatory condition associated to M2 polarization, leading to a higher plaque stability.



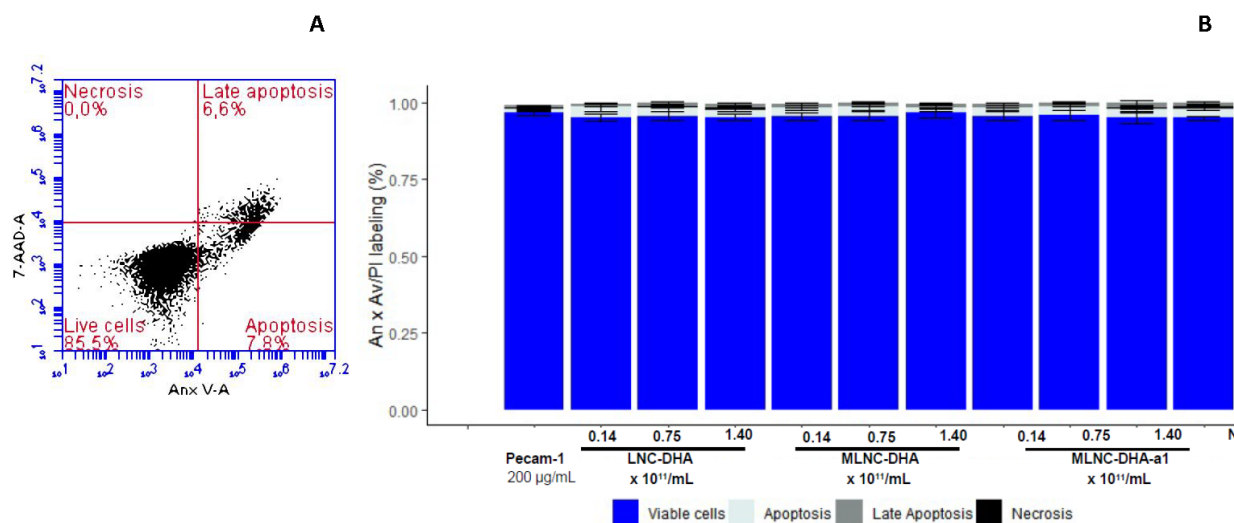
Supplementary Figure 1. HUEVEC viability, necrosis, apoptosis and late apoptosis as estimated by flow cytometry after culturing incubated with LNC-DHA, MLNC-DHA and MLNC-DHA-a1 at three concentrations (0.14×10^{11} /mL, 0.75×10^{11} /mL and 1.40×10^{11} /mL), also incubated without any nanocapsules (NT) and isolated anti-PECAM-1 at $200 \mu\text{g}/\text{mL}$ for 48h. Fig.1A: Flow cytometry colocalization of annexin-V binding and propidium iodide uptake for quantitation of HUEVEC incubated with MLNC-DHA-a1, as example. The horizontal axis depicts fluorescein-labeled annexin V; the vertical axis shows binding of propidium iodide fluorescence. Fig.1B: Proportion of HUEVEC viability, necrosis, apoptosis and late apoptosis. Vertical bars are mean \pm SEM. No difference was observed among the samples according to cell viability ($p = 0.98$) necrosis ($p = 0.96$), apoptosis ($p = 0.81$) and late apoptosis ($p = 0.99$) by Kruskal Wallis analysis.



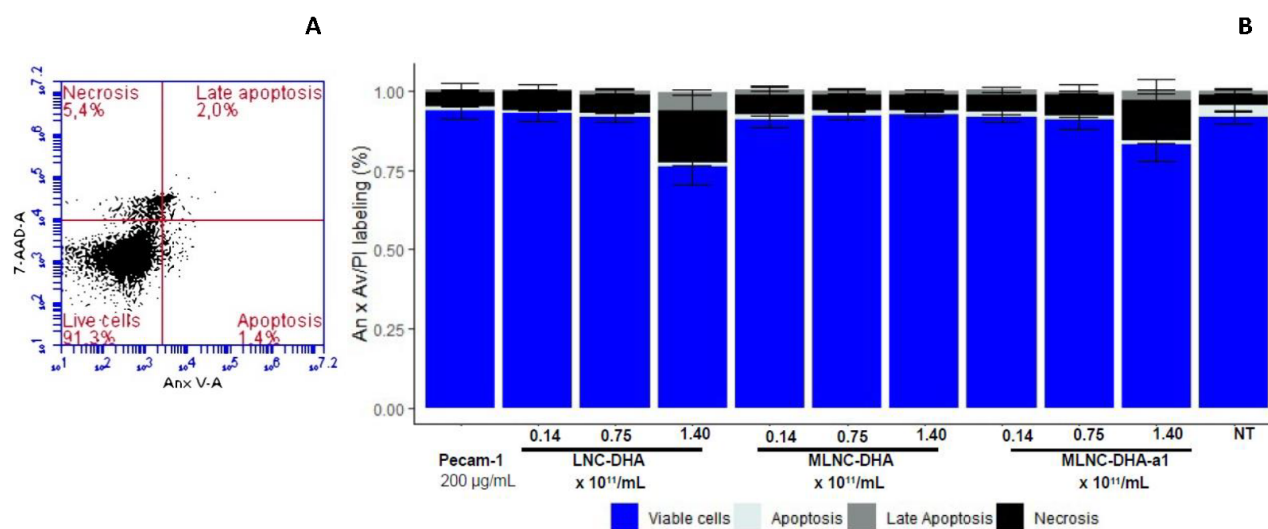
Supplementary Figure 2. HUEVEC viability, necrosis, apoptosis and late apoptosis as estimated by flow cytometry after culturing incubated with LNC-DHA, MLNC-DHA and MLNC-DHA-a1 at three concentrations (0.14×10^{11} /mL, 0.75×10^{11} /mL and 1.40×10^{11} /mL), also incubated without any nanocapsules (NT) and isolated anti-PECAM-1 at 200 µg/mL for 72h. **Fig.2A:** Flow cytometry colocalization of annexin-V binding and propidium iodide uptake for quantitation of HUEVEC incubated with MLNC-DHA-a1, as example. The horizontal axis depicts fluorescein-labeled annexin V; the vertical axis shows binding of propidium iodide fluorescence. **Fig.2B:** Proportion of HUEVEC viability, necrosis, apoptosis and late apoptosis. Vertical bars are mean \pm SEM. No difference was observed among the samples according to cell viability ($p=0.87$) necrosis ($p=0.76$), apoptosis ($p=0.99$) and late apoptosis ($p=0.43$) by Kruskal Wallis analysis.



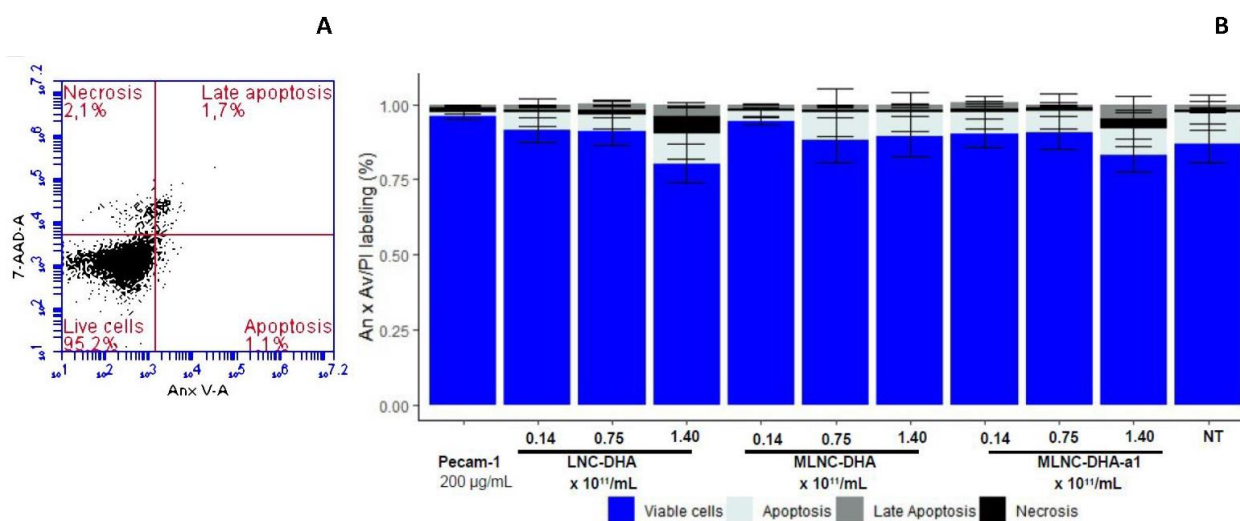
Supplementary Figure 3. U937 cells viability, necrosis, apoptosis and late apoptosis as estimated by flow cytometry after culturing incubated with LNC-DHA, MLNC-DHA and MLNC-DHA-a1 at three concentrations ($0.14 \times 10^{11}/\text{mL}$, $0.75 \times 10^{11}/\text{mL}$ and $1.40 \times 10^{11}/\text{mL}$), also incubated without any nanocapsules (NT) and isolated anti-PECAM-1 at $200 \mu\text{g}/\text{mL}$ for 48h. Fig.3A: Flow cytometry colocalization of annexin-V binding and propidium iodide uptake for quantitation of U937 cells incubated with MLNC-DHA-a1, as example. The horizontal axis depicts fluorescein-labeled annexin V; the vertical axis shows binding of propidium iodide fluorescence. Fig.3B: Proportion of U937 cells viability, necrosis, apoptosis and late apoptosis. Vertical bars are mean \pm SEM. No difference was observed among the samples according to cell viability ($p=0.73$) necrosis ($p=0.99$), apoptosis ($p=0.92$) and late apoptosis ($p=0.97$) by Kruskal Wallis analysis.



Supplementary Figure 4. U937 cells viability, necrosis, apoptosis and late apoptosis as estimated by flow cytometry after culturing incubated with LNC-DHA, MLNC-DHA and MLNC-DHA-a1 at three concentrations (0.14×10^{11} /mL, 0.75×10^{11} /mL and 1.40×10^{11} /mL), also incubated without any nanocapsules (NT) and isolated anti-PECAM-1 at 200 µg/mL for 72h. **Fig.4A:** Flow cytometry colocalization of annexin-V binding and propidium iodide uptake for quantitation of U937 cells incubated with MLNC-DHA-a1, as example. The horizontal axis depicts fluorescein-labeled annexin V; the vertical axis shows binding of propidium iodide fluorescence. **Fig.4B:** Proportion of U937 cells viability, necrosis, apoptosis and late apoptosis. Vertical bars are mean \pm SEM. No difference was observed among the samples according to cell viability ($p= 0.33$) necrosis ($p= 0.98$), apoptosis ($p= 0.89$) and late apoptosis ($p= 0.45$) by Kruskal Wallis analysis.



Supplementary Figure 5. RAW 264.7 murine macrophages viability, necrosis, apoptosis and late apoptosis as estimated by flow cytometry after culturing incubated with LNC-DHA, MLNC-DHA and MLNC-DHA-a1 at three concentrations (0.14×10^{11} /mL, 0.75×10^{11} /mL and 1.40×10^{11} /mL), also incubated without any nanocapsules (NT) and isolated anti-PECAM-1 at 200 µg/mL for 48h. **Fig.5A:** Flow cytometry colocalization of annexin-V binding and propidium iodide uptake for quantitation of RAW 264.7 murine macrophages incubated with MLNC-DHA-a1, as example. The horizontal axis depicts fluorescein-labeled annexin V; the vertical axis shows binding of propidium iodide fluorescence. **Fig.5B:** Proportion of RAW 264.7 murine macrophages viability, necrosis, apoptosis and late apoptosis. Vertical bars are mean \pm SEM. No difference was observed among the samples according to cell viability ($p= 0.25$) necrosis ($p= 0.71$), apoptosis ($p= 0.43$) and late apoptosis ($p= 0.16$) by Kruskal Wallis analysis.



Supplementary Figure 6. RAW 264.7 murine macrophages viability, necrosis, apoptosis and late apoptosis as estimated by flow cytometry after culturing incubated with LNC-DHA, MLNC-DHA and MLNC-DHA-a1 at three concentrations (0.14 x 10¹¹/mL, 0.75 x 10¹¹/mL and 1.40 x 10¹¹/mL), also incubated without any nanocapsules (NT) and isolated anti-PECAM-1 at 200 µg/mL for 72h. **Fig.6A:** Flow cytometry colocalization of annexin-V binding and propidium iodide uptake for quantitation of RAW 264.7 murine macrophages incubated with MLNC-DHA-a1, as example. The horizontal axis depicts fluorescein-labeled annexin V; the vertical axis shows binding of propidium iodide fluorescence. **Fig.6B:** Proportion of RAW 264.7 murine macrophages viability, necrosis, apoptosis and late apoptosis. Vertical bars are mean ± SEM. No difference was observed among the samples according to cell viability ($p = 0.59$), necrosis ($p = 0.78$), apoptosis ($p = 0.91$) and late apoptosis ($p = 0.18$) by Kruskal Wallis analysis.

FINAL COMMENTS

Although drug treatment for atherosclerosis has great effectiveness, cardiovascular diseases still remain in the first cause of mortality worldwide. Omega-3 fatty acids have anti-inflammatory effects that can contribute to reduce the cardiovascular diseases. In particular, DHA-derived oxylipins can switch M1 to M2 macrophages phenotype, potentially increasing the atherosclerotic plaque stability, and reducing sudden fatal events. However, one of the biggest scientific challenge is to deliver DHA to the inflamed endothelium, where the plaque is present. In this sense, we developed a stable nanoparticle functionalized with anti-PECAM-1 on its surface and containing DHA richer oil in its lipid core and observed promising results regarding to the macrophages polarization. For the next steps, new challenges must be overcome, including aggregation risk in the circulation, biodistribution, and *in vivo* anti-inflammatory effects with consequent plaque regression. It is worth to highlight that although our research represents a hopeful therapeutic strategy, classical guidelines recommendations to control atherosclerosis risks must be strongly followed by patients under primary or secondary prevention.

ATTACHMENTS



UNIVERSIDADE DE SÃO PAULO

FACULDADE DE CIÊNCIAS FARMACÊUTICAS
Comissão de Ética no Uso de Animais - CEUA

CEUA/FCF 027.2018-P555

CERTIFICADO

Certificamos que a proposta intitulada **Efeitos dos ácidos graxos EPA e DHA veiculados em nanocápsulas vetorizadas com o anticorpo Anti-PECAM-1 na aterosclerose experimental**, registrada com o nº **555**, sob a responsabilidade do(a) pesquisador(a) **Matheus de Castro Leão**, sob orientação do(a) **Profa. Dra. Inar Alves de Castro** – que envolve produção ou manutenção ou utilização de animais pertencentes ao filo Chordata, subfilo Vertebrata (exceto humanos), para fins de pesquisa científica – encontra-se de acordo com os preceitos da Lei Federal nº 11.794, de 8 de outubro de 2008, do Decreto Federal nº 6.899, de 15 de julho de 2009, e das normas editadas pelo Conselho Nacional de Controle de Experimentação Animal (CONCEA), e foi aprovada pela Comissão de Ética no Uso de Animais (CEUA) da Faculdade de Ciências Farmacêuticas da Universidade de São Paulo (FCF/USP), em reunião de **11 de maio de 2018**.

Finalidade	Pesquisa Científica
Vigência da autorização	11/05/2018 a 31/08/2019
Espécie/linhagem/raça	Camundongo – C57/BL6 knockout LDLr
Número de animais	80
Peso/Idade	20g; 3 meses
Sexo	Macho
Origem	Biotério FCF/IQ- USP

Conforme a legislação vigente, deverá ser apresentado, no encerramento do projeto de pesquisa, o respectivo **relatório final**.

São Paulo, 11 de maio de 2018.


Profa. Dra. Neuza Mariko Aymoto Hassimotto
 Coordenadora da CEUA/FCF/USP

ACADEMIC ACHIEVEMENTS

Publications:

Leão, M. D. C., Pohlmann, A. R., Alves, A. D. C. S., Farsky, S. H. P., Uchiyama, M. K., Araki, K., ... & Castro, I. A. (2021). Docosahexaenoic acid nanoencapsulated with anti-PECAM-1 as co-therapy for atherosclerosis regression. *European Journal of Pharmaceutics and Biopharmaceutics*, 159, 99-107.

Leão, M. D. C., Piazza, I. D., Broering, M. F., Farsky, S. H. P., Uchiyama, M. K., Araki, K., Pohlmann, A. R., Guterres, S. S., Castro, I. A. (2022). Effect of anti-PECAM-1 vectorized nanocapsules containing docosahexaenoic acid on macrophages polarization. *Manuscript currently under revision at "European Journal of Pharmaceutics and Biopharmaceutics"*.

Co-authorship

Rogero, M. M., **Leão, M. D. C.**, Santana, T. M., de MB Pimentel, M. V., Carlini, G. C., da Silveira, T. F., ... & Castro, I. A. (2020). Potential benefits and risks of omega-3 fatty acids supplementation to patients with COVID-19. *Free radical biology and medicine*, 156, 190-199.

Broering, M. F., **Leao, M. D. C.**, Rocha, G. H. O., Scharf, P. R. S., Alves, A. C. S., Castro, I. A., Reutelingsperger, C., Guterres, S. S., Polhmann, A. R., Farsky, S. H. P. (2022). Development of Annexin A1-surface-functionalized metal-complex multi-wall lipid core nanocapsules and effectiveness on experimental colitis. *Manuscript currently under revision at "European Journal of Pharmaceutics and Biopharmaceutics"*.

INTERNATIONAL SCIENTIFIC MEETINGS ATTENDED

EAS CONGRESS – 88th – European Atherosclerosis Society (poster presentation). October 04-07 (2020).

EAS CONGRESS – 89th – European Atherosclerosis Society (poster presentation). May 30 – June 2 (2021).



Universidade de São Paulo
Faculdade de Ciências Farmacêuticas
FICHA DO ALUNO

9132 - 10547405/1 - Matheus de Castro Leão

Email: matheusdcstr@usp.br
Data de Nascimento: 21/06/1995
Cédula de Identidade: RG - 5.013.497 - SC
Local de Nascimento: Estado de São Paulo
Nacionalidade: Brasileira
Graduação: Nutricionista - Universidade do Vale do Itajaí - Santa Catarina - Brasil - 2016

Curso: Doutorado Direto
Programa: Ciência dos Alimentos
Área: Nutrição Experimental
Data de Matrícula: 29/08/2017
Início da Contagem de Prazo: 29/08/2017
Data Limite para o Depósito: 24/08/2022
Orientador: Prof(a). Dr(a). Inar Castro Erger - 29/08/2017 até o presente. Email: inarcastro@gmail.com
Proficiência em Línguas: Inglês, 29/08/2017
Data de Aprovação no Exame de Qualificação: Aprovado em 25/10/2019
Data do Depósito do Trabalho:
Título do Trabalho:
Data Máxima para Aprovação da Banca:
Data de Aprovação da Banca:
Data Máxima para Defesa:
Data da Defesa:
Resultado da Defesa:
Histórico de Ocorrências: Primeira Matrícula em 29/08/2017

Aluno matriculado no Regimento da Pós-Graduação USP (Resolução nº 6542 em vigor de 20/04/2013 até 28/03/2018).

Última ocorrência: Matrícula de Acompanhamento em 18/07/2022

Impresso em: 24/07/2022 23:48:22



Universidade de São Paulo
Faculdade de Ciências Farmacêuticas
FICHA DO ALUNO

9132 - 10547405/1 - Matheus de Castro Leão

Sigla	Nome da Disciplina	Início	Término	Carga Horária	Cred.	Freq.	Conc.	Exc.	Situação
MPT5794-2/1	Ultraestrutura e Função Celular (Faculdade de Medicina - Universidade de São Paulo)	26/09/2017	30/10/2017	75	5	100	A	N	Concluída
FBT5790-1/1	Desenvolvimento de Lipídeos como Alimentos Funcionais e Nutracêuticos	04/10/2017	09/11/2017	45	3	100	A	N	Concluída
FBC5710-7/1	Vacinas e Adjuvantes	13/11/2017	17/12/2017	60	0	-	-	N	Matrícula cancelada
EFB5741-7/1	Integração Metabólica do Exercício Físico (Escola de Educação Física e Esporte - Universidade de São Paulo)	27/08/2018	23/09/2018	60	4	100	B	N	Concluída
FBA5728-4/7	Aprimoramento Pedagógico	02/10/2018	29/10/2018	60	4	87	A	N	Concluída
FBC5700-8/2	Aterosclerose: Fisiopatologia, Diagnóstico e Terapêutica	09/10/2018	13/11/2018	60	0	-	-	N	Turma cancelada
MCP5859-2/4	Métodos de Imagem em Pesquisa Científica Cardiovascular (Faculdade de Medicina - Universidade de São Paulo)	15/10/2018	21/10/2018	30	2	75	A	N	Concluída
FBA5907-1/1	Lipídios – Estabilidade Oxidativa e Funcionalidade Cardiovascular	11/02/2019	24/02/2019	60	4	100	A	N	Concluída

	Créditos mínimos exigidos		Créditos obtidos
	Para exame de qualificação	Para depósito de tese	
Disciplinas:	0	20	22
Estágios:			
Total:	0	20	22

Créditos Atribuídos à Tese: 172

Conceito a partir de 02/01/1997:

A - Excelente, com direito a crédito; B - Bom, com direito a crédito; C - Regular, com direito a crédito; R - Reprovado; T - Transferência.

Um(1) crédito equivale a 15 horas de atividade programada.

Última ocorrência: Matrícula de Acompanhamento em 18/07/2022

Impresso em: 24/07/2022 23:48:22